DOKUZ EYLÜL UNIVERSITY

GRADUATE SCHOOL OF NATURAL AND APPLIED SCIENCES

INVESTIGATION OF MICROCAPSULE BASED SELF-HEALING IN CEMENT BASE MATERIALS

By

Doğa EYİCE

September, 2021

İZMİR

INVESTIGATION OF MICROCAPSULE BASED SELF-HEALING IN CEMENT BASE MATERIALS

A Thesis Submitted to the
Graduate School of Natural and Applied Sciences of Dokuz Eylül University
In Partial Fulfilment of the Requirements for the Degree of Master in Civil Engineering, Construction Materials Program

By
Doğa EYİCE

September, 2021
İZMİR

M.Sc THESIS EXAMINATION RESULT FORM

We have read the thesis entitled **"INVESTIGATION OF MICROCAPSULE BASED SELF-HEALING IN CEMENT BASE MATERIALS"** completed by **DOĞA EYİCE** under supervision of **PROF. DR. HALİT YAZICI** and we certify that in our opinion it is fully adequate, in scope and in quality, as a thesis for the degree of Master of Science.

……

Prof. Dr. Halit YAZICI

Supervisor

……	……
Assoc. Prof. Dr. Tahir Kemal ERDEM	Assoc. Prof. Dr. Hüseyin YİĞİTER
(Jury member)	(Jury member)

Prof. Dr. Özgür ÖZÇELİK

Director

Graduate School of Natural and Applied Sciences

ACKNOWLEDGEMENTS

Firstly, I would like to say thank you to my supervisor, Prof. Dr. Halit YAZICI, for his sincerity and trust. It is very valuable for me that although I graduated from another university and we have not met before, he included me as a scholarship student in the TUBITAK project.

I am grateful to Assist. Prof. Dr. Ahsanollah BEGLARIGALE for his support, knowledge shearing and valuable comments during the TUBİTAK (215M793) duration. Thanks to him I have learned and challenged a lot of things in the laboratory. I would like to thank C. Eng. Bayram TUTKUN for their valuable support within the scope of the TÜBİTAK project. Also, I thank to my friends at Construction Materials Laboratory for their friendships during my master education. Thanks are also given to İ.PINAR, E. F. MORBEL, B. ERKEK, for their contributions within the scope of Undergraduate Graduation Projects.

I would like to acknowledge the financial support provided by TUBİTAK (Project No: 215M783) in terms of scholarship and project supports.

Lastly, I would like to give my whole thanks and deepest appreciation to my family; my mother Aysel, my father Şadan, my sister Deniz. It is very valuable for me that they have my back unconditionally when I say "I will do this". I would also like to thank my little niece Ekin, who was born during my thesis writing process, for making our lives colourful.

.

Doğa EYİCE

ÇİMENTO ESASLI MALZEMELERDE MİKROKAPSÜL ESASLI KENDİ KENDİNE İYİLEŞMENİN ARAŞTIRILMASI

ÖZ

Çimento esaslı malzemelerin matrislerinde meydana gelen çatlaklar kısa ve uzun vadede ciddi durabilite problemlerine neden olabilmektedir. Ayrıca, yer altı yapıları ve içinde zarar verici sıvılar bulunduran beton siloları gibi yapılarda bu çatlakların bakım-onarım çalışmaları zor ve maliyetlidir. Bu sebeple çimento esaslı malzemelerin kendi kendine iyileşme kabiliyetini geliştirmek adına birçok yaklaşım geliştirilmiştir. Bu çalışmada, lif takviyeli ultra yüksek performanslı beton (UHPC) ve normal harçlarda kendi kendine iyileşme kabiliyetini geliştirmek için sodyum silikat içeren mikrokapsüllerin üretimi gerçekleştirilip çimento esaslı kompozitlerde etkinliği incelenmiştir.

Yapılan sistematik çalışmayla UHPC ve normal harç karışımlarında mikrokapsül içermeyen kontrol karışımları ve çimentonun ağırlıkça yüzde 5'i oranında mikrokapsül içeren karışımlar üzerinde çalışılmıştır. Mikrokapsül esaslı kendi kendine iyileşme mekanizması basınç dayanımı, çekme dayanımı, toplam ve kılcal su emme, çatlak kapanma deneyi ve çatlak analizi ile incelenmiştir. Kontrol karışımlarında otojen kendi kendine iyileşme mekanizması gözlemlenirken mikrokapsüllü karışımlarla kıyaslanarak mikrokapsül esaslı iyileşmeler tespit edilmiştir.

Tüm deney sonuçlarında kayda değer iyileşme oranları elde edilmiştir. Deneylerde mikrokapsüllerin iyileşmeye olan olumlu etkisi gözlemlenirken bu etkinin normal harçlarda daha yüksek olduğu görülmüştür.

Anahtar kelimeler: Çimento esaslı kompozit, kendi kendine iyileşme, mikrokapsül, puzolan,

INVESTIGATION OF MICROCAPSULE BASED SELF-HEALING IN CEMENT BASE MATERIALS

ABSTRACT

Cracks occurring in the matrix of cement-based materials can cause serious durability problems in the short and long term. In addition, the maintenance and repair work of these cracks in structures such as underground structures and concrete silos containing damaging liquids are difficult and costly. For this reason, many approaches have been developed to improve the self-healing ability of cement-based materials. In this study, microcapsules containing sodium silicate were produced to improve the self-healing ability of fiber-reinforced ultra-high-performance concrete (UHPC) and normal mortars and their effectiveness in cement-based composites was investigated.

In a systematic study, control mixtures without microcapsules and mixtures containing microcapsules at the rate of 5 percentage by weight of cement in UHPC and normal mortar mixtures were studied. Microcapsule-based self-healing mechanism was investigated by compressive strength, tensile strength, total and capillary water absorption, crack closure test and crack analysis. While autogenous self-healing mechanism was observed in control mixtures, microcapsule-based improvements were detected by comparing with microencapsulated mixtures.

Significant recovery(self-healing) ratios were obtained in all experimental results. While the positive effect of microcapsules on healing was observed in the experiments, it was observed that this effect was higher in normal mortars.

Keywords: Cement based composite, self-healing, microcapsule, pozzolana.

CONTENTS

Page

M.Sc THESIS EXAMINATION RESULT FORM ii

ACKNOWLEDGEMENTS iii

ÖZ iv

ABSTRACT v

LIST OF FIGURES ix

LIST OF TABLES xiii

CHAPTER 1 - INTRODUCTION 1

1.1 Aim and Scope 2

CHAPTER 2 – LITERATURE REWIEV 3

1.1 Importance of Self-healing in Cementitious Composites 3

1.2 Definition of Self-Healing and Self-Healing Mechanisms 3

1.2.1 Autogenous Self-Healing Mechanism 4

1.2.2 Bacteria-based Self-Healing Mechanism 6

1.2.3 Microcapsule-based Self-Healing Mechanism 6

CHAPTER 3 – MATERIALS AND METHODS 11

3.1 Cement Based Mixtures 11

3.1.1 Materials 11

3.1.2 Design of Mixtures 14

3.1.3 Test Methods 15

3.2. Microencapsulation 25

3.2.1 Materials 26

3.2.2 Microencapsulation Method 26

CHAPTER 4 – MICROCAPSULES EFFECT ON SELF-HEALING 28

4.1 Examination of Microcapsule Based Self-Healing in UHPC Mixtures 29

4.1.1 Examination of Microcapsule Based Self-Healing Mechanism by Compressive Strength Test 29

4.1.2 Examination of Microcapsule Based Self-Healing Mechanism by Direct Tensile Strength Test 35

4.1.3 Examination of Microcapsule Based Self-Healing Mechanism by Total and Capillary Water Absorption Test 41

4.1.4 Examination of Microcapsule Based Self-Healing Mechanism by Crack-closing Test 47

4.1.5 Examination of Microcapsule Based Self-Healing Mechanism by Crack Analysis 50

4.1.6 General Evaluation of the Effectiveness of Sodium Silicate / Polyurethane Microcapsules in UHPC Mixture 53

4.2 Examination of Microcapsule Based Self-Healing in Normal Mortar Mixtures 54

4.2.1 Examination of Microcapsule Based Self-Healing Mechanism by Compressive Strength Test 54

4.2.2 Examination of Microcapsule Based Self-Healing Mechanism by Direct Tensile Test 57

4.2.3 Examination of Microcapsule Based Self-Healing Mechanism by Crack Closing Test..... 58

4.2.4 Examination of Microcapsule Based Self-Healing Mechanism by Total Water Absorption Test 59

4.2.5 Examination of Microcapsule Based Self-Healing Mechanism by Capillary Water Absorption Test..... 61

4.2.6 Examination of Microcapsule Based Self-Healing Mechanism by Crack Analysis 65

4.2.7 General Evaluation of the Effectiveness of Sodium Silicate / Polyurethane Microcapsules in Normal Mortar Mixtures..... 68

CHAPTER 5 – RESULTS AND RECOMMENDATIONS 69

REFERENCES..... 73

LIST OF FIGURES

Page

Figure 2.1 Possible mechanisms for self-healing in concrete 4
Figure 2.2 Schematic representation of the microcapsule 7
Figure 2.3 SEM images of silica/epoxy microcapsules. a) broken microcapsule, b) elemental analysis (Si= blue, C= red, Al= green), c, d and e) images of microcapsules of different sizes 9
Figure 3.1 Flow table test result of NH 16
Figure 3.2 Samples for compressive strength test 18
Figure 3.3 Details of bone-shaped sample and mold 19
Figure 3.4 Tensile loading of bone-shaped samples 20
Figure 3.5 CWA test of preloaded samples 21
Figure 3.6 a) Loading of disc-shape samples, b) measurement of crack width by OM, c) crack formation 22
Figure 3.7 Compressive strength test of cylindrical samples 23
Figure 3.8 Vacuum assembly and epoxy soak chamber 24
Figure 3.9 a) Placement of samples in chamber, b) epoxy soaking of sample in the chamber 24
Figure 3.10 Divided sample surface under UV light 25
Figure 3.11 Process of microencapsulation of sodium silicate with polyurethane wall: a) adding surfactants to oil phase, b) adding SS solution to oil phase for emulsification, c) adding wall-building solution to emulsion, d) polymerization process at 63 °C for 4 h, e, f) vacuum filtration and washing of microcapsules, g) microcapsules on the watch glass after drying process 27
Figure 4.1 Compressive strength results of 7-day samples before and after 30-day recovery period 30
Figure 4.2 Compressive strength results of 90-day samples before and after 30-day recovery period 31

Figure 4.3 Average decrease in compressive strength (damage ratio) caused by preloading in UHPC samples 32
Figure 4.4 Self-healing ratio of 7 and 90-day samples (first approach)..... 33
Figure 4.5 Self-healing ratio of 7 and 90- day samples (second approach)..... 35
Figure 4.6 7-day YM tension results..... 36
Figure 4.7 90 -day YM tension results..... 37
Figure 4.8 7 -day YM_M tension results 37
Figure 4.9 90 -day YM_M tension results 38
Figure 4.10 7-day direct tensile strength results of YM and YM_M mixtures..... 39
Figure 4.11 7-day direct tensile strength results of YM and YM_M mixtures..... 39
Figure 4.12 Regain percentages in tensile strength..... 40
Figure 4.13 TWA percentages of 7-day samples 41
Figure 4.14 TWA percentages of 90-day samples 42
Figure 4.15 Recovery in TWA (self-healing ratio)..... 42
Figure 4.16 Time-dependent capillary water absorption graph of 7-day YM samples 44
Figure 4.17 Time-dependent capillary water absorption graph of 7-day YM_M samples..... 45
Figure 4.18 Time-dependent capillary water absorption graph of 90-day YM samples 46
Figure 4.19 Time-dependent capillary water absorption graph of 90-day YM_M samples..... 46
Figure 4.20 Recovery percentages (self-healing ratios) in CWA test..... 47
Figure 4.21 Percentages of crack-closing (self-healing ratios)..... 48
Figure 4.22 a) and b) OM images of 7-day YM samples before and after 30-day recovery period; c) and d) OM images of 7-day YM_M samples before and after 30-day healing period..... 49
Figure 4.23 SEM image of two dome shaped cavities captured in the YM_M mixture 50
Figure 4.24 Crack closure percentages as a result of crack analysis (self-healing ratio) 51

Figure 4.25 a) YM mixture after 7 days preloading, b) 7 days preloaded sample under UV light and analysis after 30 days self-healing period 52
Figure 4.26 a) YM mixture after 90 days preloading, b) 90 days preloaded sample under UV light and analysis after 30 days self-healing period 52
Figure 4.27 Damage rates of NM and NM_M mixtures 55
Figure 4.28 7-day compressive strength of NM and NM_M mixtures 55
Figure 4.29 90-day compressive strength of NM and NM_M mixtures 56
Figure 4.30 Self-healing ratio of 7 and 90-day samples 57
Figure 4.32 Percentages of crack closing 58
Figure 4.33 OM images of a) before 30-day healing period of 7-day NM mixture, b) after 30-day healing period of 7-day NM mixture, c) before 30-day healing period of 7-day NM_M mixture, d) after 30-day healing period of 7-day NM_M mixture 59
Figure 4.34 TWA Percentages Of 7-Day Samples 60
Figure 4.35 TWA Percentages of 90-Day Samples 60
Figure 4.36 Self-healing in TWA (%) 61
Figure 4.37 Time-dependent capillary water absorption graph of 7-day NM samples 62
Figure 4.38 Time-dependent capillary water absorption graph of 7-day NM_M samples 62
Figure 4.39 Time-dependent capillary water absorption graph of 90-day NM samples 63
Figure 4.40 Time-dependent capillary water absorption graph of 90-day NM_M samples 64
Figure 4.41 Recovery percentages (self-healing ratios) in CWA test 65
Figure 4.42 Crack closure percentages as a result of crack analysis (self-healing ratio) 66
Figure 4.43 a) NM mixture after 7 days preloading, b) 7 days preloaded sample under UV light and analysis after 30 days self-healing period 66
Figure 4.44 a) NM_M mixture after 7 days preloading, b) 7 days preloaded sample under UV light and analysis after 30 days self-healing period 67

Figure 4.45 a) NM mixture after 90 days preloading, b) 90 days preloaded sample under UV light and analysis after 30 days self-healing period 67
Figure 4.46 a) NM_M mixture after 90 days preloading, b) 90 days preloaded sample under UV light and analysis after 30 days self-healing period 68

LIST OF TABLES

Page

Table 3.1 Properties of cement..... 12
Table 3.2 Properties of GGBFS 12
Table 3.3 Properties of steel fibers..... 13
Table 3.4 Properties of superplasticizer 13
Table 3.5 Designs of mixtures (kg/m^3) 14
Table 5.1 Summary of Self-healing ratios…….....71

CHAPTER 1

INTRODUCTION

Macro and micro cracks that occur for many reasons in cement-based composites are the most important factors affecting the strength of these materials. These cracks allow aggressive liquids and gases to penetrate, causing many durability problems and structural problems such as reinforcement corrosion. Infrastructures such as bridges and tunnels with heavy traffic congestion, or underground structures and silos containing dangerous liquids are very difficult and dangerous to repair. (Freyermuth, 2001; Mihashi & Nishiwaki, 2012; Sangadji & Schlangen, 2012; Van Tittelboom & De Belie, 2013). In most cases, these cracks are invisible or difficult to reach (S. Zhou, Zhu, & Yan, 2014). Repairing cracks in concrete is very complex and requires high cost and labor (Cailleux & Pollet, 2009; V. C. Li & Herbert, 2012; Van Breugel, 2007). It also creates environmental and social problems.

Service times of structures can be improved by using self-healing methods. Further hydration of unhydrated cement or pozzolans materials, formation of calcium hydroxide or calcium carbonate or expansion of hydrated cementitious matrix in crack walls are called autogenous (intrinsic) self-healing mechanisms in conventional concrete materials (Ter Heide, 2005).

Many researchers have discovered that autogenous self-healing is not the only mechanism for self-healing. There are many self-healing mechanisms that can be applied during the production of cement-based materials. Fracture restraint techniques (Kuang & Ou, 2008b; T. Nishiwaki, Koda, Yamada, Mihashi, & Kikuta, 2012; Van Tittelboom & De Belie, 2013), use of various pozzolans (X. Liu, Yao, Zheng, & Wu, 2005); Sahmaran, Keskin, Ozerkan, & Yaman, 2008; Sahmaran, Yildirim, & Erdem, 2013; Termkhajornkit, Nawa, Yamashiro, & Saito, 2009; ZH Zhou, Li, Xu, & Yu, 2011) and expanding agents (T. -H. Ahn & T. Kishi, 2010; Kishi, Ahn, Hosoda, Suzuki, & Takaoka, 2007; K. Sisomphon, Copuroglu, & Koenders, 2012, 2013) are applied to reduce problems in the autogenous self-healing mechanism. Unique

methods such as internal curing materials, bacteria and microcapsules are still in development. Costly repair of infrastructures and invisible/inaccessible damages will become a more important problem in developed countries. It will be possible to minimize these problems with materials with self-healing properties.

1.1 Aim and Scope

In this study, it is aimed to examine the self-healing properties of sodium silicate/polyurethane microcapsules produced in cement-based materials. For this aim, ultra-high performance concrete mixtures, containing blast furnace slag and steel fibers to restrict cracks. and normal mortars, containing steel fiber too, were used. The self-healing performance of these microcapsules were investigated by compressive strength test, direct tensile test, total and capillary water absorption test, crack-closing test and crack analysis experimental methods. It is planned to obtain the required healing values by comparing them with the control mixtures without microcapsules.

CHAPTER 2

LITERATURE REVIEW

2.1 Importance of Self-healing in Cementitious Composites

In many developed countries, the annual maintenance and repair cost of infrastructures is higher than a new infrastructure work (V. C. Li & Herbert, 2012). Christopher Joseph, Gardner, Jefferson, Isaacs & Lark (2010) stated that maintenance and repair costs in Great Britain account for 45% of all construction costs. Similar statistics are presented by Cailleux & Pollet (2009) for European countries.

As mentioned before, repair work in infrastructures such as bridges and tunnels with heavy traffic problems or in underground structures and tanks containing dangerous liquids is very dangerous and difficult (Freyermuth, 2001; Mihashi & Nishiwaki, 2012; Sangadji & Schlangen, 2012; Van Tittelboom & DeBelie, 2013). In addition to the direct cost, this situation brings indirect economic difficulties together with the decrease in efficiency and traffic problem (Van Tittelboom & De Belie, 2013). It is thought that the cost caused by the traffic problem is 10 times more than the cost of maintenance and repair (Freyermuth, 2001). In addition, in many cases, it is not possible to see and reach the cracks (Van Tittelboom & De Belie, 2013).

2.2 Definition of Self-Healing and Self-Healing Mechanisms

Self-healing is the ability to self-renew and/or repair damage in plants, animals, man-made materials (self-healing materials) (de Rooij, Van Tittelboom, De Belie, & Schlangen, 2013; Ghosh, 2009). Self-healing materials can recover definite damages automatically/independently or with a small external trigger (de Rooij et al., 2013; Ghosh, 2009). Self-healing strategies and approaches are used in many developed materials such as ceramics, polymers and metals, in particular cement-based materials.

In 1836, the French Academy of Sciences observed the self-healing mechanism, autogenous healing of cracks, in cracked structures such as concrete retaining structures, culverts and pipes (de Rooij et al., 2013; Van Breugel, 2007).

2.2.1 Autogenous Self-Healing Mechanism

Autogenous self-healing mechanism takes place in concrete by nature. Ter Heide (2005) demonstrated the self-healing types which occur along cracks in concrete as follows (Figure 2.1): i) Calcium hydroxide or calcium carbonate formation. ii) clogging of the crack with concrete particles or impurities from water. iii) Subsequent reaction of unreacted cement and cement-like additives. iv) Expansion of calcium-silicate-hydrate on the crack surface. While the subsequent reaction of unreacted cement particles in the early ages of the concrete is the main healing mechanism, CaCO3 formation becomes the main mechanism in later ages (Neville, 2002). Van Tittelboom & De Belie (2013) emphasized that the autogenous healing mechanism occurs effectively in narrow cracks, only in the presence of water, and it is difficult to control. For this reason, autogenous self-healing mechanism should be developed with some approaches.

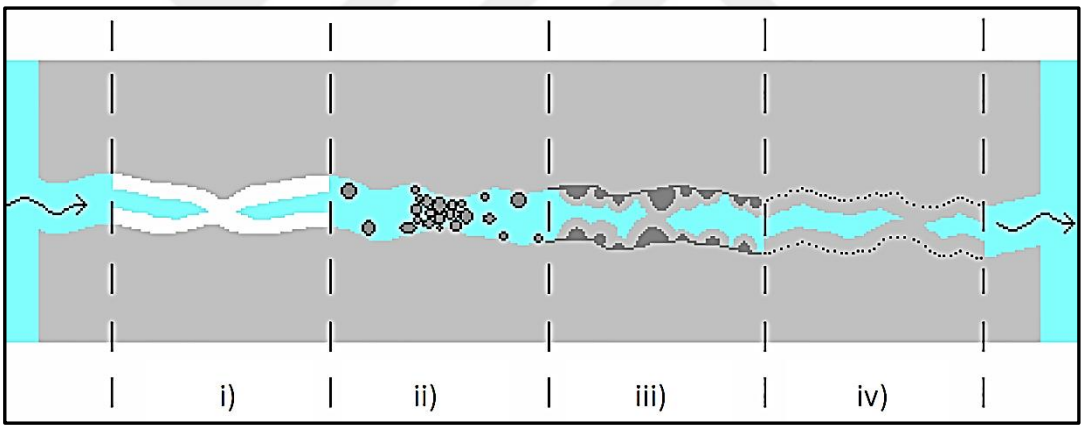

Figure 2.1 Possible mechanisms for self-healing in concrete (Ter Heide, 2005)

Soluble in water calcium hydroxide, one of the cement hydration products, is present along the crack surface. Wu, Johannesson & Geiker (2012) summarized the reaction of calcium ions in the crack with carbon dioxide as follows: “Free calcium ions formed as a result of cement hydration react with carbon dioxide dissolved in water. The self-healing crystals that form develop on the crack surface and fill the gaps.” (p. 573).

Beyond the mentioned, different mechanisms also cause autogenous self-healing depending on the environment and environmental conditions of the structure. Palin,

Wiktor & Jonkers (2015) examined the autogenous self-healing capacities of mortar samples prepared in freshwater and seawater environments. In their study, mortar samples prepared with traditional portland cement have the maximum self-healing capacity in the seawater environment. This is due to the magnesium, calcium and carbonate ions found in sea water.

The efficiency of autogenous self-healing mechanism can be increased by restriction of the crack width. It means, the narrower cracks are tend to be closed by the autogenous self-healing mechanism (Van Tittelboom & De Belie, 2013). Different fibers usage is greatly contributing to the autogenous self-healing by restricting the crack width (Kunieda, Choonghyun, Ueda, & Nakamura, 2012). Fiber reinforced cementitious composite (FRCC) can be mentioned as a self-healing material (Beglarigale, 2018).

Synthetic fiber ECC has been used in self-healing investigations. (Hung, Su, & Hung, 2017; M. Li & Li, 2011; VC Li et al., 1998; HZ Liu, Zhang, Gu, Su, & Li, 2017a; HZ Liu et al., 2017b; Qian, Zhou, & Schlangen, 2010; Sahmaran et al., 2007; Sahmaran & Li, 2009; Siad, Lachemi, Sahmaran, & Hossain, 2017; YZ Yang et al., 2009). Also, the effectiveness of self-healing was also investigated in cementitious composites with various steel fiber (Homma, Mihashi, & Nishiwaki, 2009; Kim, Kang, & Ahn, 2014; T. Nishiwaki, Kwon, Homma, Yamada, & Mihashi, 2014). Kim et al. (2014) investigated the self-healing capacity of crack in high performance steel fibered cement based composites in terms of improvement of mechanical properties. In the study, multiple microcracks were formed by applying 0.3% unit deformation under tensile stress to all 90-day prestressed specimens. It was observed that the first crack stress in the preloaded samples, which was applied tensile stress again after 3, 7 and 14 days, improved by 36% after 14 days of water curing (Kim et al., 2014). In other cracks, a healing rate of 100% was achieved.

Pozzolans as fly ash (FA) and granulated blast furnace slag (GBFS) are frequently used in cement-based composites and provide many advantages. Hydration of pozzolans at later ages supports the development of autogenous self-healing (Van Tittelboom & De Belie, 2013). Sahmaran et al. (2008) investigated the self-healing behaviour in self-compacting concrete mixtures. In the prepared mixtures, low-lime

FA was used at 0%, 35% and 55% replacement rates. The samples were subjected to water curing for 30 days after being preloaded to 70% and 90% of their maximum compressive strength. Sahmaran et al. (2008) self-healing behavior of preloaded samples was determined by the changes in parameters before and after 15 and 30 days water curing (self-healing process) (compared to the same-aged witness samples). In the test results, 27% compressive strength loss was determined in the samples subjected to 90% preload. The loss in compressive strength decreased to 7% after the 30-day self-healing period. In the mixtures without FA replacement, the loss in compressive strength before and after the self-healing process is 19% and 13%, respectively.

2.2.2 Bacteria-based Self-Healing Mechanism

The idea of using bacterial spores in concrete as a healing agent and accumulation of CaCO3 was first discussed by Ramachandran, Ramakrishnan, & Bang (2001). Jonkers (2007), on the other hand, summarized the bacteria-based self-healing mechanism as follows: "Bacteria on the surface of the fresh crack formed will start to multiply activated by the penetration of water and minerals such as calcite (CaCO3) will accumulate. In this way, the crack will be repaired and the reinforcements will be protected from chemical attacks in the long run." This approach is a topic of interest to many researchers around the world. The encapsulation of bacterial spores and bacterial nutrients continues today thanks to the developed unique test methods and materials (Bhaskar, Hossain, Lachemi, Wolfaardt, & Kroukamp, 2017; Sangadji, Wiktor, Jonkers, & Schlangen, 2017; J. Wang, Jonkers, Boon, & De Belie, 2017; JY Wang, Snoeck, Van Vlierberghe, Verstraete, & De Belie, 2014; JY Wang, Soens, Verstraete, & De Belie, 2014; Wiktor & Jonkers, 2011; Xu & Yao, 2014).

2.2.3 Microcapsule-based Self-Healing Mechanism

Conservation of the curing agent for the capsule is one of the most promising methods of self-healing. Thanks to the advantages of microencapsulation, it attracts more attention compared to other encapsulation methods. First, White et al. (2001) proposed the microcapsule-based self-healing method for polymer composites.

Microencapsulation is the process of covering various materials with a protective membrane called a shell or wall. As seen in Figure 2.2, a microcapsule consists of core/inner material and wall/cladding material. The core material can be solid, liquid or even gaseous. Jia et al. (2016) summarized the function of a microcapsule as follows: “Theoretically, microcapsules not only isolate a large amount of active inner material from the external environment and store it for a long time, but also keep the process stable by releasing the inner material in a controlled manner in the target area with an external stimulus.” (p. 221-222).

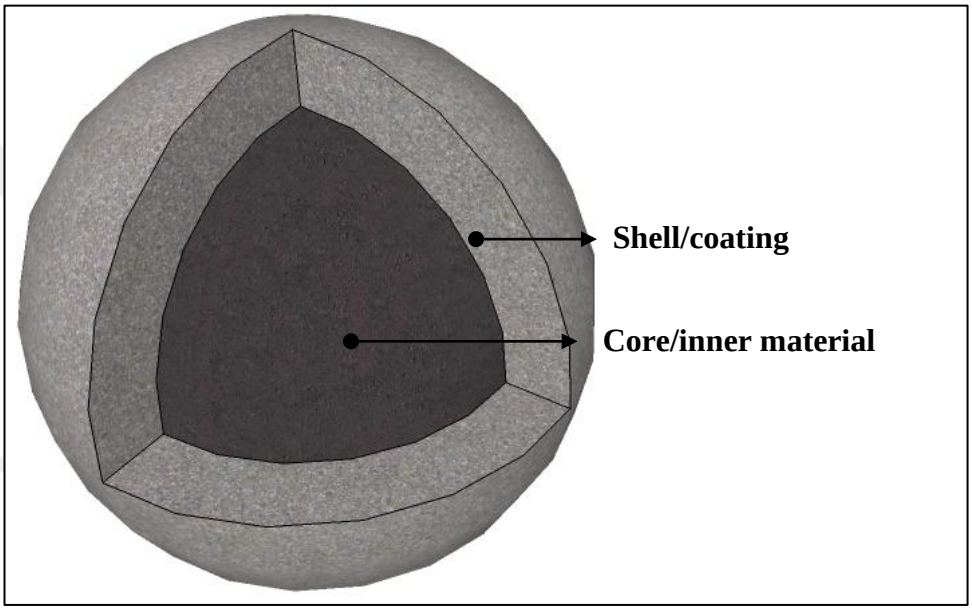

Figure 2.2 Schematic representation of the microcapsule (Beglarigale, 2018)

In addition to polymer composites, the microcapsule-based self-healing approach is quite new in cement-based composites. Prior to 2011, only a few studies have addressed the microcapsule-based self-healing method in cement-based composites (Xing et al., 2008; Z. X. Yang, Holler, He, & Shi, 2010). Due to the completely different natural structure of cement-based materials, microcapsules used in polymer composites may not be able to form an effective self-healing mechanism when used in cement-based composites. Z. X. Yang, Hollar, He & Shi (2011) encapsulated methylmethacrylate and triethylborane as curing agents and catalysts and investigated the self-assembly process at the crack interface. The wall of these microcapsules is a silica-based material formed as a result of the sol-gel reaction. Z. X. Yang et al. (2011)

summarized their suggestive methods as follows: “The self-healing for uncured mortar is triggered by the crack formed along the microcapsule. Afterwards, the curing agent and catalyst were released into the environment by breaking depending on the cracking strength of the microcapsule”.

Z. X. Yang et al. (2011) clearly obtained self-healing ratios in the preloaded samples they used in their studies. He also added that microcapsules containing silica-based wall material form a strong bond with the cement matrix. The wall establishes a chemical and physical bond with the matrix, ensuring that the microcapsule remains stable for years without being damaged. This means that the adhesion between the wall and the matrix must be quite high. If the wall-matrix bond strength is low, the crack will form at the capsule-matrix interface without breaking the microcapsule (S. Zhou et al., 2014). In another study, Perez, Erkizia, et al. (2015) synthesized silica wall-based microcapsules and investigated the mechanism of self-healing in cement-based composites (Figure 2.3). The researchers encapsulated the Epothin® (epoxy component) material as a curing agent with a sol-gel reaction. Z. X. Yang et al. (2011) Similar to the hypothesis, Perez, Erkizia, et al. (2015) include the following finding in their work: “A good bond is formed between the capsule wall and the matrix, and the silica capsules maintain their stability by reacting with a high proportion of lime.” (p. 47). The effectiveness of the produced microcapsules has been investigated in many different studies (Calvo et al., 2017; Perez, Gaitero, Erkizia, Jimenez, & Guerrero, 2015). Calvo et al. (2017) reported that although silica/epoxy microcapsules integrate well with the cement matrix, they may cause a decrease in the mechanical performance of cement-based composites.

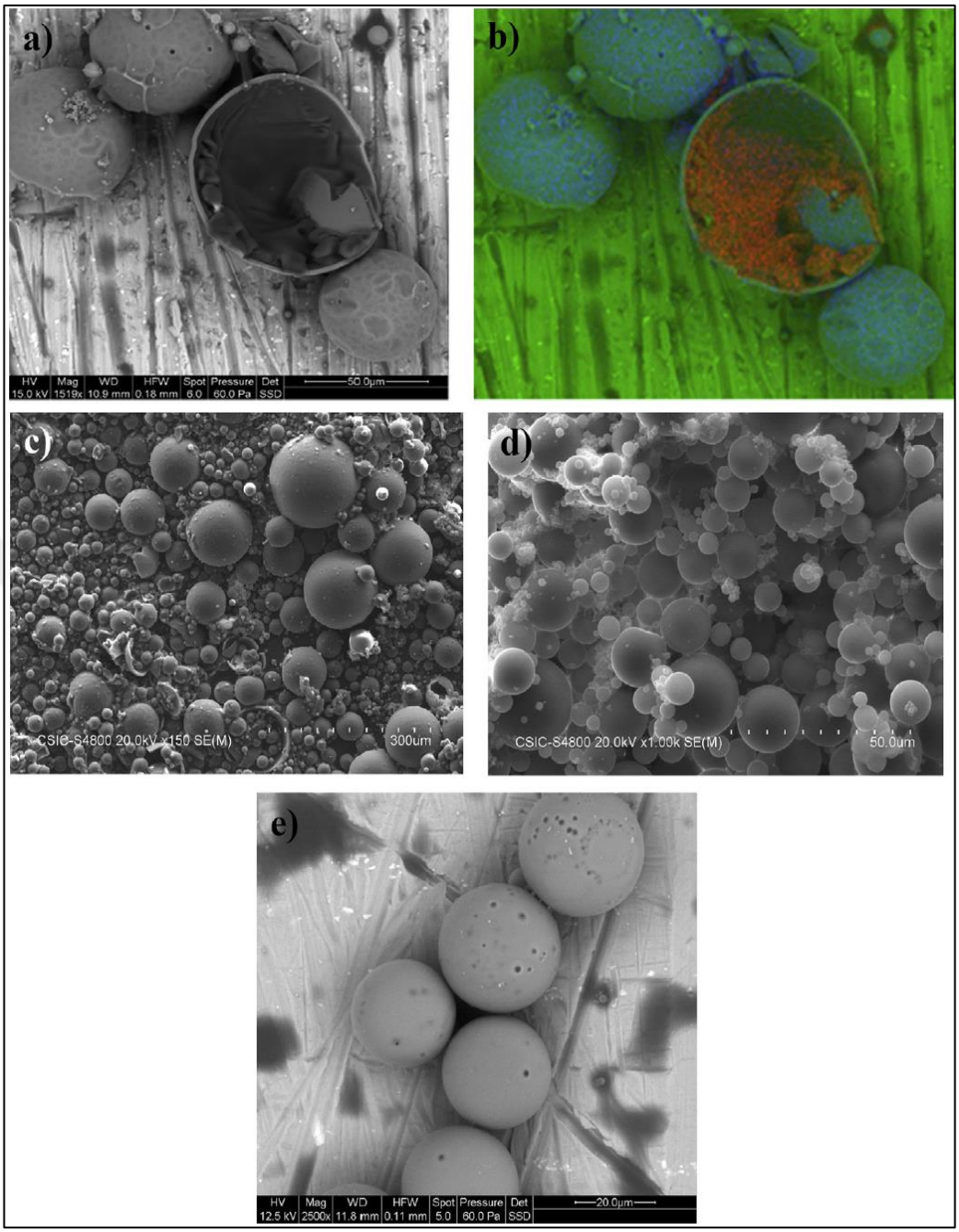

Figure 2.3 SEM images of silica/epoxy microcapsules. a) broken microcapsule, b) elemental analysis (Si= blue, C= red, Al= green), c, d and e) images of microcapsules of different sizes (Perez, Erkizia, et al., 2015)

Dicyclopentadiene, which is used as a healing agent in cement-based materials, is also encapsulated with phenol-formaldehyde resin Lv et al. (2016). The stability properties of the produced capsules were investigated in artificial concrete pore water

and cement paste. In the test results, microcapsules show high stability in artificial concrete pore water as well as in real cement environment (Lv et al., 2016).

All the conditioning agents mentioned so far react with a second component (microencapsulated) to the cement matrix. In bi-component agents, the ratio of the first component and the second component is often uncontrollable. Especially in epoxy resins, this ratio is important to complete the polymerization. For this reason, single-component healing agents are more suitable for use as there is no need for a second component.

$Ca(OH)_2$, one of the product of hydrated cement, can react with SiO_2 came from pozzolanic materials such as fly ash (Sahmaran et al., 2008; Termkhajornkit et al., 2009; Z. H. Zhou et al., 2011) and ground-granulated blast-furnace slag (Sahmaran et al., 2013; Z. H. Zhou et al., 2011). In studies conducted in the past years, silica-based microcapsules have been used as SiO_2 source within the scope of cement-based composites (Giannaros, Kanellopoulos, & Al-Tabbaa, 2016; Kanellopoulos, Giannaros, & Al-Tabbaa, 2016; Kanellopoulos, Giannaros, Palmer, Kerr, & Al-Tabbaa, 2017; Pelletier, Brown, Shukla, & Bose, 2011; Tan, Keung, Choi, Lam, & Leung, 2016). Pelletier et al. (2011) presented the idea of microencapsulation of aqueous sodium silicate solution (SS) by interfacial polymerization with polyurethane. Colloidal silica has also been used as a curing agent and SO_2 source in similar microcapsules (Tan et al., 2016). There are also studies in the literature in which the SS solution is microencapsulated with gelatin/gum arabic and the coacervation technique is used (Kanellopoulos et al. ,2017). The self-healing mechanism of these microcapsules is based on the cracking of the microcapsule wall along the crack formed in the cement matrix and the reaction of SS or colloidal silica with $Ca(OH)_2$. As a result of the reaction, a secondary calcium-silicate-hydrate gel is formed.

Gilford et al. (2014) tried to microencapsulate aqueous sodium silicate solution (SS) with urea-formaldehyde wall. During the encapsulation of SS as a curing agent, they used in-situ polymerization proposed by Brown, Kessler, Sottos, & White (2003) and adapted to their own work. Brown, Kessler, Sottos & White (2003) microencapsulated dicyclopentadiene monomer (DCPD) with poly(urea-formaldehyde) in their study where they proposed the polymerization method.

CHAPTER 3

MATERIALS AND METHODS

3.1 Cement Based Mixtures

Two different cement-based mixtures which are ultra-high performance concrete (UHPC) and normal mortar (NM) are worked in the scope of thesis studies. UHPC mixture has high amount of binder material because of low w/c ratio and containing ground granulated blast furnace slag. When the self-healing behaviour of this mixture is handled, the autogenous mechanism is dominant due to high amount of binder especially in 90 days cured specimens. It is originated from late reactivity of pozzolanas (Beglarigale, 2018). Aim of choosing mortar mixture is to minimize other self-healing mechanism and observe microcapsule activity on self-healing behaviour in cement-based composites.

3.1.1 Materials

3.1.1.1 Cement and Ground Granulated Blast Furnace Slag

The properties of CEM I 42.5 R Portland cement given in Table 3.1 is purchased from Denizli Cement. A ground granulated blast furnace slag (GGBFS) is supplied from İskenderun iron and steel factory in Turkey. The properties of GGBFS is represented in Table 3.2.

Table 3.1 Properties of cement

Chemical Composition (%)		**Physical Properties**	
SiO_2	19,1	Space surface (Blaine) (m^2/kg)	369
Al_2O_3	4,40	Initial setting time (min)	110
Fe_2O_3	3,96	Final setting time (min)	166
CaO	61,85	Volume Expansion (mm)	1,00
MgO	2,05		
Na_2O	0,27		
K_2O	0,7	**Compressive Strength**	
SO_3	3,72	2 days (MPa)	27,1
Cl^-	0,0004	7 days (MPa)	43,3
Loss on Ignition	1,82	28 days (MPa)	56,0

Table 3.2 Properties of GGBFS

Chemical Composition (%) of GGBFS	
SiO_2	39,95
Al_2O_3	11,46
Fe_2O_3	0,54
CaO	34,07
MgO	6,45
Na_2O	0,3
K_2O	1,02
SO_3	0,55
Cl^-	0,0246
Free CaO	0,13
Loss on Ignition	2,95

3.1.1.2 Aggregates

For UHPC mixture, three different size 0-0.4, 0.5-1, 1-3 mm quartz aggregate were used. The specific gravity of aggregate is 2.66 and water absorption is 0.1.

In mortar mixture, crushed limestone sized 0-5 mm is used. Aggregate specific gravity was 2.55 and the water absorption is 1.63.

3.1.1.3 Steel Fibers

Same straight brass-coated steel fiber (6 mm and 13 mm in length) were used for two cement-based mixtures. However, specimens prepared for direct tensile strength test had 13 mm length steel fiber was used due to test procedure. Other specimens were prepared with 6 mm steel fiber. Properties of steel fibers taken from manufacturer were given in Table 3.3.

Table 3.3 Properties of steel fibers

Length (mm)	**Diameter (mm)**	**Aspect ratio (L/d)**	**Tensile strength (MPa)**
6	0.16	37.5	2000
13	0.2	65	2750

3.1.1.4 Chemical Admixture

Polycarboxylic ether-based superplasticizer (MasterGlenium® ACE 450) was used to develop consistency properties. The superplasticizer (SP) is supplied from BASF and properties were presented in Table.3.4

Table 3.4 Properties of superplasticizer

Properties	**Comments**
Structure of material	Polycarboxylic ether based
Form	Liquid
Color	Amber
pH value	5 - 7 (20 ºC)
Density	1.069 – 1.109 kg/lt (20 ºC)
Solubility in water	Miscible

3.1.2 Design of Mixtures

Normal mortar mixture and UHPC mixture designs are given in Table 3.5. Called NM was used as control normal mortar mixture without microcapsules. In NM_M mixture, Microcapsules have been used up to 5% by mass of the cement amount. By keeping the water, cement and micro-fiber dosage constant, the volume required for the microcapsules was deducted from the amount of aggregate. The specific gravity of the microcapsules was assumed to be 1.00 g/ cm^3. This assumption is based on the specific gravity of the raw materials and the high stability of the water-microcapsule mixture. Kanellopoulos et al. (2016) also used SS microcapsules with a density of ~ 0.98 g / cm^3 in their study.

YM_M from UHPC mixture that ground granulated furnace slag is substituted 50% of cement by weight and bearing 5% microcapsule of cement amount by weight. UHPC mixture which has not any microcapsules YM's test results were completed during TÜBİTAK (2020) project studies and presented in Phd Thesis of Ahsonallah Beglarigale (2018) and Beglarigale et al. (2021) studies. For experimental studies in this thesis, YM mixture test results were used as Control results to compare YM_M mixture bearing microcapsule and contribution of microcapsules to self-healing behavior was investigated.

Table 3.5 Designs of mixtures (kg/m^3)

Mixture (kg/m^3)	**w/c**	**Water**	**Cement**	**Micro-capsule**	**Fiber**	**Aggregate 0-5**	**SP**
NM	0.5	250	500	-	143	1372	1
NM_M	0.5	250	500	25	143	1309	2.5

Table 3.5 continuous

Mixture (kg/ m^3)	w/b	Water	Cement	GGBFS	Microcapsule	Fiber	Quartz Aggregate			SP
							0-0.4	0.5-1	1-3	
YM	0.22	264	800	400	-	143	189	265	303	11
YM_M	0.22	264	800	400	40	143	165	230	264	17

3.1.3 Test Methods

3.1.3.1 Mixtures and Mixing Procedure

While preparing the NM mixture, firstly the dry materials were mixed by using mortar mixer. Then water and super plasticizer were added to the mixture. In the NM_M mixture, dry materials except microcapsules were mixed in the mortar mixer to avoid harm microcapsules. The microcapsules were taken into a beaker, mixed in 90% of the design water using magnetic stirrer for 10 minutes. Then superplasticizer was added and mixed with magnetic stirrer continued for 5 minutes. It was observed that the microcapsules dispersed better in the design water when the super plasticizer was added. Also they dispersed in water because of their small size and similar specific gravity to water. This application (mixing microcapsules with design water previously) is made to keep the microcapsules hydrated and prevent agglomeration in mixtures. In addition, this application can be effective in dispersing microcapsules homogeneously in the cement- based matrix.

Normal mortar mixes were obtained by adding the microcapsules dispersed in the design water and the remaining design water to the dry mixture. Both of two mixtures mixed normal speed during 1 minute and then high rate speed during 4 minutes.

After mixing process, NM and NM_M mixture mini-flow table test value was 200 ±10 mm. It was also the criteria to indicate superplasticizer amount that was used (Figure 3.1). It should be noted that in the mini-flow experiment, the mixtures were placed conical mold which is made of brass has dimensions of 100 mm base dia. x 70 mm gun dia. X 50mm height.

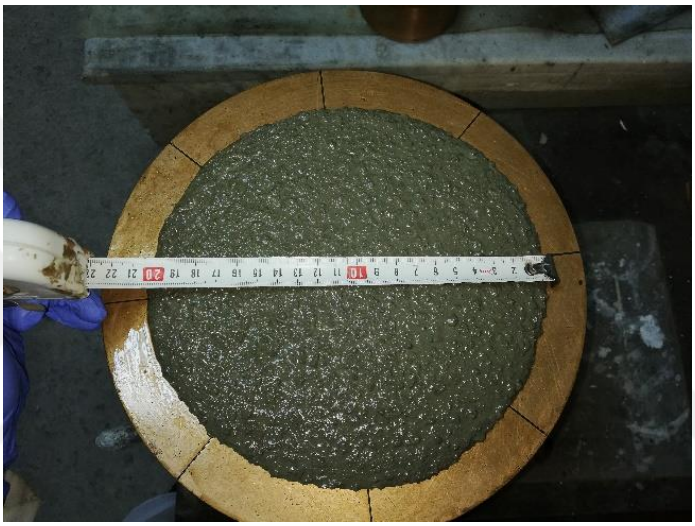

Figure 3.1 Flow table test result of NH (Personal archive, 2019)

For YM mixture, firstly the dry materials were mixed for five minutes. Then, half of the design water was added to the dry mix. The remaining design water was mixed with the required superplasticizer and added to the mixer. After 5 minutes of mixing at normal speed, mixing was continued for 15 minutes at high rate speed. The workability of each mixture was checked by a mini-flow table test. The required amount of superplasticizer was determined to be 260 ± 10 mm of diameter.

3.1.3.2 Compressive Strength Test

For the compressive strength test, mixtures of normal mortar and UHPC mixtures were poured into 50x50x50 mm cube molds. Compressive strength was determined at

different ages in the cube samples prepared with all mixtures with/without microcapsule.

18 cubic samples were prepared for each mixture in the determination of self-healing capacities by compressive strength test (Figure 3.2). After 7 and 90 days of water cure, 18 samples that prepared for each 7 and 90-day samples, were removed from the water and kept in the laboratory for one day. Firstly, the average compressive strength was determined by applied compressive strength tests over 7 of the 18 samples prepared. To create damage, compressive loading of 90% of the average compressive strength was applied on 8 samples. Compressive strength test was performed on these preloaded 8 samples in order to determine the damage rate (decrease in compressive strength). However, the results of the experiments conducted showed that there was no decrease (Beglarigale, 2018). For this reason, the experiment was repeated by producing new samples. After the average compressive strength of the first 7 samples was determined, 100% of the average compressive strength was applied on 8 samples. When the loading reaches 100% of the average strength, the loading was stopped immediately in order to prevent the samples from being crushed. To determine the damage rate caused by the 100% loading, the compressive strength test was carried out on 4 of the preloaded 8 samples. The remaining 4 samples from the preloaded 8 samples were subjected to 30 days of water cure (self-healing process). The remaining 3 samples from the 18 samples were left to water cure for 30 days as witness samples without any experimentation and damage. After 30 days of water curing, damaged and witness samples were subjected to compressive strength test, and the self-healing (recovery in strength) rates were determined.

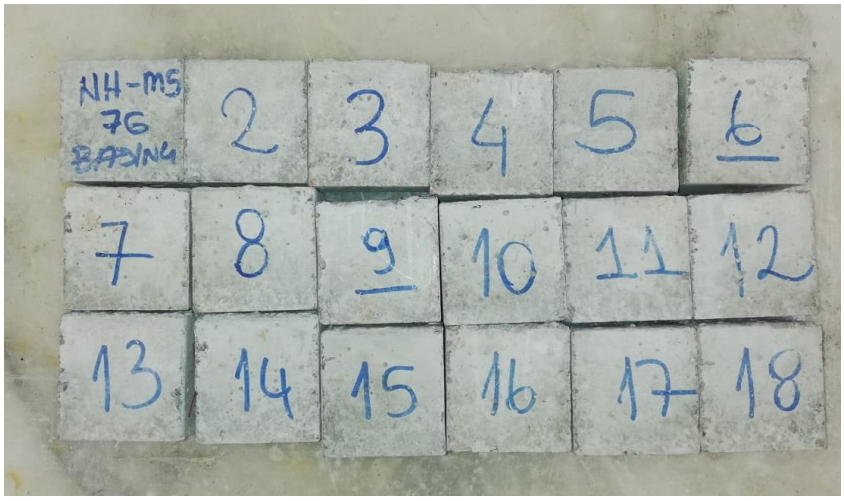

Figure 3.2 Samples for compressive strength test (Personal archive, 2019)

3.1.3.3 Direct Tensile Test

The direct tensile test is one of the test methods applied to Normal mortar and UHPC mixture samples and used to determine the KKI capability (recovery in tensile strength). The experiment was carried out on specially designed bone-shaped specimens with a gauge length of 80 mm (Beglarigale, 2018, 2019). Details of bone-shaped samples and special design molds are shown in Figure 3.3

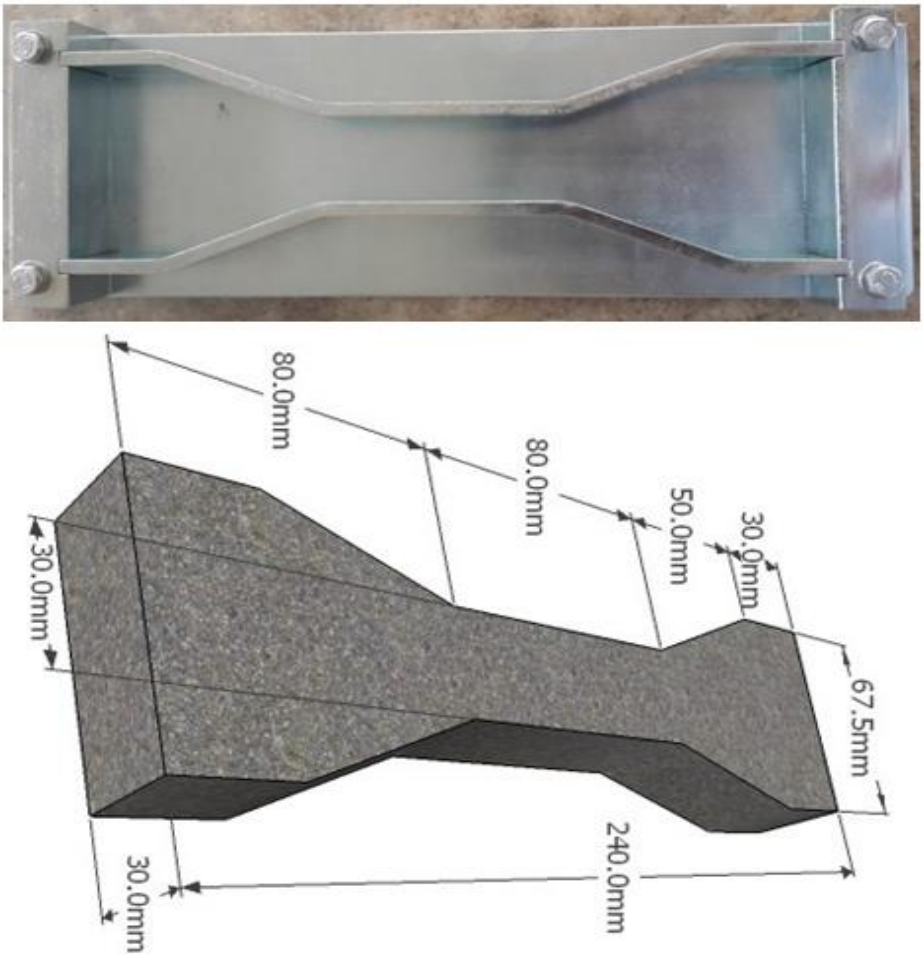

Figure 3.3 Details of bone-shaped sample and mold (Beglarigale, 2018)

In this test, samples were prepared with 13 mm micro-fibre instead of 6 mm micro-fibre that was used in other tests. The reason is that 6 mm micro-fibres were pull off quickly due to their short adherence length and causes sudden drop in tensile stress-strain diagram. This situation prevented damage rate properly.

For all mixtures, 12 bone shaped sample prepared and exposed water cure during 7 and 90 days. After that, the tensile strength test applied on 3 samples to obtain average tensile strength. 6 bone shaped samples were loaded until a decrease in loading was observed regardless of the crack control and the test was stopped when the decrease was observed (Figure 3.4). Together with the preloaded (damaged) samples obtained and 3 witness samples which were not conducted any loading were subjected to the direct tensile test after 30 days of recovery process and the self-healing ratios were determined.

Figure 3.4 Tensile loading of bone-shaped samples (Personal archive, 2019)

3.1.3.4 Total and Capillary Water Absorption Test

In total water absorption (TWA) and capillary water absorption (CWA) test, 18 cubic samples of 50x50x50 mm were prepared. After 7 and 90 days of standard water curing, at least 16 samples were removed from the water saturated with lime and dried under laboratory conditions for one day. 7 samples were used to determine the average compressive strength of the mixture. 8 samples were preloaded, corresponding to ~ 100% of their compressive strength. The loading is stopped when the desired preload value was reached in order not to cause further damage. Subsequently, all samples were kept in water for at least 24 hours and their dry surface saturated weights were measured. It was then dried in an oven at 50^{o}C for three days. Although the weight of the cement-based materials is usually taken after drying in the 105^{o}C oven for 24 hours, this effect has been minimized by drying at 50^{o}C for a longer time as the high temperature will affect the hydration of the unreacted cement and pozzolana particles in the sample. After the oven-dry weights of the samples were measured, they were subjected to the CWA test from the preloaded surfaces (Figure 3.5). In the samples, weight gain due to capillary water absorption was determined by measurements at 30, 60, 90, 120, 150, 180, 240, 300 and 360 minutes. After the CWA test, all samples were

put into water again and following 30-day recovery period, all samples, including the witnesses, were examined by TWA and CWA tests.

Figure 3.5 CWA test of preloaded samples (Personal archive, 2019)

3.1.3.5 Crack-closing Test

Four disc-shaped samples were prepared with mixtures of UHPC and normal mortar included with steel micro-fibre. Plastic molds in the form of discs with a diameter of 30 mm and a height of approximately 10 mm were used. After 7 and 90 days of water curing, the samples were subjected to tensile splitting test and a crack was formed (Figure 3.6-a). Crack width is adjusted by following a digital microscope (Figure 3.6-b). In the middle of the sample, a line was drawn perpendicular to the load and when the crack width reached 100 μm ± 10 on the line, the loading was stopped (Figure 3.6-c). The crack surface areas were determined by drawing at least five points along the crack with a red marker to be read throughout the test procedure. Readings were made with a digital microscope at the determined points. The surface area of the cracks was measured at five marked locations on the surface by using digital microscope software. Immediately after the measurements, samples were subjected to water curing (self-healing process) for 30 days.

The self-healing capacity of each mixture was determined by calculating the crack closure rate at each position of the four samples (20 positions) by the following equation:

$$\boldsymbol{H = \frac{a-b}{a} \times 100} \qquad (3.1)$$

Here, H= crack closure rate (self-healing ratio-%), a=original crack surface area and b=crack surface area after self-healing process

Figure 3.6 a) Loading of disc-shape samples, b) measurement of crack width by OM, c) crack formation (Personal archive, 2019)

3.1.3.6 Crack Analysis

As part of the crack analysis, a low viscosity epoxy (EpoFix Resin) that can penetrate the cracks under vacuum was provided. In addition, fluorescent dye (EpoDye) was used to make the cracks become apparent during image analysis. Cylindrical small samples were produced to ensure that the epoxy penetrated all the cracks of the damaged samples. In addition, small samples were thought to be advantageous due to the high cost of the epoxy and paint. In this context, 8 pieces of 30 × Ø30 mm cylinder samples were prepared for each mixture. After 7 and 90 days of water curing, 4 samples were subjected to compressive strength tests and the maximum strength of the samples were determined (Figure 3.7). The other four samples were loaded up to ~ 100% of the maximum strength to prevent further damage to the samples Half of the damaged samples (two) were dried at 40 ° C for three days after loading and then subjected to epoxy impregnation under vacuum. The other half (two) of the samples were subjected to 30 days of water curing (self-healing process). Then they were dried and impregnated epoxy. In addition, one of the samples used to determine the maximum strength of the mixtures was used before self-healing and one was used for crack analysis after self-healing.

Figure 3.7 Compressive strength test of cylindrical samples (Personal archive, 2019)

A strong vacuum assembly and epoxy soak chamber were designed for the experiment. (Figure 3.8). As seen in Figure 3.9-a, the samples were placed in a cylindrical mold and vacuumed in the vacuum chamber for at least two hours. In this way, all cracks were vacuumed. During vacuum, the epoxy is directed to the molds in

the chamber (Figure 3.9-b). After the epoxy has covered samples, the air valve is opened slowly, allowing the air to enter the chamber and thus the epoxy to penetrate the cracks.

Figure 3.8 Vacuum assembly and epoxy soak chamber (Tubitak, 2020)

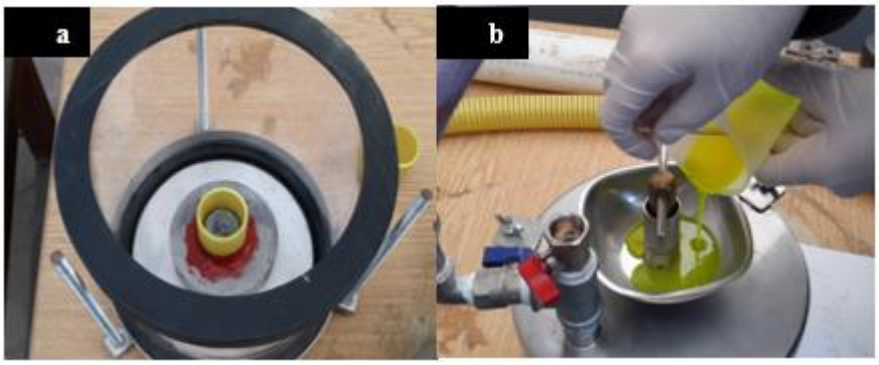

Figure 3.9 a) Placement of samples in chamber, b) epoxy soaking of sample in the chamber (Tubitak, 2020)

The samples were removed from the mold after 24 hours of epoxy stiffing time. Then, the samples were divided in the middle with a precision concrete cutting machine and the divided samples' inner surfaces were polished. Image analysis (ImageJ program) was performed on the samples under ultraviolet (UV) light source (Figure 3.10). Matrix-crack contrast was well observed using fluorescent dyed epoxy and image analysis was carried out.

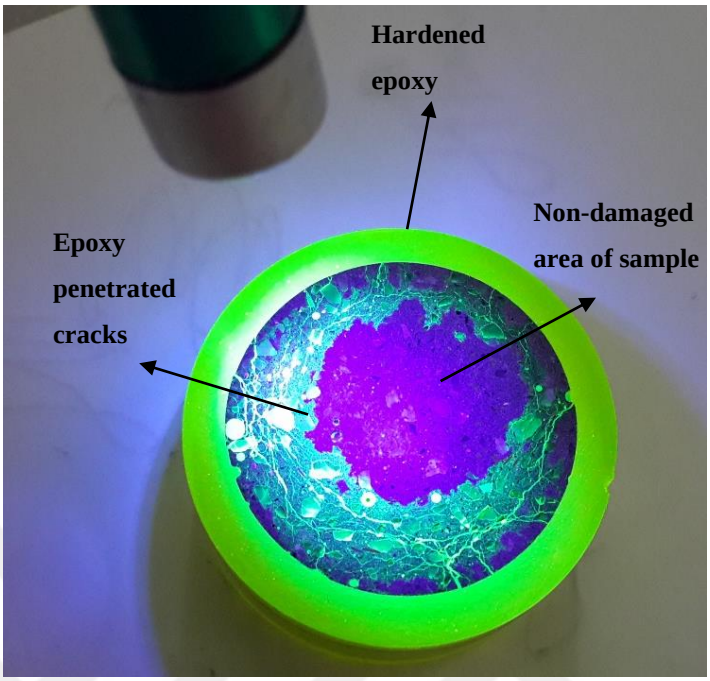

Figure 3.10 Divided sample surface under UV light (Tubitak, 2020)

3.2. Microencapsulation

In this section, the materials and methods used in the microencapsulation of sodium silicate, which is healing agents, are discussed.

Pelletier et al. (2011) produced polyurethane microcapsules containing aqueous sodium silicate (SS) with the method proposed by Saihi, Vroman, Giraud, and Bourbigot (2006) for the microencapsulation of di-ammonium hydrogen phosphate. In the study, the SS solution was emulsified using toluene, insoluble in water, using two different surfactants. After dispersion of SS in the organic phase (toluene), the wall-building monomer, methylene diphenyl diisocyanate (MDI), was added to initiate an interfacial reaction of MDI and water on the surface of the SS solution droplets (Saihi et al., 2006). Similar interface polymerization method Tan et al. (2016) used in the microencapsulation of colloidal silica.

3.2.1 Materials

In microencapsulation, sodium silicate solution (SS) (Na_2O, ~ 10.6% and SiO_2, ~ 26.5%) supplied from Sigma-Aldrich was used as core material together with deionized water. The monomer 4,4'-Methylenebisphenyl isocyanate (98%) (MDI) forming the wall, Span85 (Sorbitantriolcat) and poly(ethylene glycol) diolcat (POEDO) used as surfactant were also supplied from Sigma-Aldrich. Additionally, dibutyltin dilaurate (95%, Sigma-Aldrich) was used as a catalyst. Emulsification of sodium silicate was carried out in organic phase Toluene (Sigma-Aldrich).

3.2.2 Microencapsulation Method

The synthesis of microcapsules was carried out in a 100 ml beaker with a 30 mm long cylindrical stirring bar on a magnetic stirrer. As previously mentioned, microcapsules were described by Saihi et al. (2016) by the in-situ interface polymerization method. However, in this study, some necessary changes were made as a result of preliminary trials. This method consists of two main steps: 1) Dispersion of the aqueous SS solution in the organic phase (water-in-oil emulsion), 2) Addition of the monomer forming the wall to the emulsion. Material ratios and mixing parameters were determined as a result of many trials. The three solutions required in the synthesis process were prepared as follows: 1) Surfactant solution in 45 ml of toluene: S1 solution formed by adding 2 g Span85 and 1 g POEDO, 2) S2 solution in which MDI and a few drops of catalyst are added to a mixture of 12.5 ml toluene and 7.5 ml S1, 3) S3 solution formed with 7.5 g SS and 7.5 g deionized water. It should be noted at this point that various SS/water ratios were analysed as core material. further, morphological optimization tests were carried out using different types of magnetic stirring bars in a 250 ml beaker (two layers of material).

During the microencapsulation process, S3 was emulsified in S1 solution at 1000 rpm for 20 minutes. After the aqueous SS microdroplets dispersed and stabilized in the organic phase, the S2 solution was added to the emulsion. In the study, different amounts of MDI were used to examine the effects of diisocyanate monomer on the microcapsule, based on the results of trials. For primary membrane formation, the mixture was stirred at 900 rpm for 20 minutes at room temperature (Saihi et al., 2006).

Then, while the stirring speed was reduced to 800 rpm, the temperature was gradually increased to 63 °C. Stirring was continued for 4 hours at 800 rpm and 63 °C to thicken the membrane. After vacuum filtration in a Buhner funnel, the microcapsules were washed with toluene and surfactant to remove MDI residues and with ethanol-water mixture to remove unencapsulated SS residues. The microcapsules were allowed to dry for 48 hours at room temperature and weighed for yield calculations. Figure 3.11 shows the microencapsulation process of SS with polyurethane. Polyurethane formation occurs as a result of the reaction of the hydrophobic ends of the surfactants and the MDI monomer.

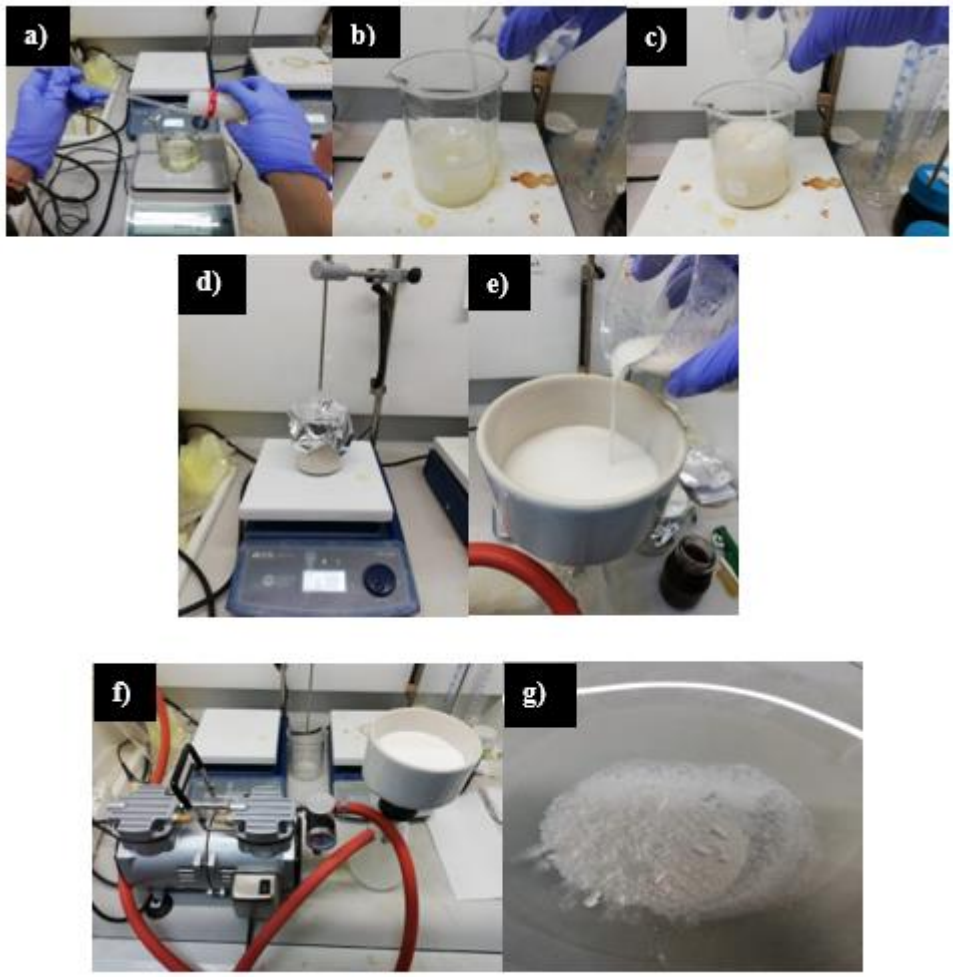

Figure 3.11 Process of microencapsulation of sodium silicate with polyurethane wall: a) adding surfactants to oil phase, b) adding SS solution to oil phase for emulsification, c) adding wall-building solution to emulsion, d) polymerization process at 63 °C for 4 h, e, f) vacuum filtration and washing of microcapsules, g) microcapsules on the watch glass after drying process (Personal archive, 2019)

With the microcapsule production procedure described in this section, sodium silicate-polyurethane microcapsules with an average diameter of 50-60μm and a wall thickness of 3-4 μm were produced.

Many optimization studies were carried out within the scope of Tubitak, 2019 study until the final recipe was found during the microcapsule production phase. Optimization of the microcapsule is a very important process to effect self-healing performance. For example, the too small size of the microcapsules causes the microcapsules to not have enough healing agents. While homogeneous size distribution is observed in small microcapsules, a homogeneous size distribution cannot be observed in the procedure in which large-sized microcapsules are obtained. Considering the wall thickness, a very thin wall thickness will not sufficiently protect the self-healing agent, while a very thick wall thickness causes the crack to progress at the microcapsule-cement matrix interface instead of breaking the wall of the crack and revealing the healing agent. Obtaining efficient microcapsules from all materials is another criterion in optimization studies.

CHAPTER 4

MICROCAPSULES EFFECT ON SELF-HEALING

The self-healing efficiency of Sodium silicate / polyurethane microcapsules produced in normal mortar and UHPC mixtures was investigated by compressive strength test, direct tensile test, total water absorption test, capillary water absorption test, crack closure and crack analysis. The procedure for these tests is described in detail in section 3.1.3.

4.1 Examination of Microcapsule Based Self-Healing in UHPC Mixtures

Microcapsules have been used up to 5% by mass of the cement amount (40 kg / m3). The design of microencapsulated UHPC mixtures is presented in Table 3.5. Water, cement, GGBFS, micro fiber dosage was kept constant. The volume required for microcapsules is provided by deducting from the amount of aggregate. The specific gravity of the microcapsules is considered to be 1.00. This assumption is based on the high stability of the water-microcapsule mixture. As expected, the use of microcapsules increased the need for SP in the YM mixture (Table 3.5). As mentioned previously, the required amount of superplasticizer was determined to achieve a free flow diameter of 260 ± 10 mm.

4.1.1 Examination of Microcapsule Based Self-Healing Mechanism by Compressive Strength Test

Compressive strength test was carried out with the test method detailed under the topic 3.1.3.2. Considering the results of the experiment (Figure 4.1), it is seen that the compressive strength of 7-day-old samples decreased by about 28% in microencapsulated samples. This may be due to the microcapsules being substituted for the inert material and quartz aggregate, which will not cause hydration and not affect the self-healing mechanism. As stated before, microcapsules with a specific weight of ~ 1 have been substituted for aggregate by volume, up to 5% by weight of the cement amount. This situation causes the microcapsules in the cement matrix to act as a void and negatively affect the strength. As it is known, the average size of the

microcapsules used in the mixtures is ~ 60μm. This causes the microcapsules to behave like entrained air void. The fact that the voids of 50-60 μm in concrete technology are large and it explains the decrease in strength. This difference in compressive strength does not create a problem in comparison, because the ratio of self-healing is calculated for each sample group. This decrease in compressive strength is around 34% in 90-day samples (Figure 4.2). It is thought that, decrease in compressive strength can be reduced with some precautions like reduction of water / binder ratio and microcapsule diameter, etc.

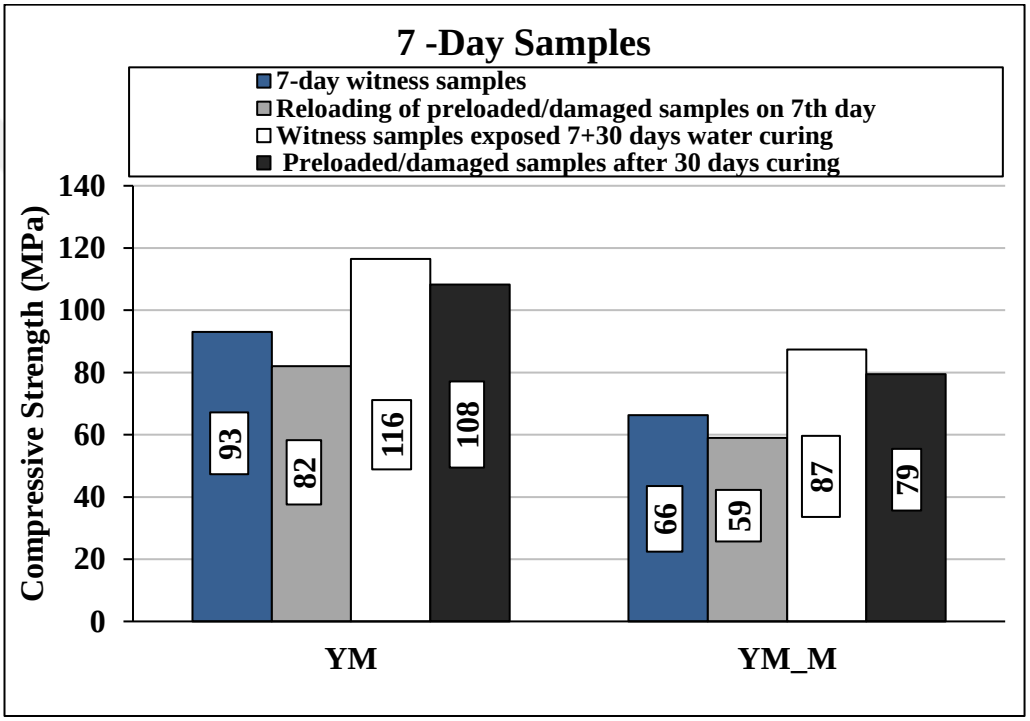

Figure 4.1 Compressive strength results of 7-day samples before and after 30-day recovery period

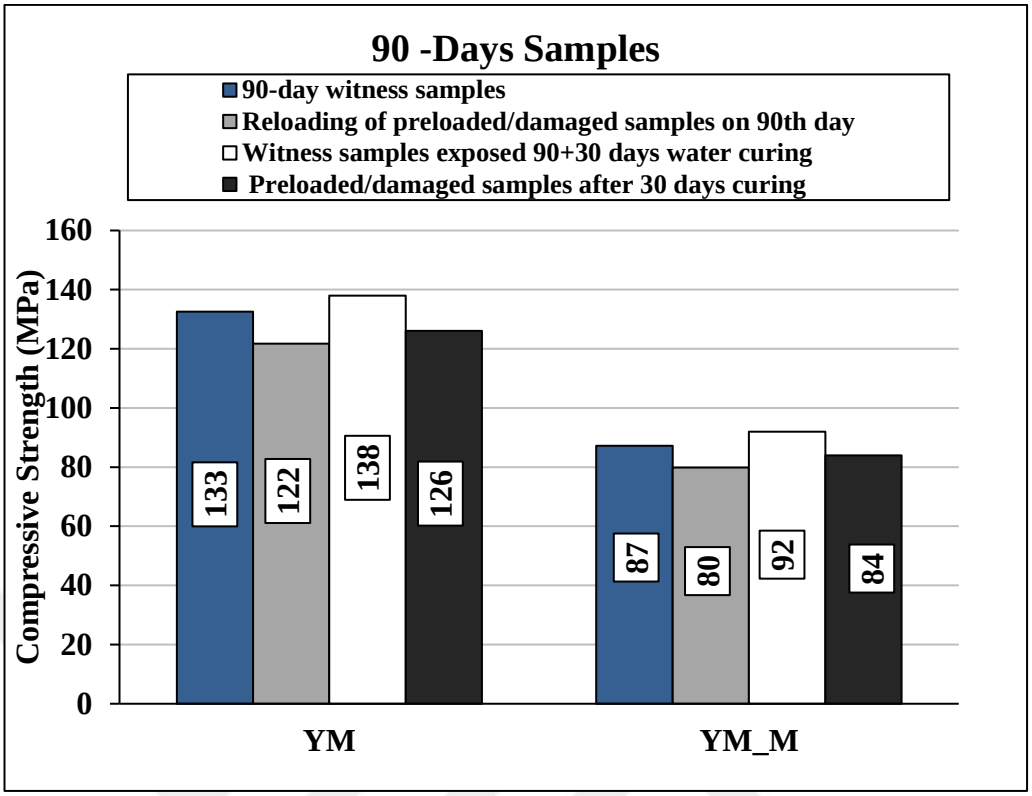

Figure 4.2 Compressive strength results of 90-day samples before and after 30-day recovery period

In the experimental method, samples were damaged by preloading and damage rates of 7 and 90-day samples are shown in Figure 4.3. As can be seen, the damage rates of YM and YM_M mixtures are very close to each other in 7 and 90- day samples. These very close degree damage provides a better examination of the effect of microcapsules on the healing mechanism. Despite the preloading made up to 100% of the average compressive strength, the damage of samples is at the most 12%.

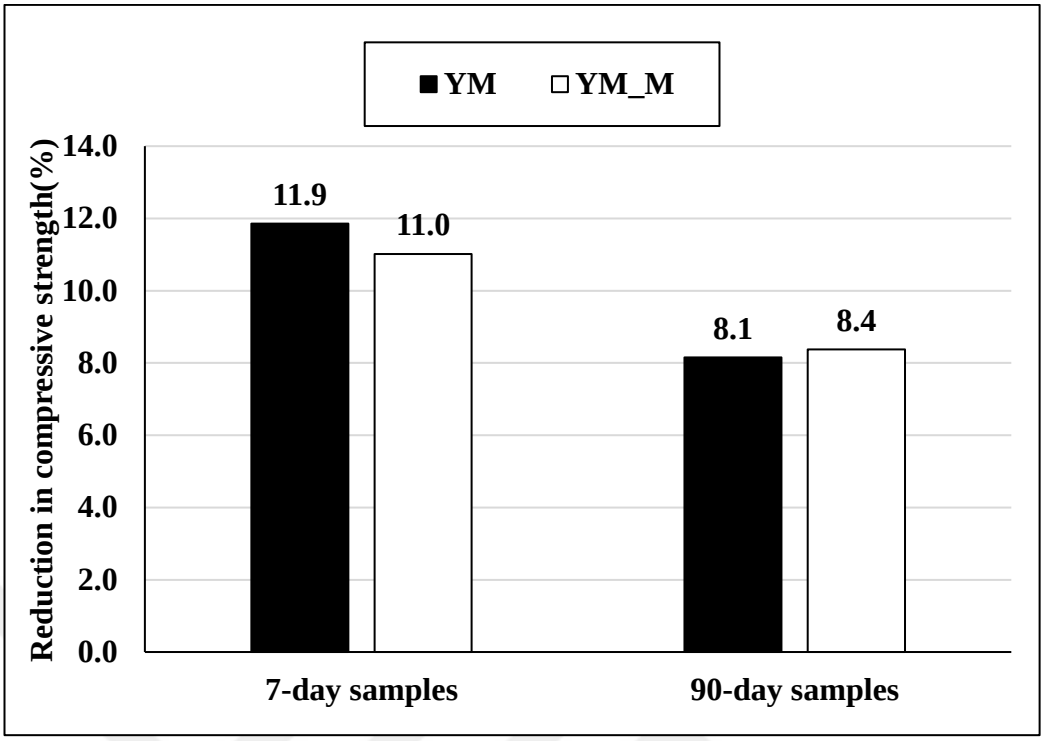

Figure 4.3 Average decrease in compressive strength (damage ratio) caused by preloading in UHPC samples

As it is known, concrete and cement-based materials in general without fiber are brittle construction materials. This negative behaviour can be reduced by using fiber. The positive results of the use of steel fiber in the mixtures are that the damage is less in the samples, despite the preloading up to the compressive strength level. Most of the strength is preserved after reloading immediately. Less preload damage in 90-day samples compared to 7-day samples can be explained by the development of fiber-matrix and aggregate-matrix adherence over time.

Self-healing mechanism in compressive strength can be expressed with different approaches. It is only possible to determine a realistic self-healing ratio, or in other words, its recovery in strength with a correct perspective.

First approach:

$$S(\%) = \frac{c-b}{d-b}\ x\ 100 \qquad (4.1)$$

In this equation, the expression "S" indicates the ratio of self-healing, and the terms "b" and "c" represent preloading which is ~ 100% of the compressive strength (damaged samples after 7 and 90 days of water cure), respectively, before and after the self-healing process (30 days water cure). The average compressive strength of the witness samples after 7 + 30 and 90 + 30 days of water curing is indicated with the expression "d".

The self-healing ratios given in Figure 4.4 were investigated with the first approach, which gives the most realistic result in samples without microcapsules.

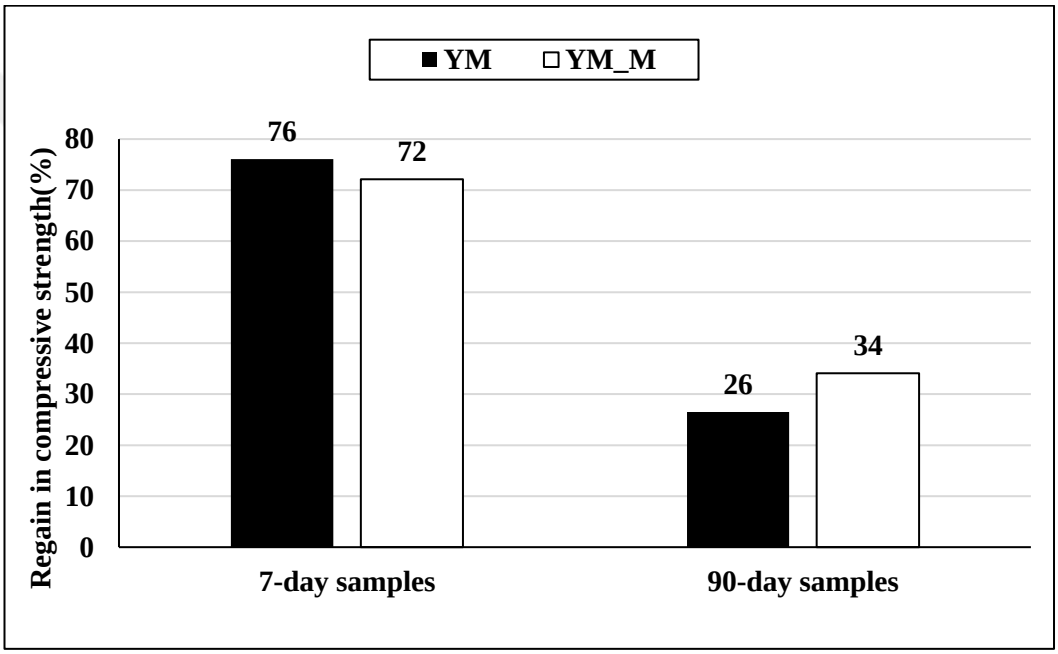

Figure 4.4 Self-healing ratio of 7 and 90-day samples (first approach)

When the results of the 7-day samples are examined, it is seen that there is no additional self-healing developed with microcapsules in the compressive strength of the UHPC mixtures. In 90-day samples, the self-healing ratio of YM and YM_M mixtures is 26% and 34%, respectively. The healing mechanism in the YM mixture is provided from the autogenous healing mechanism. So that, efficiency of microcapsules on self -healing can be determined compare with YM and YM_M. The 8% improvement between the two mixtures is the self-healing rate achieved with the contribution of microcapsules. The SS solution, which is the healing agent in the microcapsule, may have reacted with $Ca(OH)_2$ in the matrix to form the secondary C-

S-H gel. However, it is clear that the microcapsule efficiency on UHPC mixtures does not have a large self-healing contribution in the compressive strength. Additionally, the difference in damage rate of 4% between 7-day samples and 90-day samples may have affected this mechanism. However, the products of the self-healing agent have a low contribution to the compressive strength.

Second approach:

$$S(\%) = \frac{c-b}{d-a} \times 100 \quad (4.2)$$

In this equation, the expression "S" indicates the ratio of self-healing, and the terms "b" and "c" represent preloading which is ~ 100% of the compressive strength (damaged samples after 7 and 90 days of water cure), respectively, before and after the self-healing process (30 days water cure). The average compressive strength of 7 and 90 -day samples is indicated with the expression "a". The average compressive strength of the witness samples after 7 + 30 and 90 + 30 days of water curing is shown with the expression "d".

Average recovery (self-healing rate) in strength calculated with the second approach is shown in Figure 4.5. In this approach, recovery rates in strength were obtained by considering the compressive strengths of 7 and 90 -day witness samples. In other words, the 30-day self-healing process has been neglected in the witness samples. Thus, hydration and pozzolanic reactions that continue during the 30-day self-healing process were not considered.

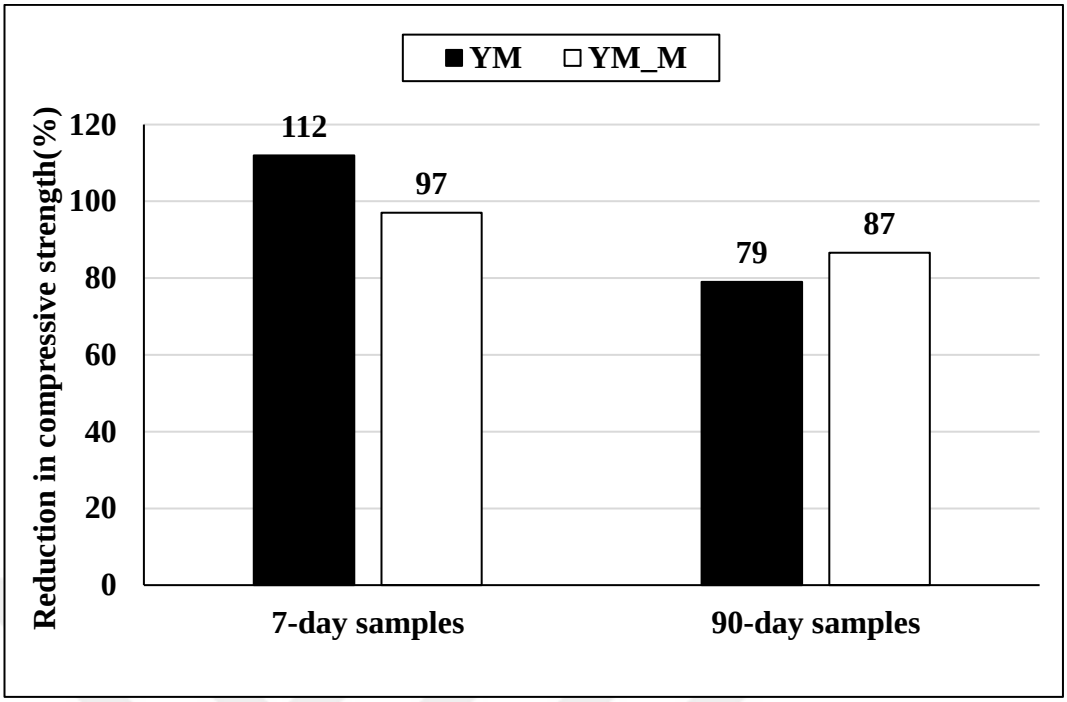

Figure 4.5 Self-healing ratio of 7 and 90- day samples (second approach)

As seen in Figure 4.5, it is seen that microcapsule-based improvement has an effect on 90-day samples. Unreacted cement particles were reduced for autogenous self - healing in 90-day samples. So that, it can be said that microcapsules appear to be an additive here.

4.1.2 Examination of Microcapsule Based Self-Healing Mechanism by Direct Tensile Strength Test

As explained in detail in the previous section, the direct tensile test was performed on a mixture of 13 mm steel fibers. In the direct tensile test, which it was aimed to be damaged, crack control is relatively easier, especially in 7-day samples. However, a more brittle behavior is observed in 90-day samples due to the nature of the cement-based material. The samples using 6 mm steel fiber exhibited a sudden load drop without showing any deformation hardening/softening with the formation of the first crack (damage). This sudden drop made it impossible to observe self-healing in the direct tensile test, which is very sensitive and difficult. For this reason, it was able to show deformation hardening/softening under direct tensile load by providing crack control by using 13 mm steel fiber (Beglarigale, 2018). Figure 4.6 and Figure 4.7

show the stress-strain curves of a sample that best represents the 7 and 90-day direct tension behaviour of UYPB mixtures without microcapsules (YM) and Figure 4.8 and Figure 4.9 shows stress-strain curves of a sample that best represents the 7 and 90-day direct tension behaviour of UYPB mixtures containing microcapsules (YM_M). To reiterate, when the samples reach maximum strength and a decrease in the curve is observed, the loading is stopped (black line on curves).

Also, it can be seen in Figure 4.6, the results of direct tensile test were represented. Self-healing ratios are obtained by using following equation which is thought to give the best results;

$$SDT(\%) = \frac{c-b}{d-b} \times 100 \tag{4.3}$$

In this equation, SDT, recovery percentage in direct tensile test, “b” and “c” are tensile strength of preloaded samples before and after 30-day healing process respectively, “d” is tensile strength of witness samples after 7+30- and 90+30-day water curing.

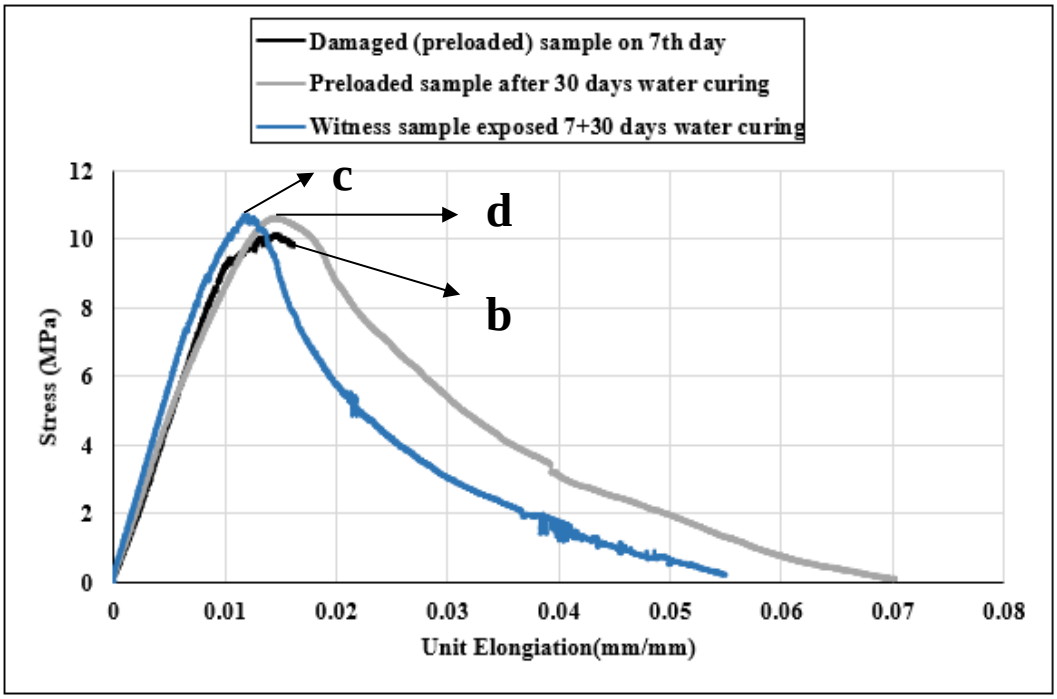

Figure 4.6 7-day YM tension results

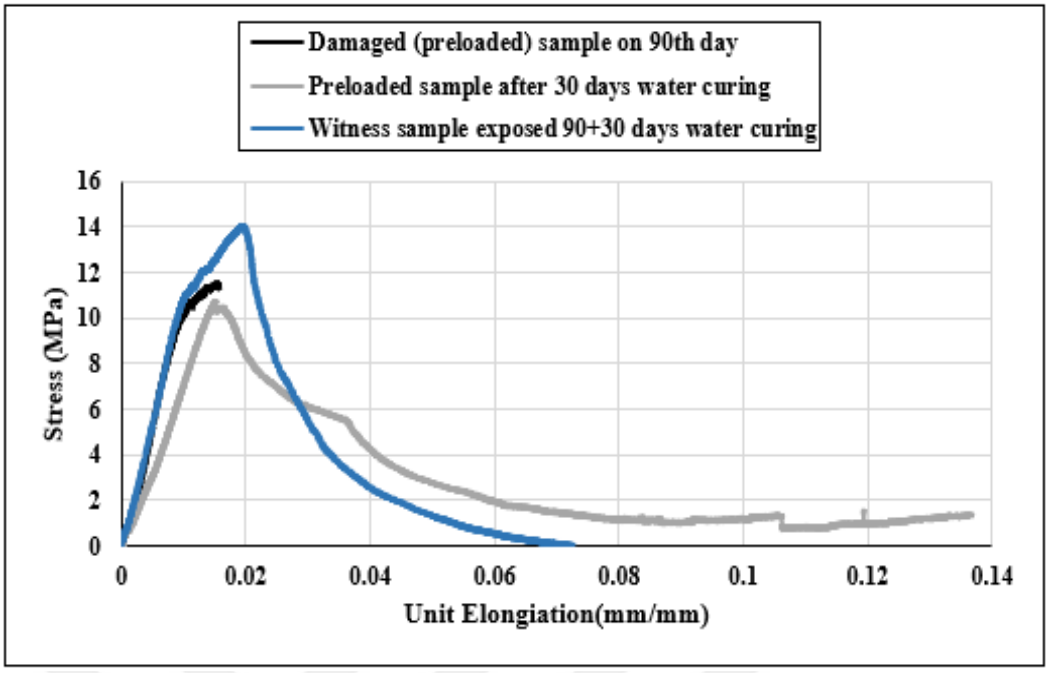

Figure 4.7 90 -day YM tension results

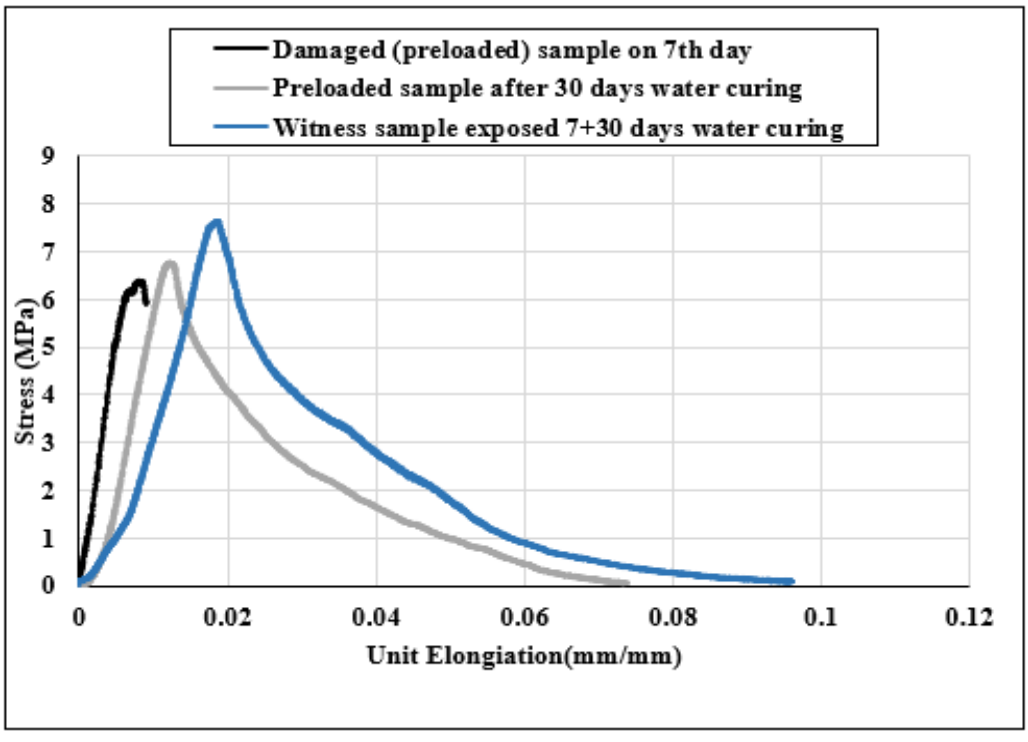

Figure 4.8 7 -day YM_M tension results

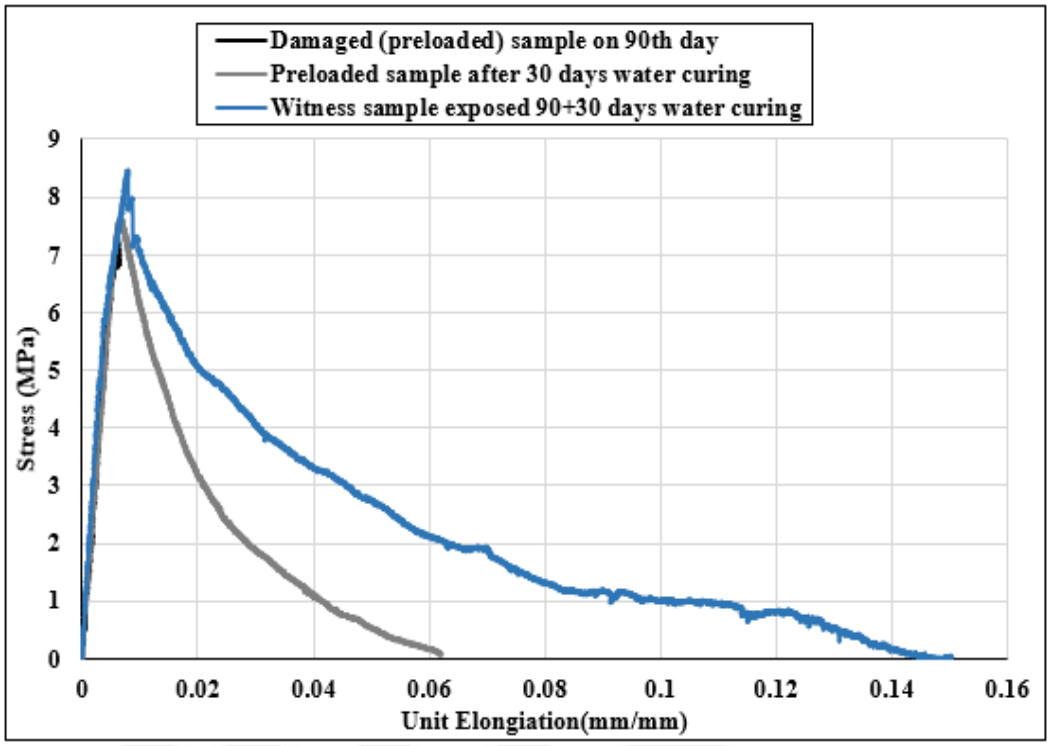

Figure 4.9 90 -day YM_M tension results

In Figure 4.10 and Figure 3.11, tensile strength test results are given. When the results are examined, it is seen that the use of microcapsules reduces the tensile strength of UHPC mixtures, similar to the compressive strength. The negative effects of microcapsules on the mechanical properties of UHPC mixtures, which were explained in detail in the previous section, are more clearly observed in the direct tensile test.

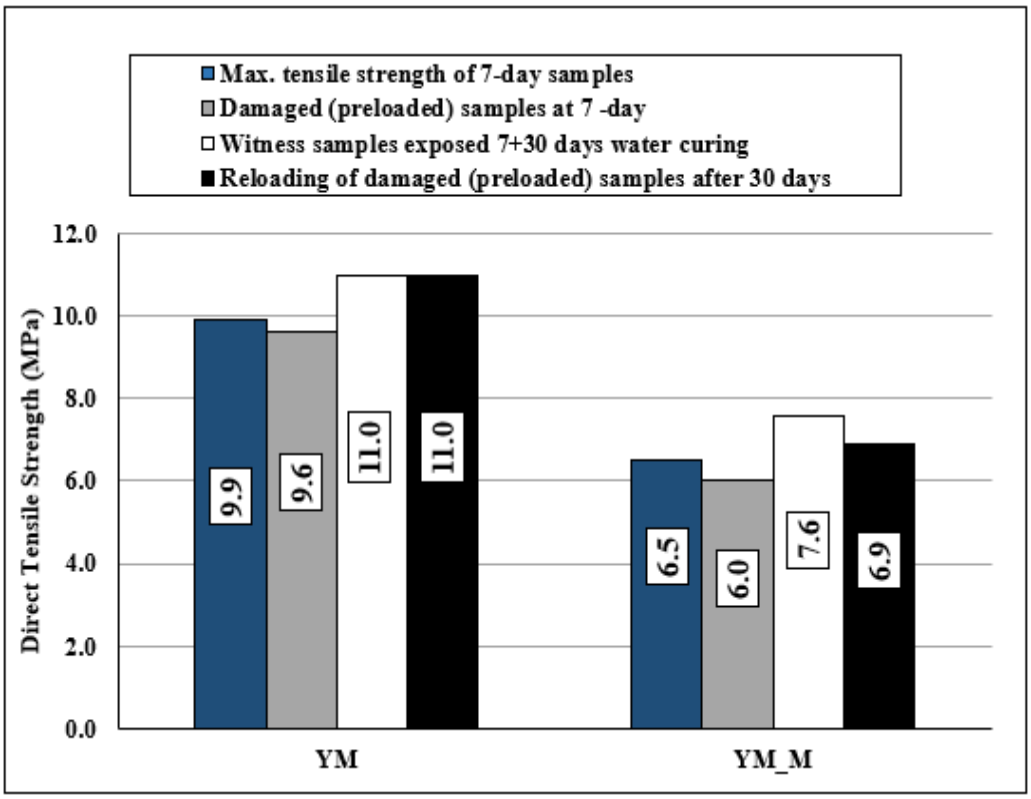

Figure 4.10 7-day direct tensile strength results of YM and YM_M mixtures

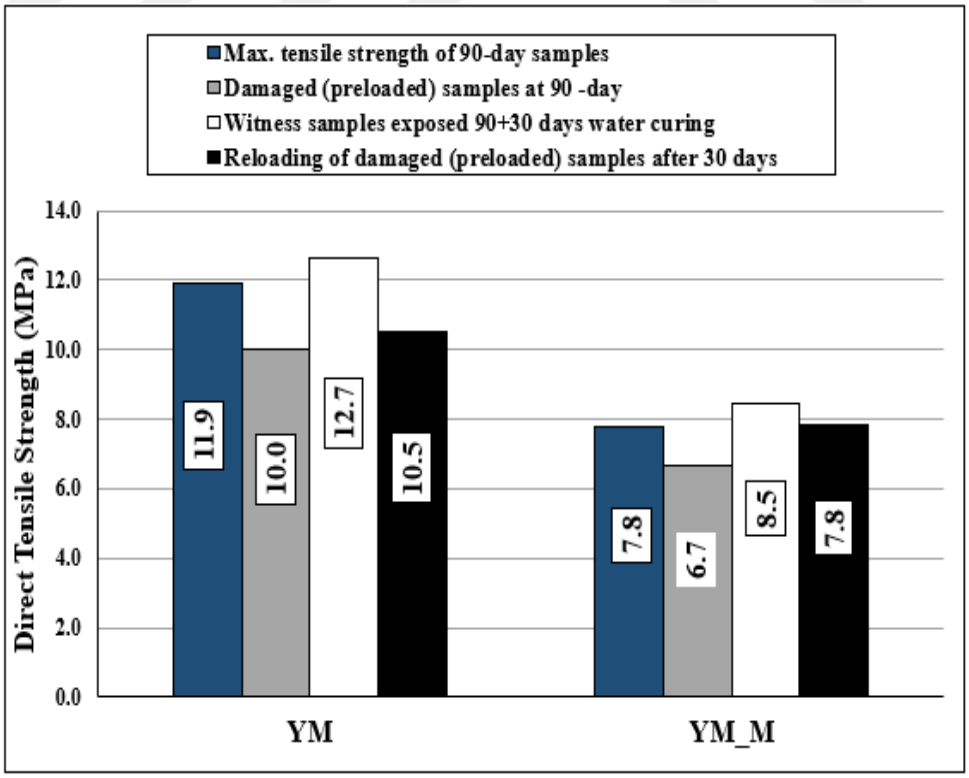

Figure 4.11 7-day direct tensile strength results of YM and YM_M mixtures

Average recovery (self-healing ratio) in direct tensile strength calculated with the first approach (4.1) is shown in Figure 4.12. When the results were examined, an average 7% higher self-healing ratio was obtained in 7-day samples of the microencapsulated mixture, and an average 45% additional self-healing ratio (compared to the mixture without microcapsules) was reached in the 90-day samples. Although the compressive strength of the microcapsule-bearing UHPC mixtures have a low self-healing ratio, it can be considered as an optimistic result to obtain a high self-healing ratio in tensile strength. One of the reasons for the occurrence of this result is that the self-healing mechanisms in the two-test process are different. While the fiber-matrix interface improvement and micro crack filling in the direct tensile strength test is the more active mechanism, filling of micro cracks was not effective in compressive strength test. Observing the 90-day test results, it is seen that the ratio of self-healing is higher. The reason for this is that the activity of autogenous healing was slowed in 90 days. For this reason, microcapsules create a more pronounced effect.

→Another important point is that the microcapsules significantly reduce the tensile strength. For that reason, it will be more difficult for a mixture with high tensile strength to regain the strength as a result of self-healing after damage.

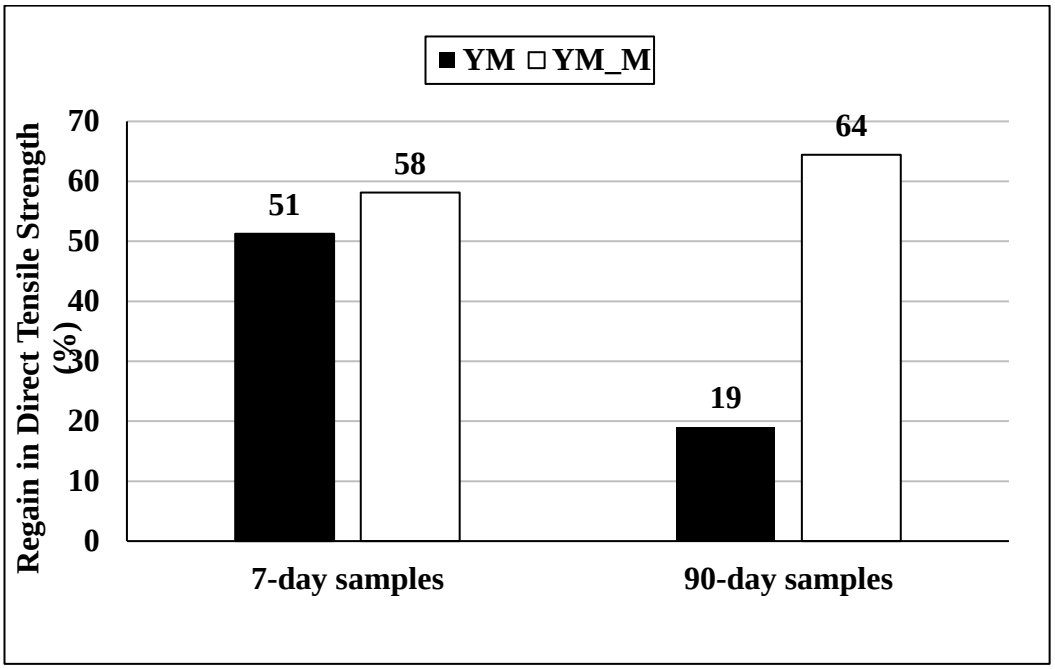

Figure 4.12 Regain percentages in tensile strength

4.1.3 Examination of Microcapsule Based Self-Healing Mechanism by Total and Capillary Water Absorption Test

The total water absorption (TWA) percentages of the 7-day YM and YM_M samples are shown in Figure 4.13. The 0.9% water absorption of the YM mixture indicates that it absorbs less water than the 7-day-old samples. However, when we look at the witness samples after 30 days of water cure, an important decrease was observed in the water absorption rate of the YM_M mixture. In short, while the substitution of microcapsules instead of quartz aggregate in 7-day samples (keeping binder dosage and b / w ratio constant) increased water absorption, it tolerated this disadvantage and achieved less water absorption rates during the 30-day additional water cure (self-healing process).

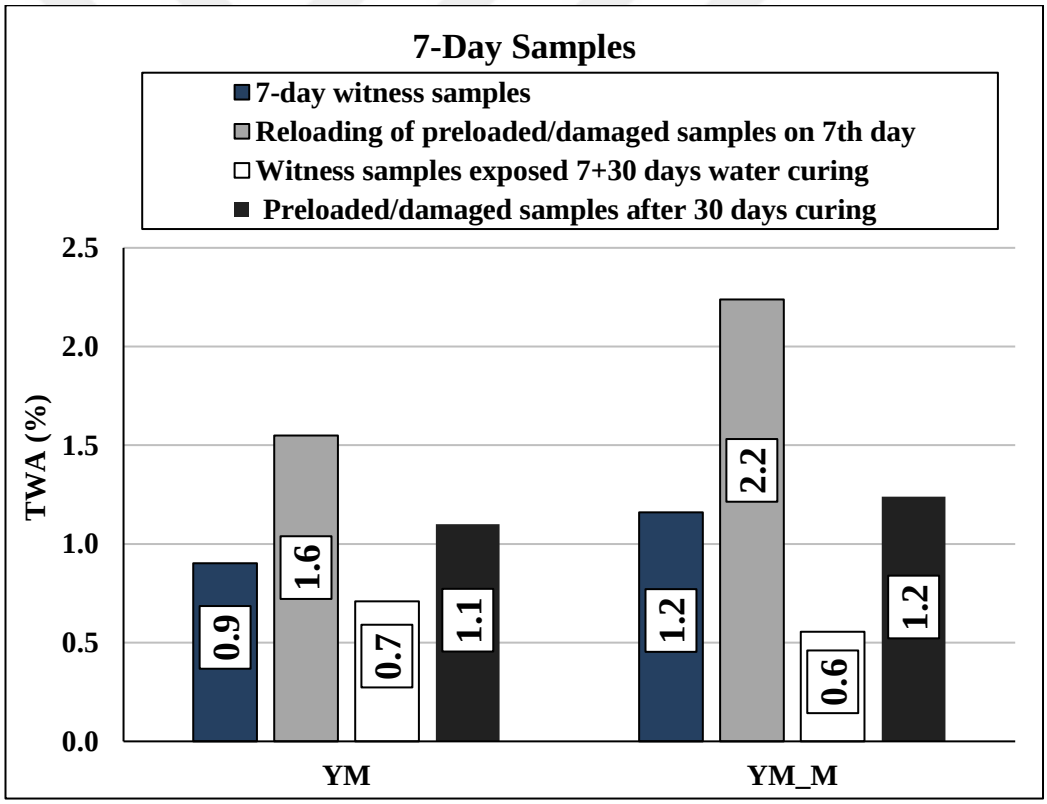

Figure 4.13 TWA percentages of 7-day samples

Total water absorption (TWA) percentages of 90-day samples are 0.4% and 0.5%, respectively (Figure 4.14). When the 90-day samples of the two mixtures are

compared, it is seen that The water absorption rate of the mixture containing microcapsules is higher (36%).

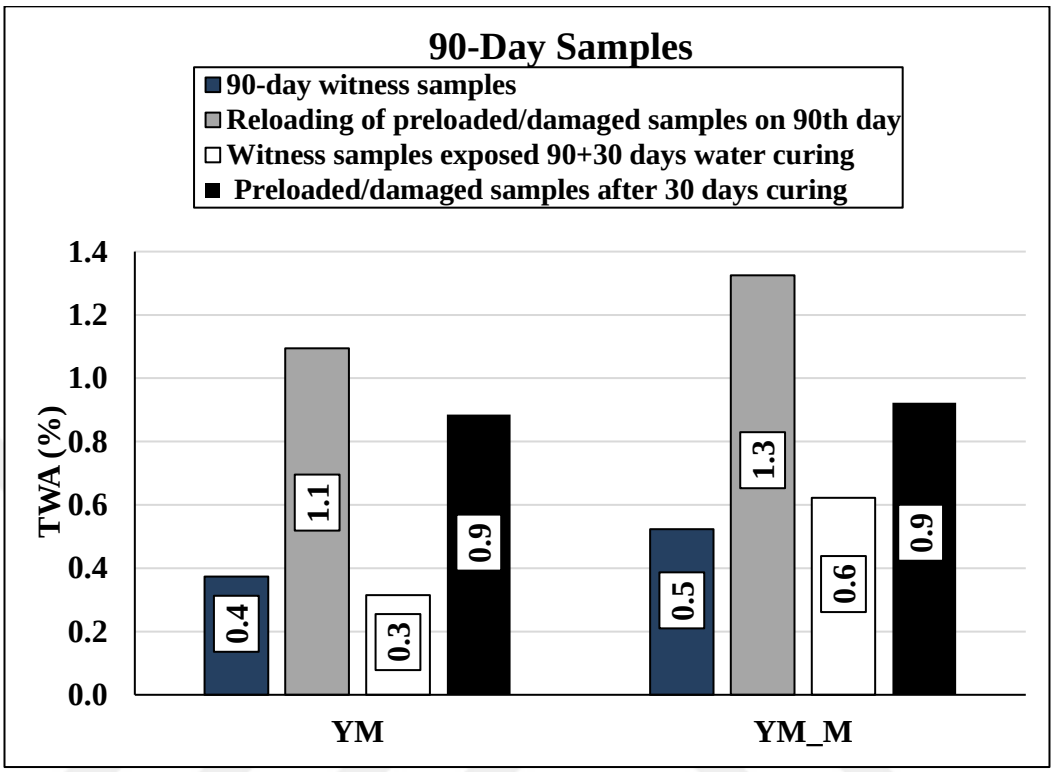

Figure 4.14 TWA percentages of 90-day samples

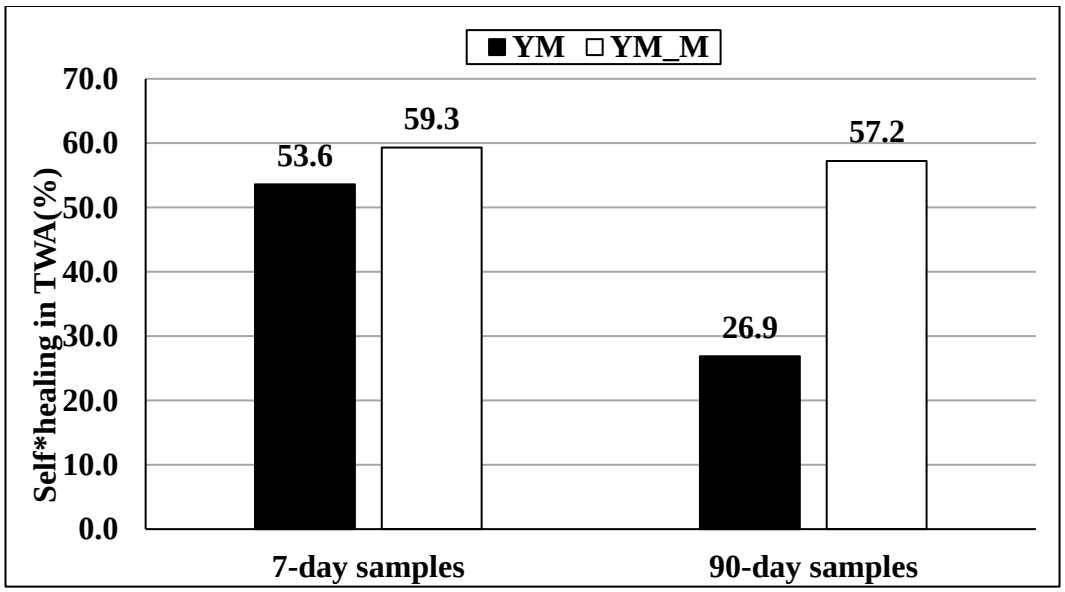

Figure 4.15 Recovery in TWA (self-healing ratio)

Figure 4.15 shows the recovery (self-healing) rates in TWA obtained by the total water absorption test of the mixtures. Results are obtained by using following equation which is thought to give the best results;

$$STWA(\%) = \frac{c-b}{d-b} x100 \quad (4.4)$$

In this equation, STWA, recovery percentage in TWA, "b" and "c" are TWA percentages of preloaded samples before and after 30-day healing process respectively, "d" is TWA percentage of witness samples after 7+30 and 90+30 day water curing.

Accordingly, the recovery rates of YM and YM_M samples in 7-day samples are 54% and 59%, respectively. These results, which are close to each other, show that the microcapsule-based recovery is only 5.7%. In 90-day samples, it is seen that the healing mechanism of microcapsules is 30.3% more effective.

The achievement of better results in the water absorption test can be explained by a different self-healing mechanism. Micro cracks that occur after the preloading damage increase the water permeability coefficient of the samples. However, the reaction of sodium silicate with $Ca(OH)_2$, which is formed by the breaking of microcapsules, and also the crystallization of the agent itself, may have provided a certain blocking.

It is thought that as a result of the procedure of TWA and CWA experiments, obtained ratio of self-healing may be less than the real rate. In here, It should be explained how the TWA and CWA values of the damaged samples were obtained. Eight samples were preloaded corresponding to ~ 100% of their compressive strength. Subsequently, all samples were kept in water for at least 24 hours and their dry surface saturated weights were measured. It was then dried in an oven at 50^{o}C for three days. After the oven-dry weights of the samples were measured, TWA values were calculated by taking their dry weights, and then they were subjected to the CWA test. The reason for keeping the drying temperature lower than normal is that it is not desired to create additional micro-cracks caused by temperature. Because of all, TWA and CWA values can be calculated 4 days after the samples are damaged. However, in these 4 days, the reaction of unreacted particles and most importantly, the reaction of

broken microcapsules continues. Therefore, the water absorption rates of these damaged samples, which are kept in water for 24 hours and then kept at 50°C for 72 hours, will be lower than the water absorption rates immediately after the damage. In addition, the unhydrated particles expected to react during the 30 days of self-healing and the concentration of the released sodium silicate will have decreased little in the said 4 days. It is thought that the theoretically realized self-healing rates in TWA and CWA of the samples are higher than the experimentally obtained rates.

The 7-day capillary water absorption (CWA) test results (CWA- time curve) of the YM and YM_M mixtures are given in Figure 4.16 and Figure 4.17, respectively. Considering the results, it is seen that the capillary water absorption amount of the 7-day YM_M mixture is about half of the YM mixture. In addition, an increase is observed in the CWA values of preloaded samples in all mixtures as expected. It is seen that the preloaded samples waited in 30 days water cure in the YM_M mixture are very close to the CWA value of the 7-day witness samples.

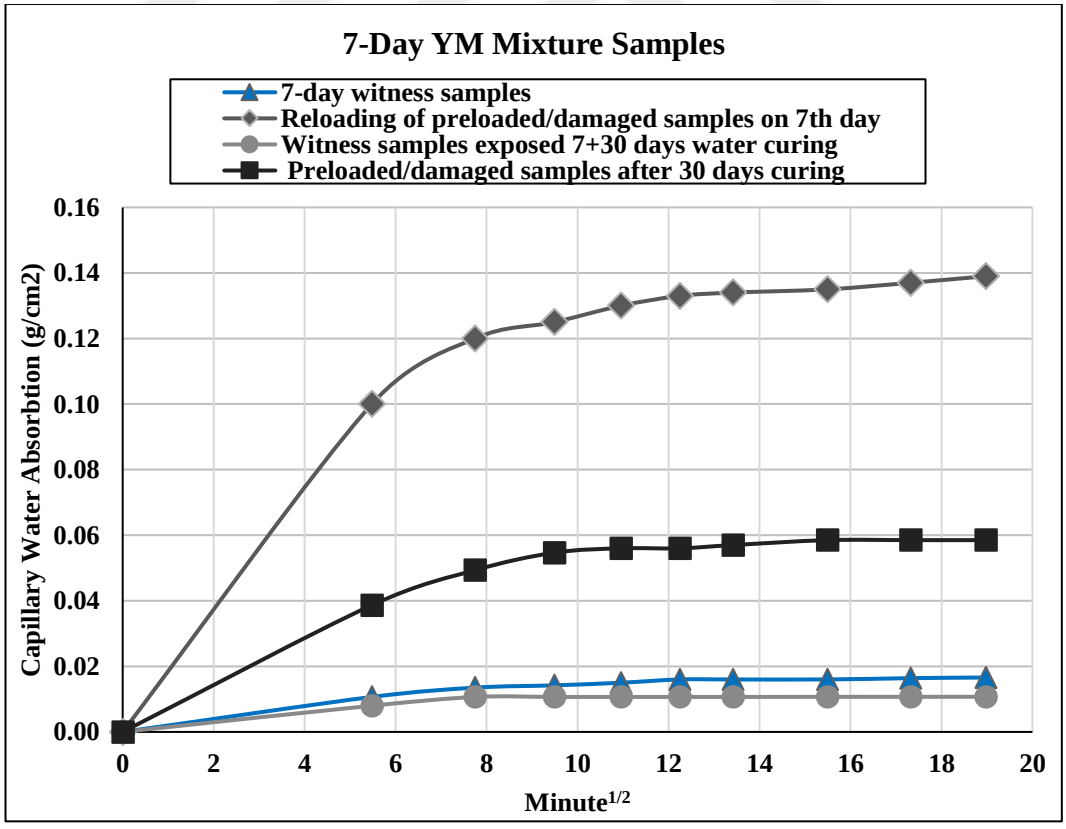

Figure 4.16 Time-dependent capillary water absorption graph of 7-day YM samples

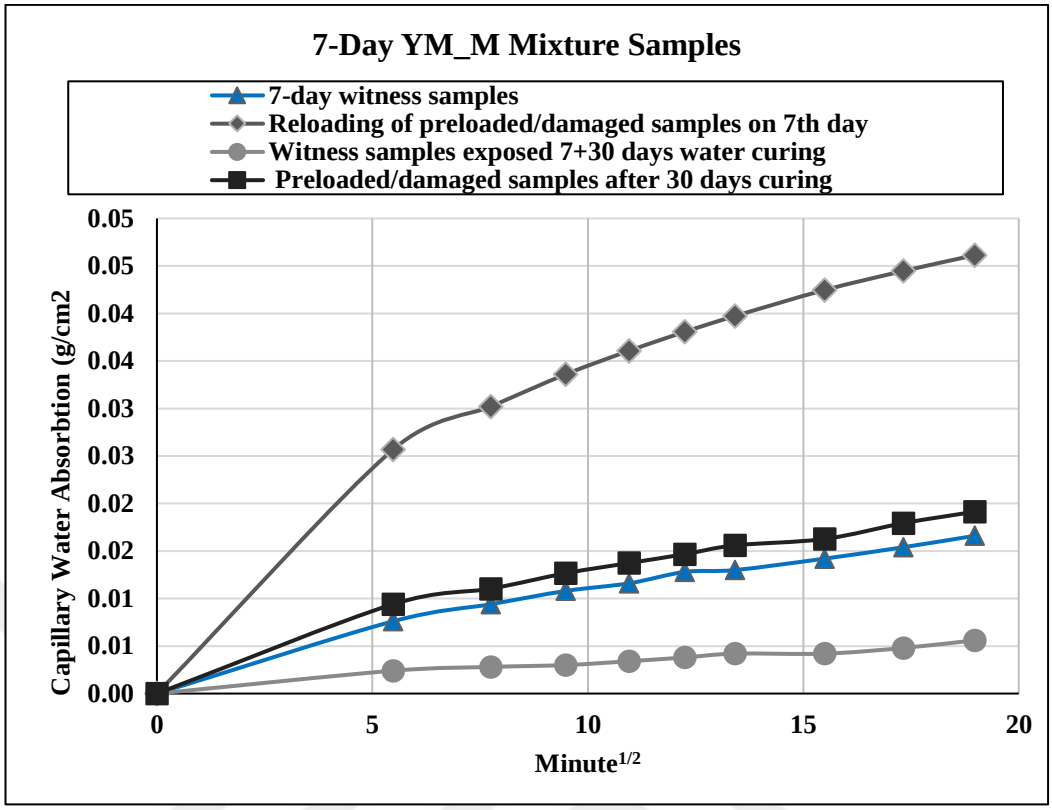

Figure 4.17 Time-dependent capillary water absorption graph of 7-day YM_M samples

When the 90-day CWA values of the mixtures are examined (Figure 4.18 and Figure 4.19), it is seen that the CWA values of the witness samples of both mixtures before and after the 30-day self- healing process did not change too much as expected. This is due to the inability to mention about a self-healing since no damage was done. There is only maturation of cement-based material.

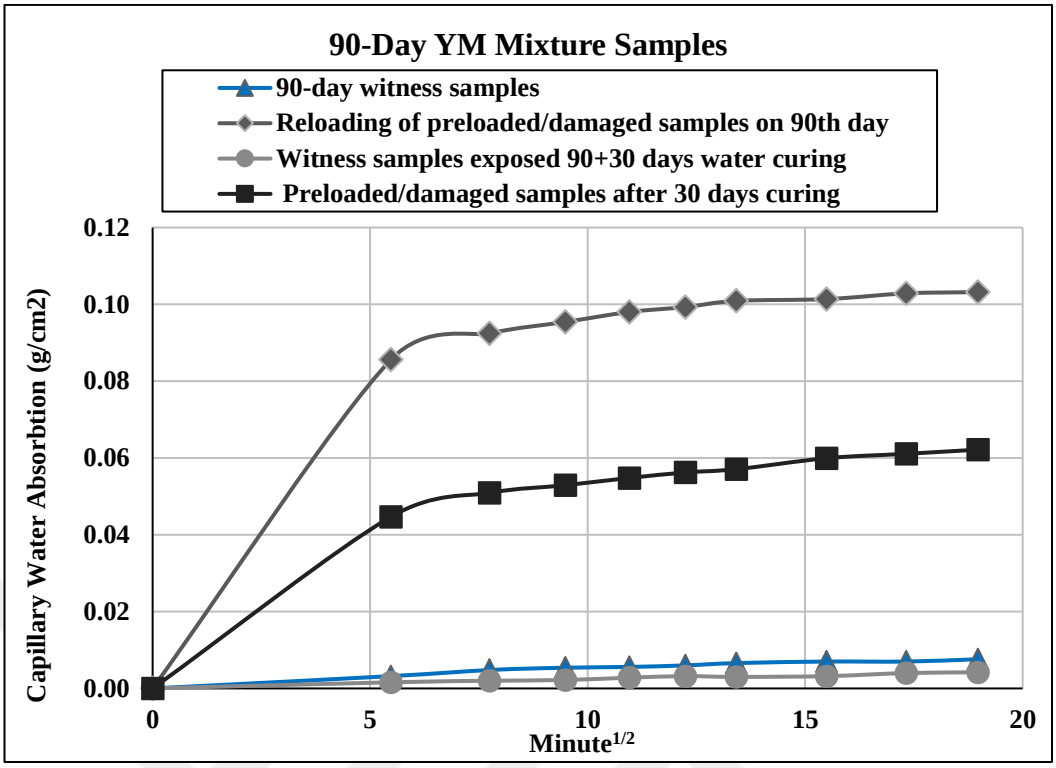

Figure 4.18 Time-dependent capillary water absorption graph of 90-day YM samples

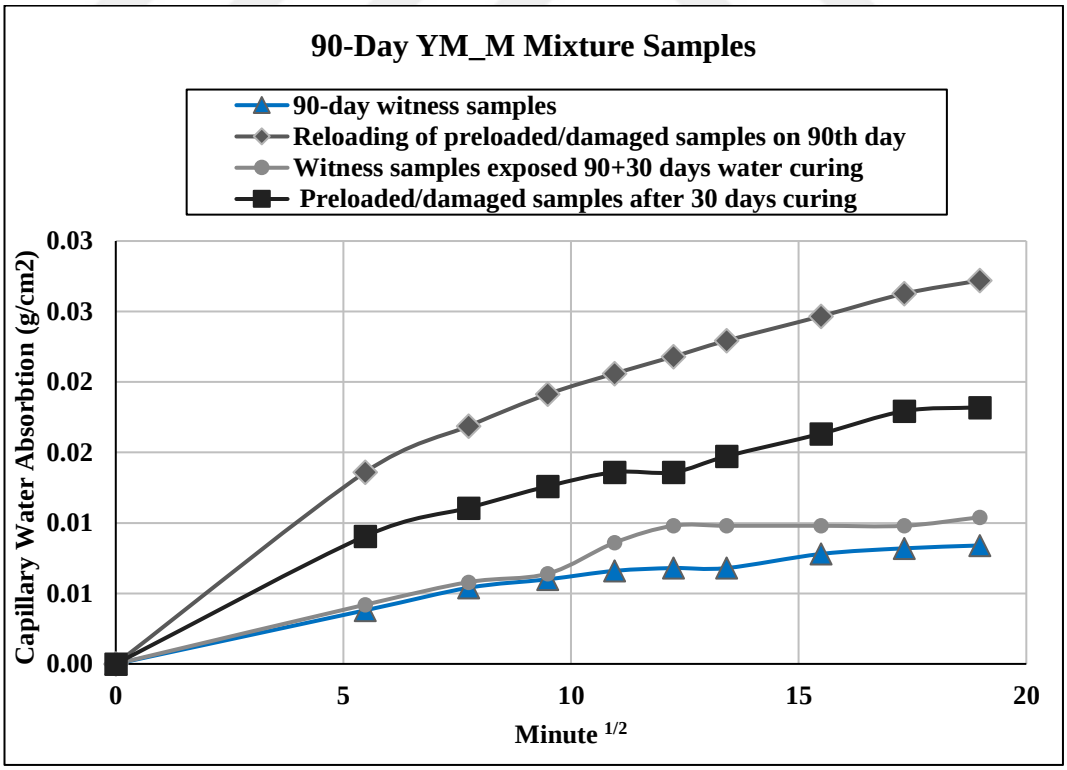

Figure 4.19 Time-dependent capillary water absorption graph of 90-day YM_M samples

The recovery rates in the CWA (self-healing ratio) were calculated with the equation (4.4) at the end of 360 minutes results. The recovery results in the CWA are given in Figure 4.20. As can be seen, while a microcapsule-based recovery of 3.8% was achieved in 7-day samples, 12.2% recovery was achieved in 90-day samples. To reiterate, these ratios was found by subtracting the self-healing ratio (autogenous recovery, 62.8% and 41.4%) in mixtures without microcapsules from the self-healing ratio based on autogenous + microcapsule in mixtures containing microcapsules (66.6% and 53.6%). The self-healing ratio obtained with the CWA test shows that the microcapsule-based healing mechanism works in 90-day samples. It can be thought that the points explained in the total water absorption test can be valid for the noteworthy self-healing performance in the CWA.

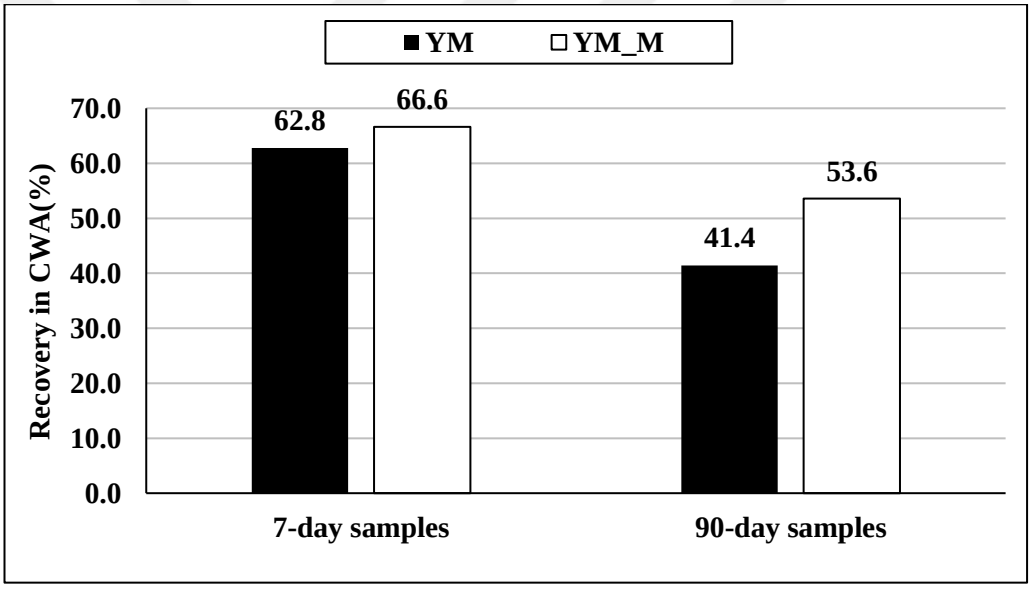

Figure 4.20 Recovery percentages (self-healing ratios) in CWA test

4.1.4 Examination of Microcapsule Based Self-Healing Mechanism by Crack-closing Test

Crack-closing test was performed comparatively on samples of 7 and 90 days old, YM and microencapsulated YM_M samples. As in the 7-day YM samples and as expected, 100% recovery is observed in the YM_M mixture (Figure 4.21). For this reason, it appears that the crack-closing test in 7-day samples is not suitable for comparing the microcapsule-based self-healing and autogenous self-healing

mechanism. Images obtained with optical microscope (OM) are shown in Figure 4.22. In 90-day samples, 56% recovery was achieved in YM mixture, while 58.62% recovery was achieved in YM_M mixture. Although it can be said that approximately 3% recovery is caused by microcapsules, the very close recovery rates are not sufficient for definitive interpretations. This situation can be explained by the fact that the crack -closing test is performed only on the sample surface. Additionally, the microcapsules are damaged and lost their effectiveness on the open side. It is thought that microcapsules stored in crack depths may be more effective in three dimensions.

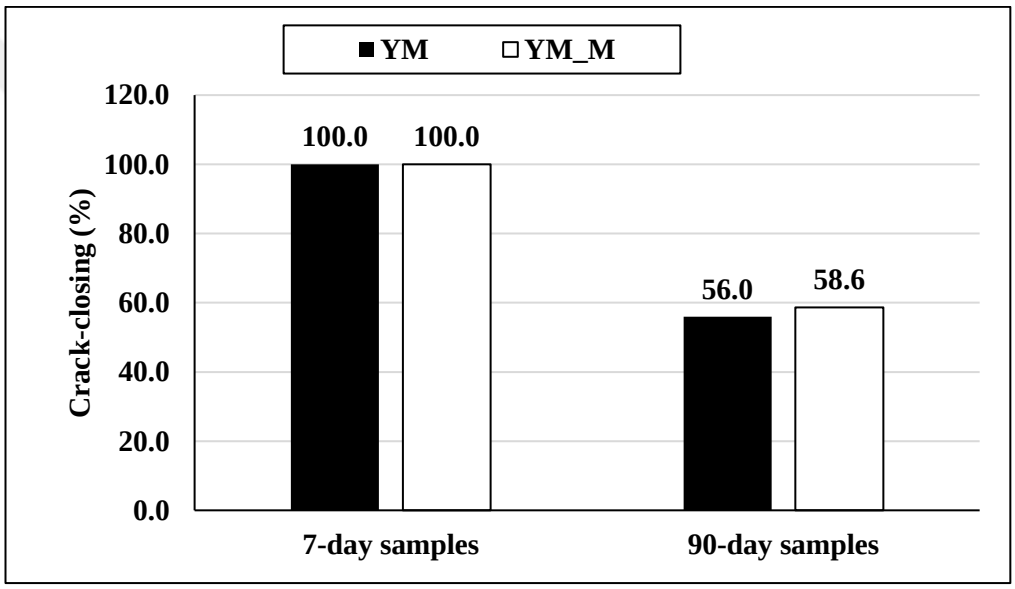

Figure 4.21 Percentages of crack-closing (self-healing ratios)

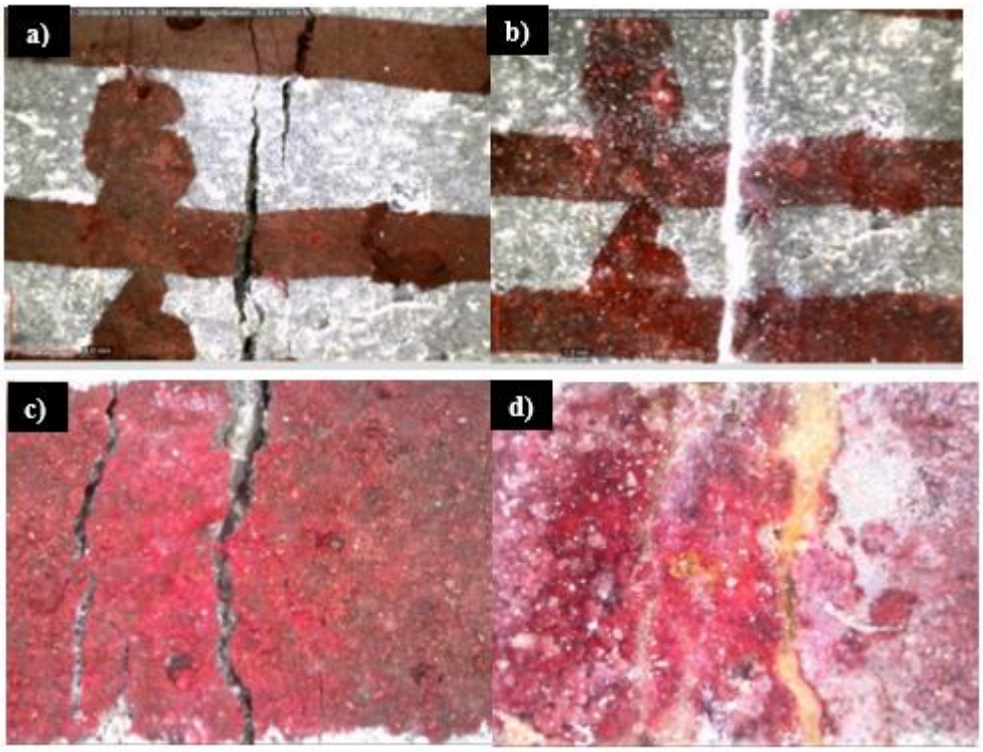

Figure 4.22 a) and b) OM images of 7-day YM samples before and after 30-day recovery period (Beglarigale, 2018); c) and d) OM images of 7-day YM_M samples before and after 30-day healing period (Personal archive, 2019)

After 30 days of healing period, the disc-shape sample were separated from the cracks by hand in order not to damage the sample itself. SEM / EDS analyses were performed on the fracture surface to see healing products and broken microcapsules. Figure 4.23 is a SEM image of two close dome shaped cavities captured in the YM_M mixture. The broken surface and one of the dome-shaped cavities are covered with massive healing products, especially CaCO3. Other cavities are air bubbles according to the EDS analysis result and appearance. Another one may be a broken microcapsule, where healing products are formed on its inner surface after releasing the core material (SS). This can be explained by the fact that the inner surface of the microcapsules is very rough. However, the inner surface of the air cavity is quite smooth. These findings have been observed in many regions of the fracture surface (Beglarigale, 2018).

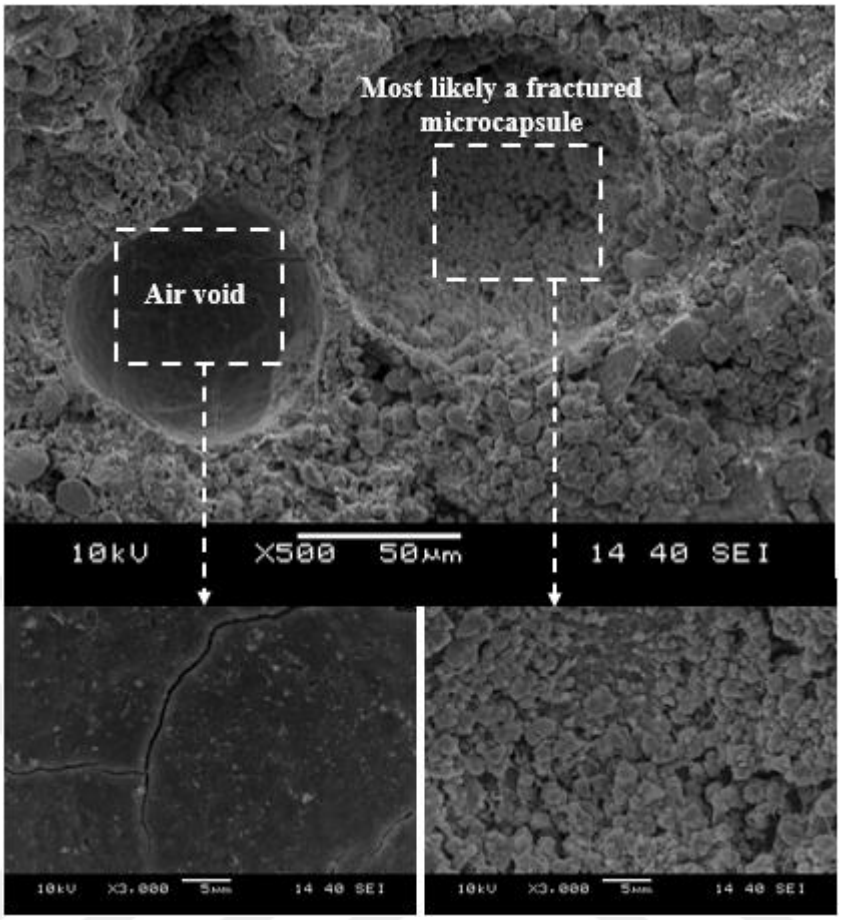

Figure 4.23 SEM image of two dome shaped cavities captured in the YM_M mixture (Beglarigale, 2018, 2019)

4.1.5 Examination of Microcapsule Based Self-Healing Mechanism by Crack Analysis

Figure 4.24 shows the crack analysis ratios (self -healing ratio) as a result of crack analysis which is executed by penetrating epoxy to 7 and 90 -day samples of YM and YM_M mixtures.

Results are calculated by the following equation;

$$CA(\%) = \frac{a-b}{a} x100 \quad (4.5)$$

In this equation CA, healing percentage with each closing analysis, “a” and “b” are the percentage of epoxy impregnated crack area of damaged samples before and after the 30-day healing process, respectively.

Figure 4.25 and Figure 4.26 are the analysis images of the 7-day and 90-day YM samples as examples. As can be seen from the results, there is, definitely, self-healing of samples. However, no additional contribution of microcapsules in self-healing was observed with crack analysis instead of existing self-healing. As previously explained, the epoxy impregnation was carried out under a severe vacuum effect. Therefore, the resulting self-healing products may have been affected by this high pressure. It is clear is that the efficacy of microcapsules in UHPC mixtures cannot be determined by this test method.

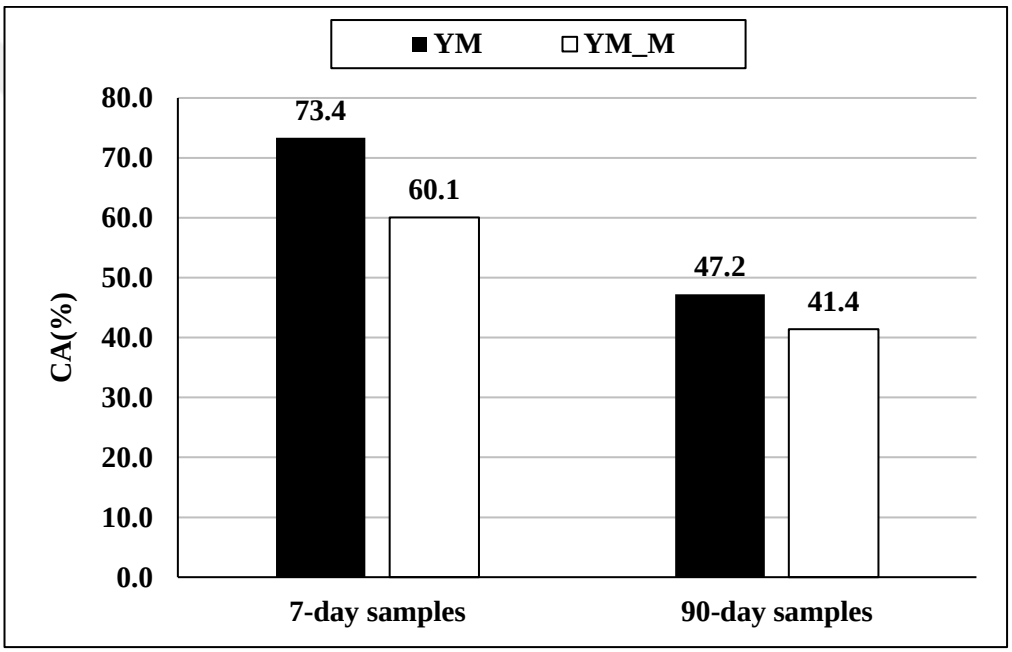

Figure 4.24 Crack closure percentages as a result of crack analysis (self-healing ratio)

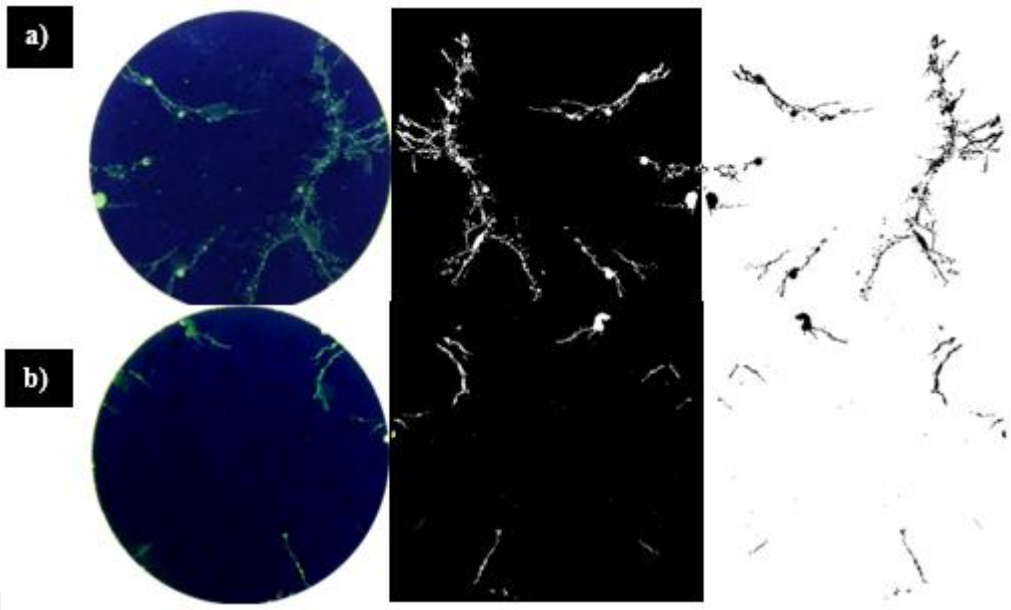

Figure 4.25 a) YM mixture after 7 days preloading, b) 7 days preloaded sample under UV light and analysis after 30 days self-healing period (Personal archive, 2019)

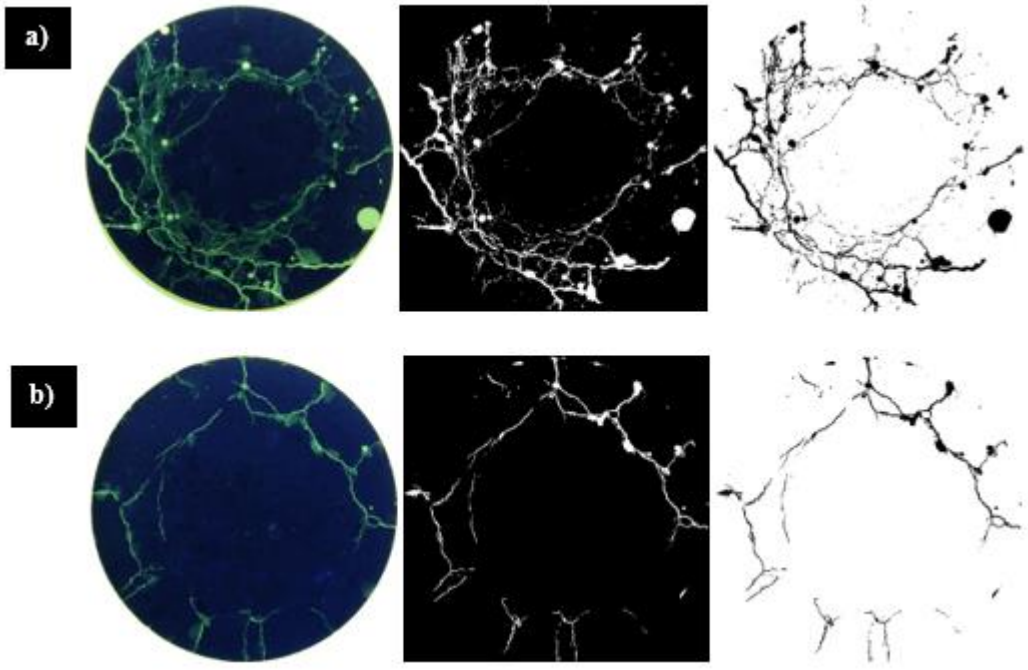

Figure 4.26 a) YM mixture after 90 days preloading, b) 90 days preloaded sample under UV light and analysis after 30 days self-healing period (Personal archive, 2019)

4.1.6 General Evaluation of the Effectiveness of Sodium Silicate / Polyurethane Microcapsules in UHPC Mixture

As seen from the experimental study, microcapsules negatively have affected the mechanical properties of the mixture as an expected result. The absence of a significant self-healing contribution to the compressive strength of the UHPC mixture may be due to different reasons. The fact that self-healing products are not very strong in micro cracks may be an important reason. On the other hand, it can be thought that some optimistic self-healing ratios may have been obtained in the direct tensile test. Crack-closing and crack analysis tests were found to be insufficient for the self-healing measurement at this stage. In addition, in UHPC mixtures with low water / cement ratio, there is the possibility of damaging microcapsules if they are mixed in the mixer for a long time in order to gain workability with super plasticizer additives. On the other hand, it is usual to obtain very good results in total and capillary water absorption tests. In these experiments, there is no return in mechanical properties, but recovery of impermeability. Since any product that occurs in cracks will reduce the permeability, it is normal for the self-healing to be higher.

Considering the results in general, Although the difference in self-healing ratios was low in mixtures with and without microcapsules, the ratios of recovery(self-healing) was observed with all methods. It is seen that the microcapsules developed are not very beneficial in UHPC mixtures. So that, studies were investigated in normal mortar mixture to examine the effectiveness of microcapsules in a healthier way. There is less cement in normal mortar mixes. Autogenous self-healing effect will be less. Since microcapsules are added by the weight of cement, less capsules will create less void effect in total. The mixing procedure of normal mortars is much shorter. It does not need to be mixed for a long time as in UHPC. The risk of breakage of microcapsules during mixing is less compared to UHPC. For all these reasons, the effectiveness of microcapsules has been investigated on classical mortar in this scope.

4.2. Examination of Microcapsule Based Self-Healing in Normal Mortar Mixtures

The properties of the normal mortar mixture prepared to examine the microcapsule-based self-healing mechanism are given in Table 3.5. Two different normal mortar mixtures with 0.5 water / cement ratio and 2% by volume of fiber were prepared: The mixture without microcapsules is abbreviated NM and the mixture in which 5% by weight of the cement is replaced by microcapsule instead of aggregate (NM_M).

4.2.1 Examination of Microcapsule Based Self-Healing Mechanism by Compressive Strength Test

A certain level of damage (decrease in compressive strength) has occurred in the preloaded samples on which the compressive strength test was applied, depending on the mixture design. As can be seen, preloading that is ~ 100% of the average compressive strength caused a certain degree of damage in the samples. Despite such a high level of preloading, the decrease in compressive strength does not exceed 18% (Figure 4.27). The damage to the samples by preloading was determined as 17.7% and 14.3% for NM and NM_M mixtures, respectively. This means that the healing mechanism is examined in similarly damaged samples.

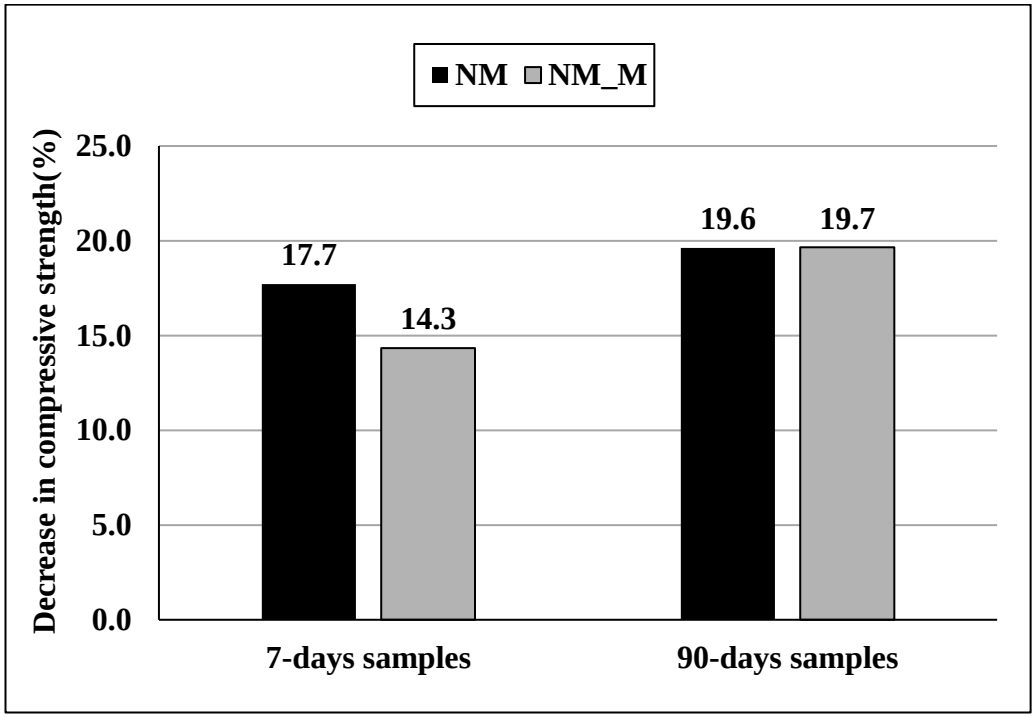

Figure 4.27 Damage rates of NM and NM_M mixtures

Figure 4.28 and Figure 4.29 gave the compressive strengths of 7-day and 90-day samples before and after 30-day self-healing process. The 7-day compressive strengths of NM and NM_M mixtures are 46.75 MPa and 40.73 MPa, respectively. Likewise, in 90-day samples, it is 70.54 MPa and 54.83 MPa, respectively. As can be seen, the compressive strength of the NM_M samples is lower than the NM samples. This is due to the substitution of microcapsules instead of aggregates by volume. In addition, microcapsules create a large macro-void effect like entrained air spaces. As expected, the 7-day compressive strength of the NM_M samples is lower than the NM samples. It is seen that the decreases are higher in 90-day samples.

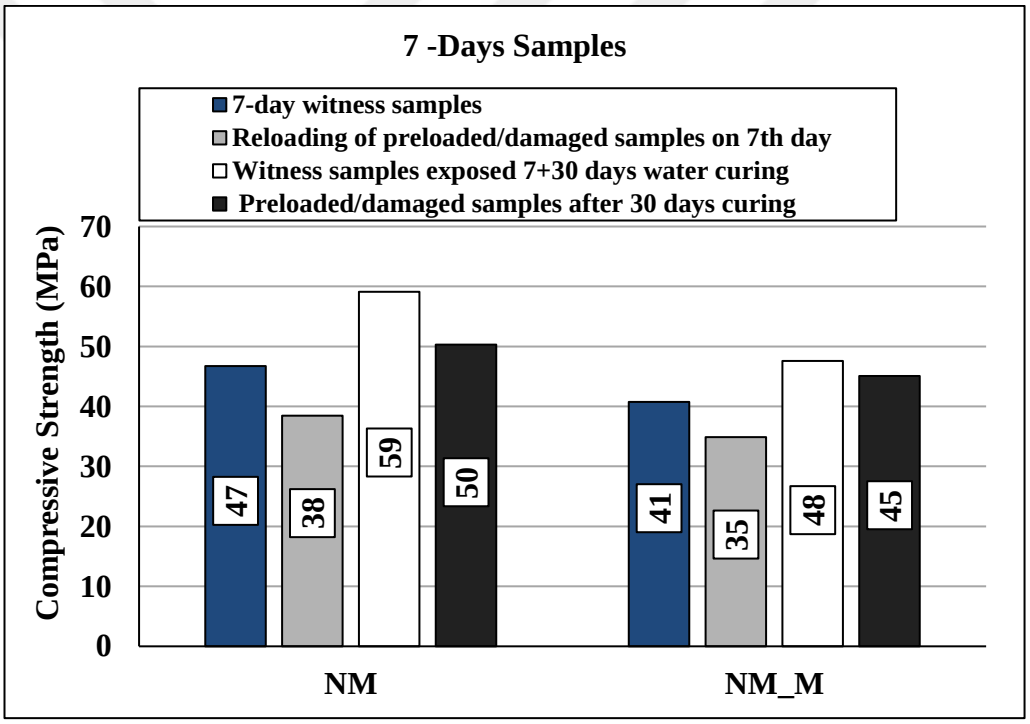

Figure 4.28 7-day compressive strength of NM and NM_M mixtures

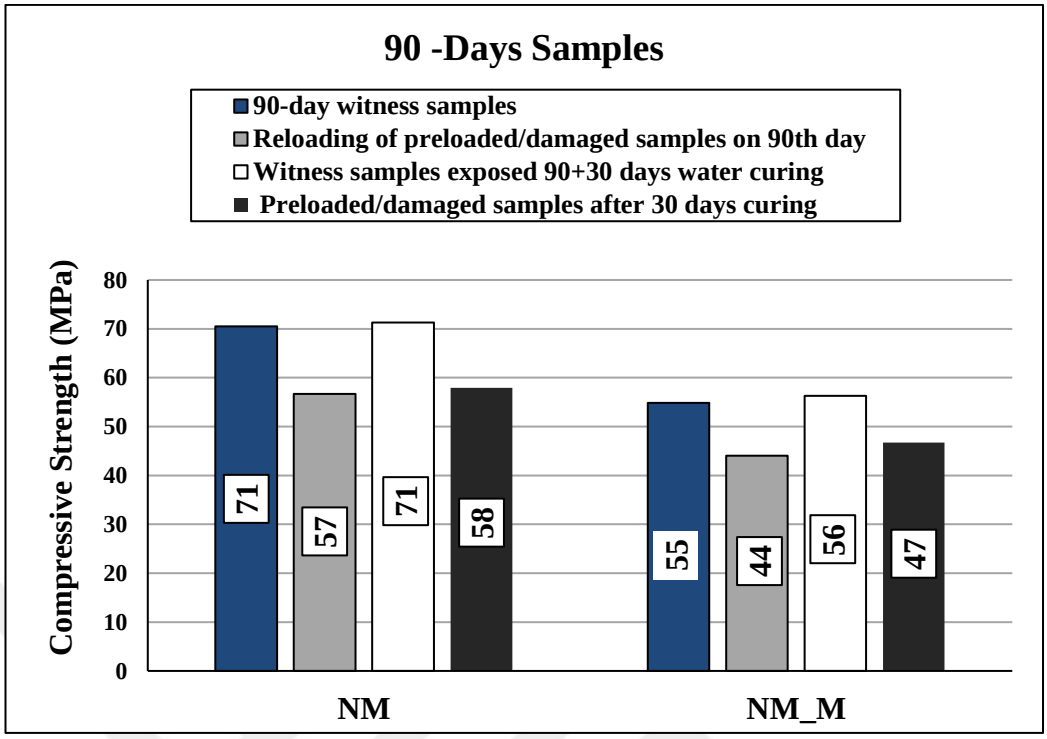

Figure 4.29 90-day compressive strength of NM and NM_M mixtures

Figure 4.30 shows the recovery (self-healing ratio) of the 7-day and 90-day samples after the 30-day water cure healing period. These ratios are calculated by equation (4.1) presented in the 4.1 chapter. When the 7-day samples are examined, 57% healing is seen in the NM mixture. This healing is due to the autogenous self- healing mechanism that takes place within the mortar. The ongoing hydration of non-hydrated cement particles is quite high in 7-day samples. In the NM_M mixture, the recovery at the rate of 80% represents the sum of autogenous and microcapsule-based recovery. In this case, the microcapsule-based self-healing in 7-day samples can be expressed as 23%. This ratio is difference between 7-day NM and NM_M mixtures self-healing ratios. In the 90-day samples, a lower rate of autogenous recovery was detected with the completion of cement hydration at later ages. In this experimental group, the ratio of self-healing resulting from microcapsule-based heling is around 14%. As can be seen, the efficiency of microcapsules on the compressive strength of normal mortar is much higher than that of an UHPC mixture. Here, because microcapsules are in the size of large voids, the total voids are decreased at the same time. In addition, mixing NM mixtures in a much shorter time compared to UHPC mixtures reduced the risk of damage to microcapsules and increased their efficiency.

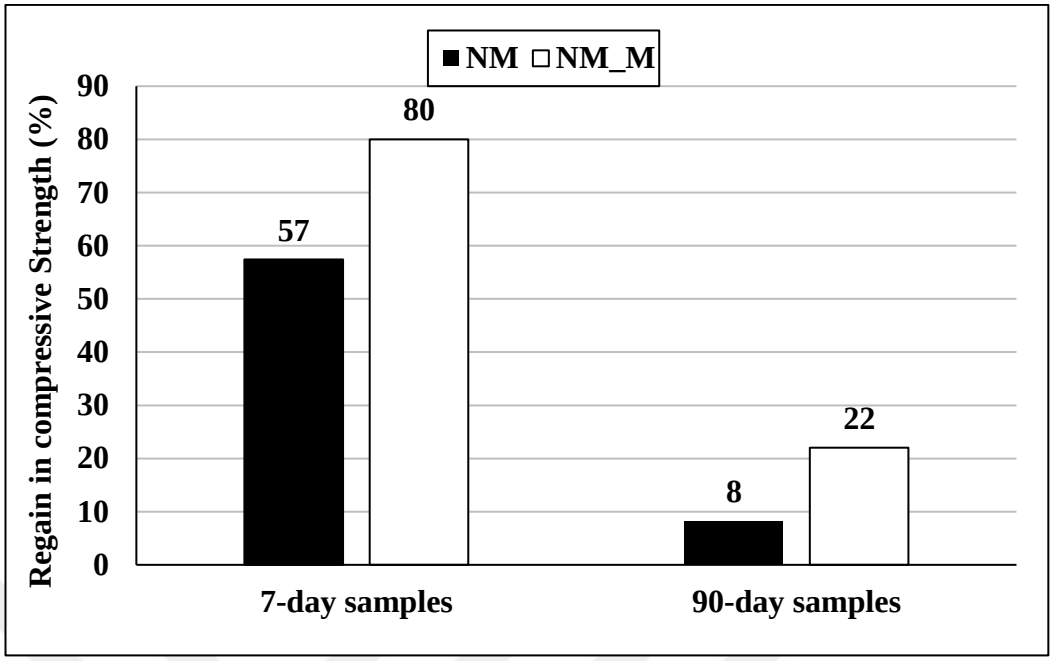

Figure 4.30 Self-healing ratio of 7 and 90-day samples

4.2.2 Examination of Microcapsule Based Self-Healing Mechanism by Direct Tensile Test

When normal mortar mixes were modified with 13 mm long steel fibers suitable for direct tensile testing, a mixture with suitable workability was not obtained. Due to the low amount of binder encountered in normal mortar mixtures, the locking of the fibers also occurred in the normal mortar mixtures prepared (Figure 4.31) and therefore the direct tensile test was not carried out.

Figure 4.31 The 13 mm fiber locking of normal mortar mixtures

4.2.3 Examination of Microcapsule Based Self-Healing Mechanism by Crack Closing Test

Crack closing test in 7- and 90-day samples of NM and NM_M mixtures is given in Figure 4.32. The crack closing ratio of 7-day NM and NM_M mixtures is 47.4% and 50.7%, respectively. In this case, it is seen that the microcapsule-based healing is 3.3%. When the 90-day samples were examined, 7.2% microcapsule-based healing was obtained. Although the healing was higher in the 90-day samples, it cannot be said to be a significant self-healing ratio. This situation can be explained by the fact that the crack closing test is performed only on the sample surface, as in UHPC mixtures, and the microcapsules are damaged and lost their effectiveness on the open side. It is thought that microcapsules stored in crack depths may be more effective in three dimensions. In Figure 4.33, optical microscope (OM) images of the 7-day samples before and after the healing process are shown as example.

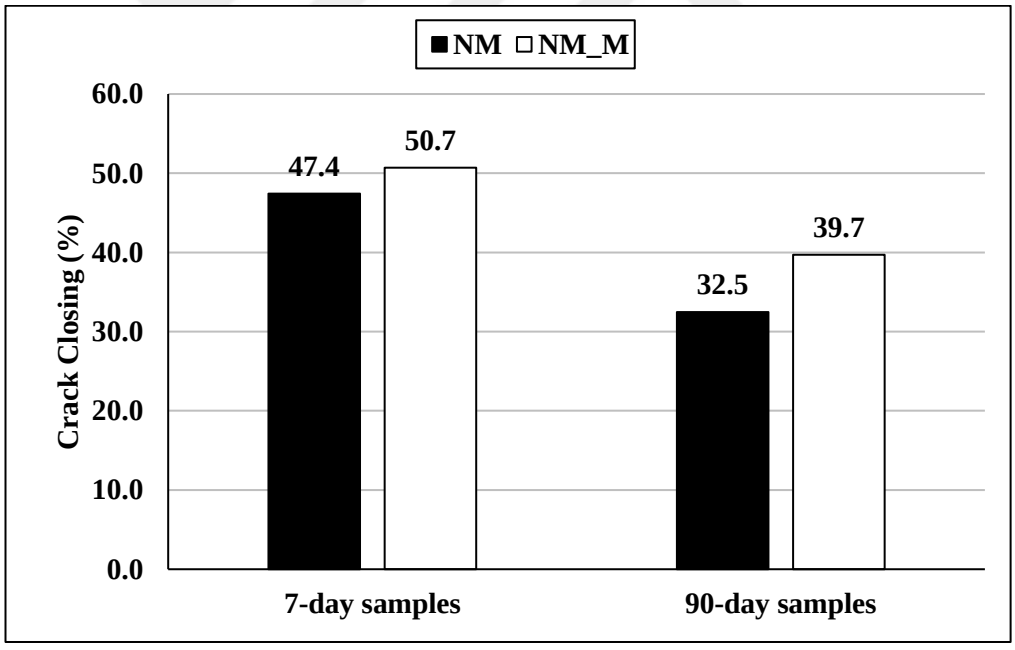

Figure 4.31 Percentages of crack closing

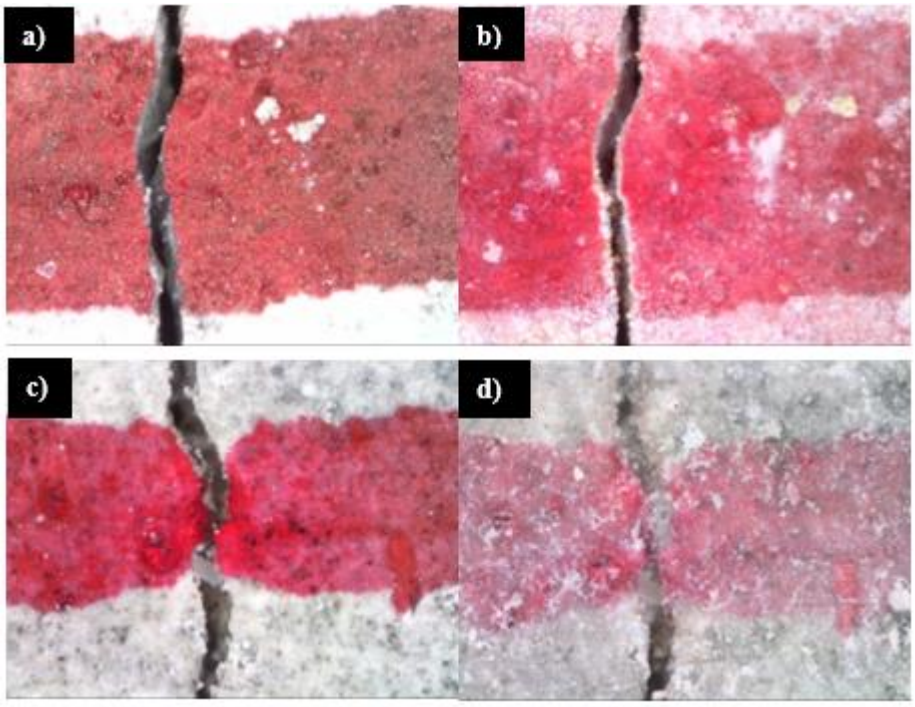

Figure 4.32 OM images of a) before 30-day healing period of 7-day NM mixture, b) after 30-day healing period of 7-day NM mixture, c) before 30-day healing period of 7-day NM_M mixture, d) after 30-day healing period of 7-day NM_M mixture (Personal archive, 2019)

4.2.4 Examination of Microcapsule Based Self-Healing Mechanism by Total Water Absorption Test

The total water absorption (TWA) percentages of 7-day NM and NM_M mixtures are shown in Figure 4.34. The water absorption of the normal mortar mixtures is higher than that of UHPC mixtures. The presence of microcapsules in normal mortar mixtures does not appear to significantly affect the total water absorption rate. Total water absorption percentages of 90-day samples are given in Figure 4.35. As can be seen from the graphics, there is a decrease in the water absorption rates after the 30-day healing period in the preloaded samples.

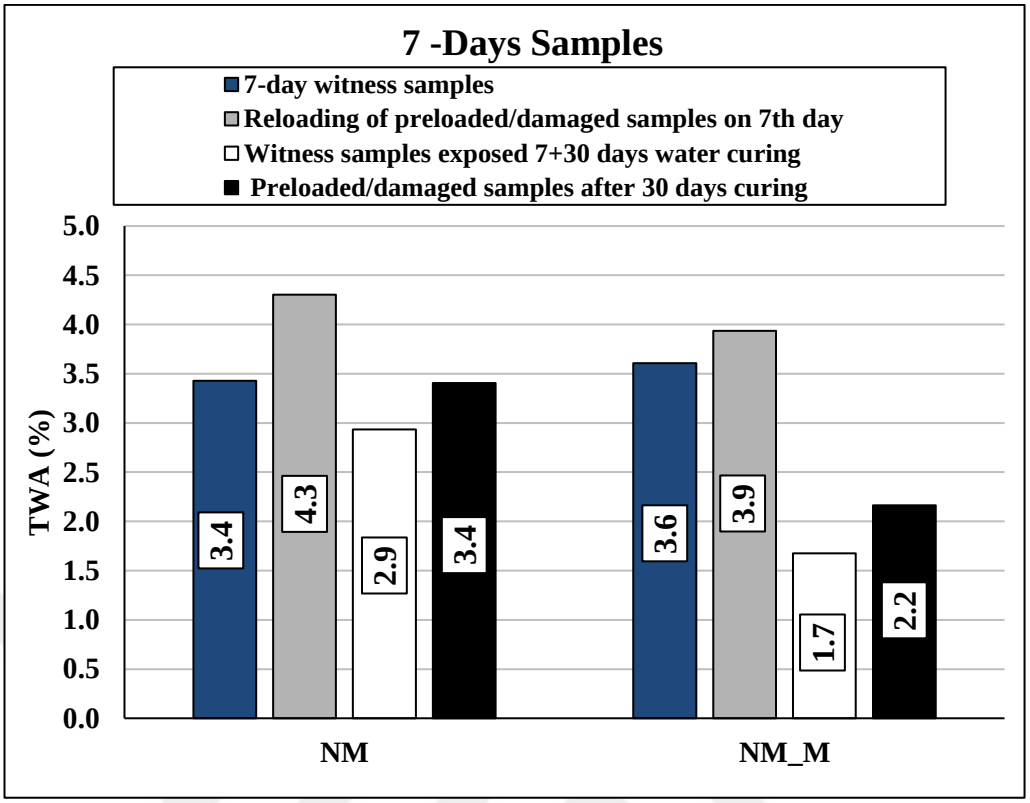

Figure 4.33 TWA Percentages Of 7-Day Samples

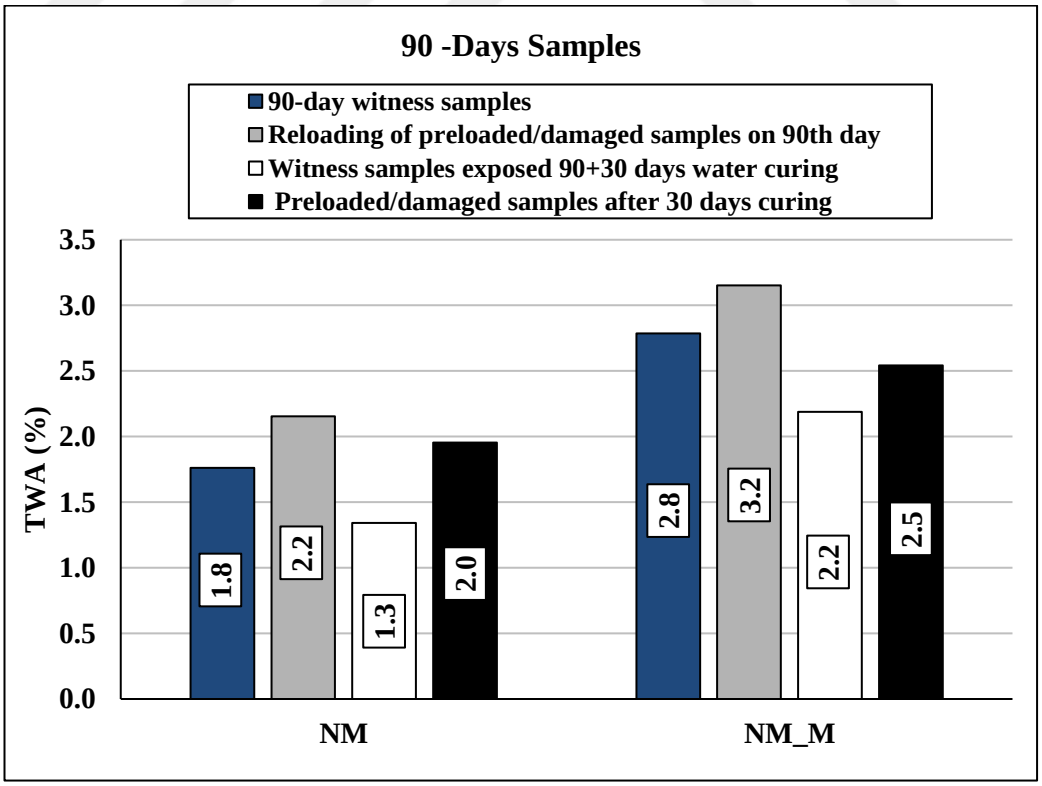

Figure 4.34 TWA Percentages of 90-Day Samples

Figure 4.36 shows the recovery (self-healing) ratio of the mixtures in TWA. The results are obtained by using equation (4.1), which is thought to give the most realistic result in the 4.1 section. Accordingly, the ratio of self-healing of NM and NM_M mixtures in 7-day samples is 65.5% and 78.5%, respectively. It is seen that the effect of microcapsules on the self-healing mechanism in 7-day-old samples is 13%. In 90-day samples, improvement by microcapsules is at the level of 38.4%. As can be seen, microcapsules significantly increased the self-healing ratio of the NM mixture.

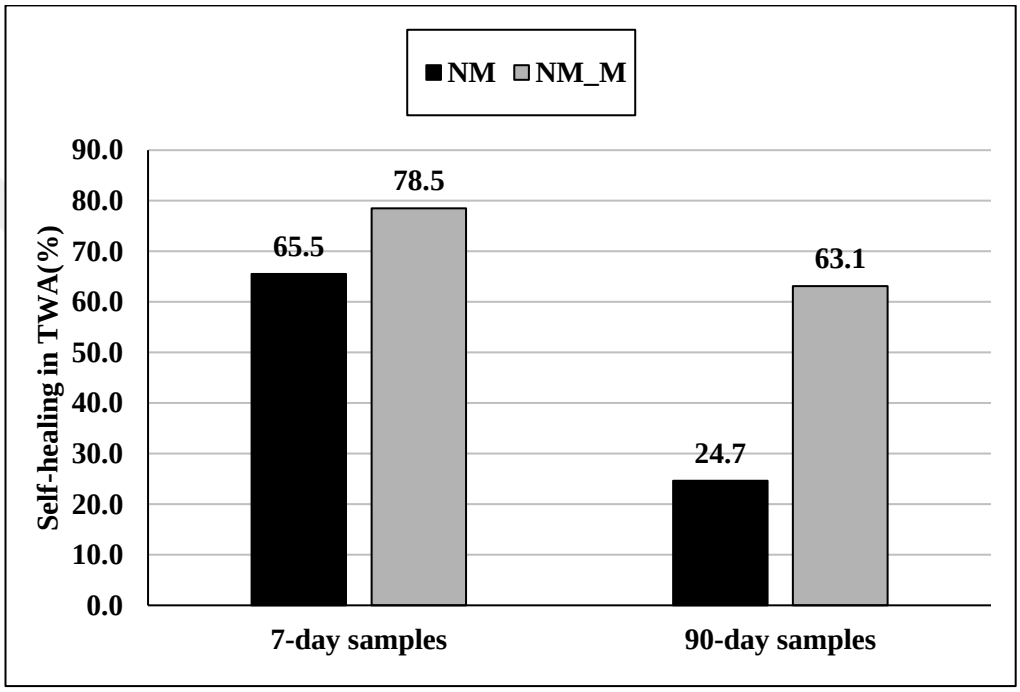

Figure 4.35 Self-healing in TWA (%)

4.2.5 Examination of Microcapsule Based Self-Healing Mechanism by Capillary Water Absorption Test

7-day capillary water absorption (CWA) test results (CWA - time curve) of NM and NM_M mixtures are given in Figure 4.37 and Figure 4.38, respectively. Considering the results, it is seen that the capillary water absorption amount of the 7-day NM_M mixture is about half of the NM mixture. In addition, a large increase is observed in the CWA values of preloaded samples in all mixtures. It is seen that the preloaded samples left for 30 days water cure in the YM_M mixture are very close to the CWA value of the 7-day witness samples.

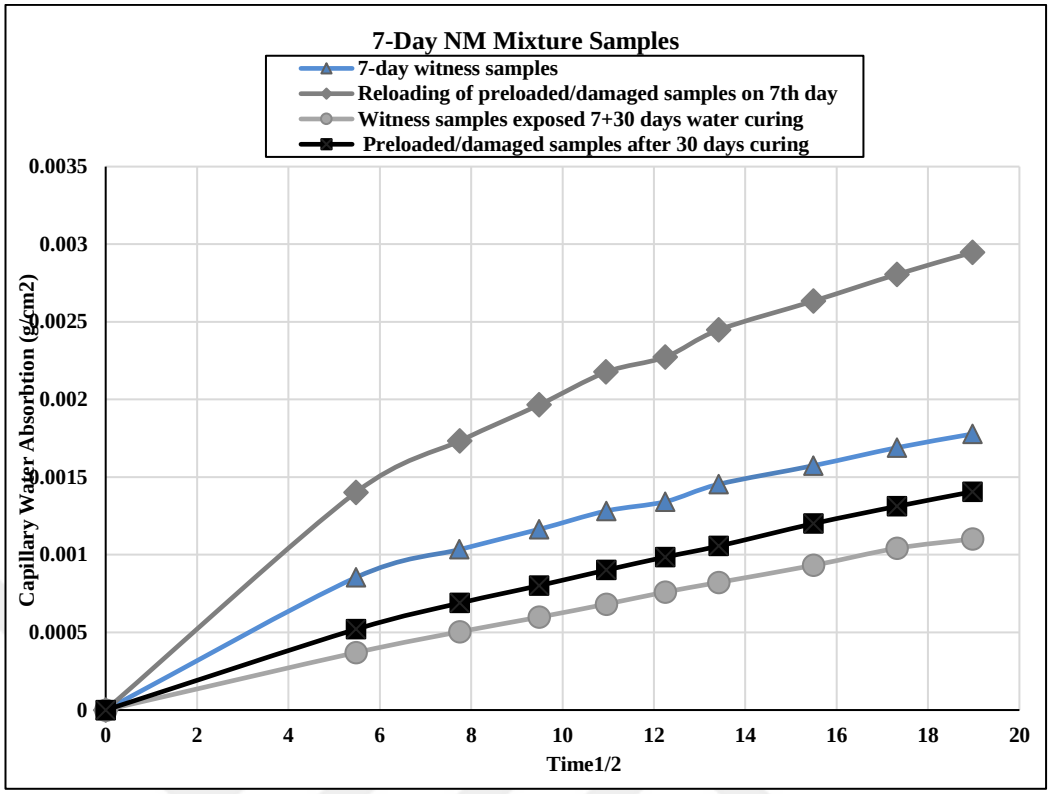

Figure 4.36 Time-dependent capillary water absorption graph of 7-day NM samples

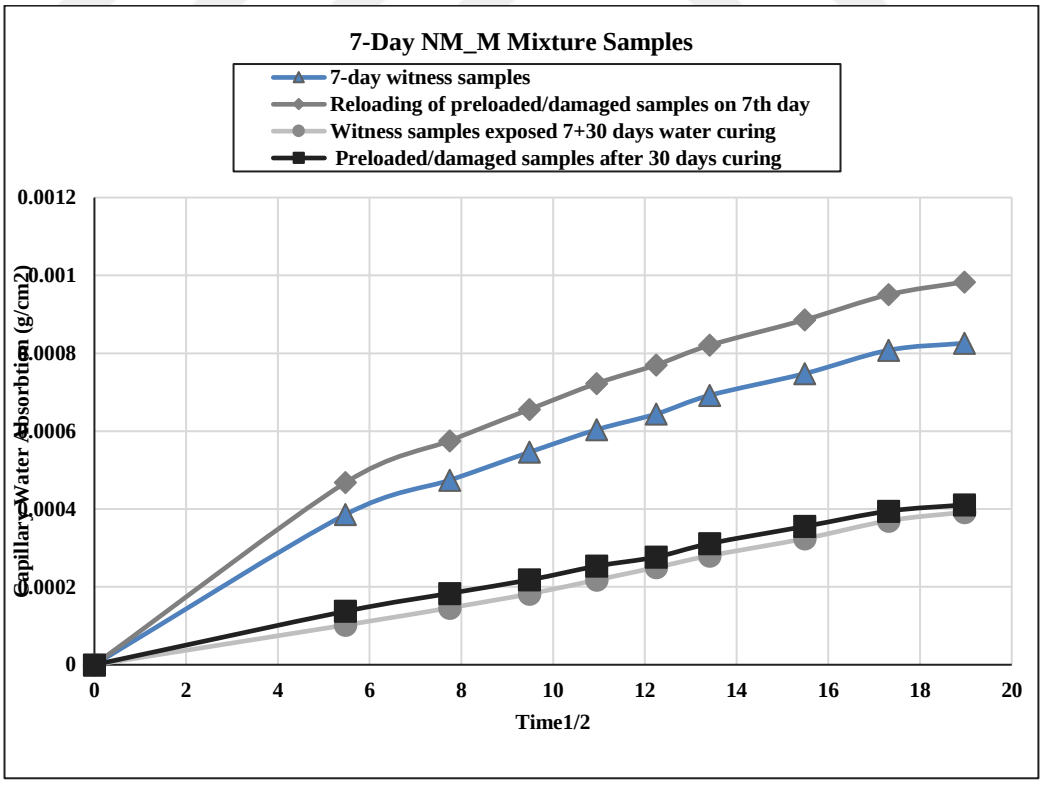

Figure 4.37 Time-dependent capillary water absorption graph of 7-day NM_M samples

When the 90-day CWA values of the mixtures are examined (Figure 4.39 and Figure 4.40), it is seen that the CWA values of the witness samples of both mixtures after 90 days and 30 days of self-healing period do not change significantly. Although the CWA values of the damaged samples of the NM mixture did not change significantly after the healing period, it was observed that there was a significant decrease in the CWA value in the 90-day NM_M mixture due to self-healing.

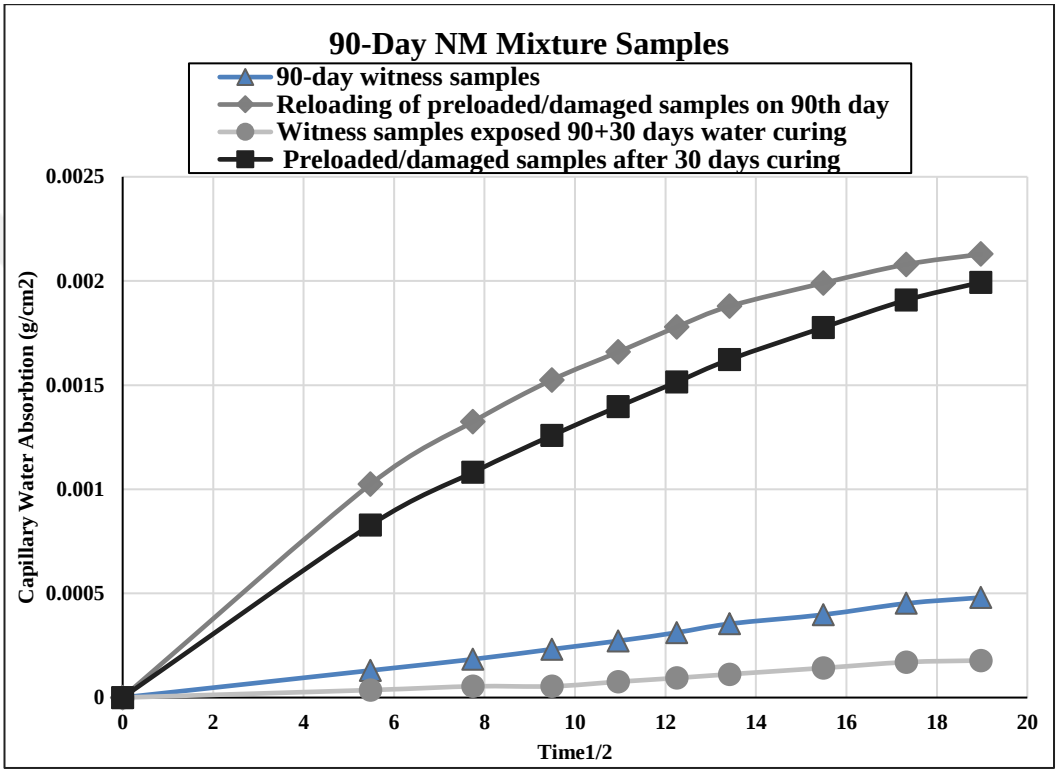

Figure 4.38 Time-dependent capillary water absorption graph of 90-day NM samples

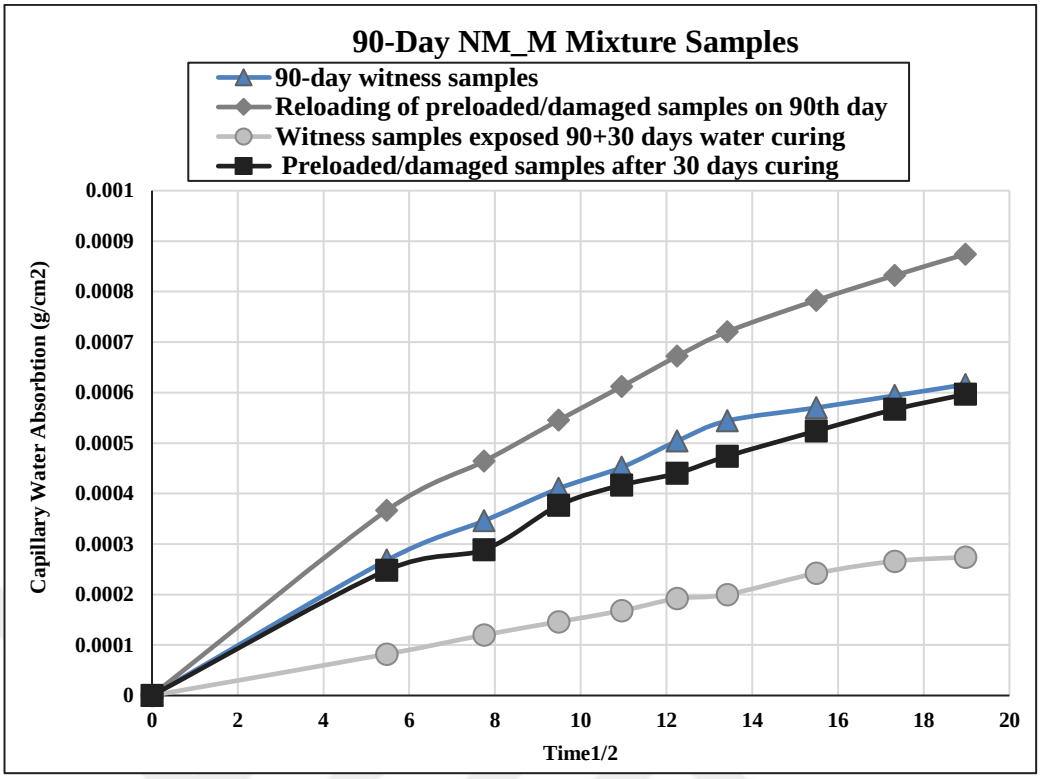

Figure 4.40 Time-dependent capillary water absorption graph of 90-day NM_M samples

As seen in Figure 4.41, microcapsule-based self-healing is 13.3% in 7-day normal mortar samples, while it is 39.3% in 90-day samples. Microcapsule-based healing examined with the CWA experiment gives better results in older samples. Because the autogenous self-healing potential in 90-day samples is low, the contribution of the microcapsule can be measured better.

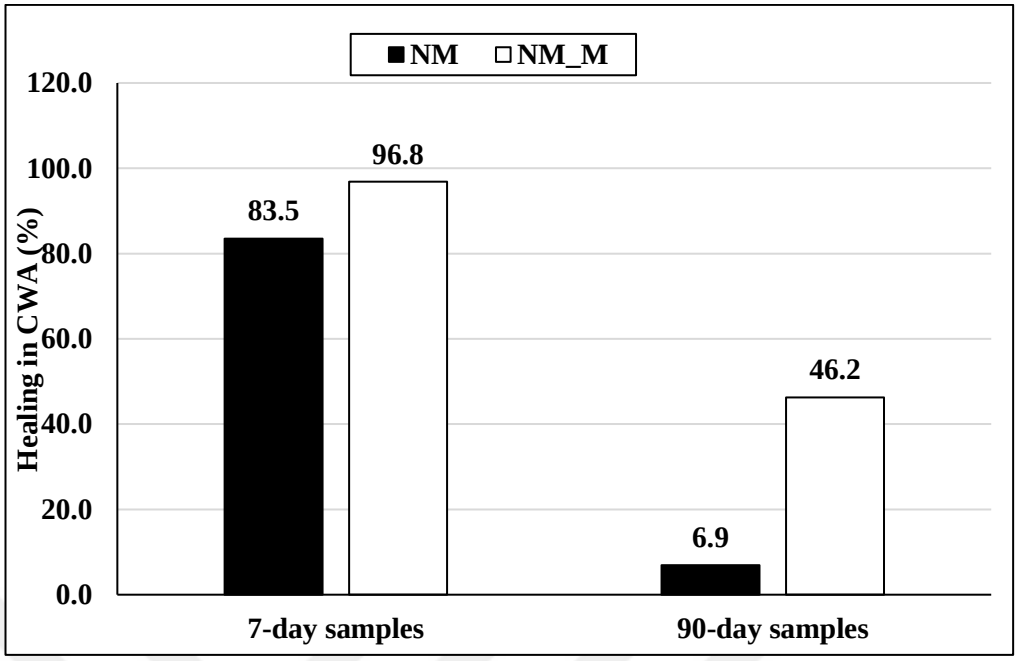

Figure 4.41 Recovery percentages (self-healing ratios) in CWA test

4.2.6 Examination of Microcapsule Based Self-Healing Mechanism by Crack Analysis

Figure 4.42 shows the crack analysis ratio (CA ratio) calculated by the equation (4.1) presented in the 4.1 section as a result of crack analysis in 7- and 90-day samples of NM and NM_M mixtures. Due to the hydration process completed in 90-day samples, less recovery(self-healing) rate is obtained. However, at the same time, microcapsule-based healing can be observed better in these samples. Considering the results, microcapsule-based recovery(self-healing) can be found by subtracting the autogenous recovery(self-healing) in samples without microcapsules from the recovery(self-healing) ratio in mixtures with microcapsules. The microcapsule-based healing is observed at a ratio of 30% in 7-day samples, while this rate is 37.2% in 90-day samples. Figure 4.43 and Figure 4.44 show optical microscope (OM) and analysis images of 7-day samples of NM and NM_M mixtures and Figure 4.45 and Figure 4.46 show optical microscope (OM) and analysis images of 90-day samples of NM and NM_M mixtures before and after the healing process with 30-day water cure. Although the self-healing activity of microcapsules in the UHPC mixture was not well determined by this test, it appears that there is an important self-healing contribution in normal mortar mixtures as in other test methods.

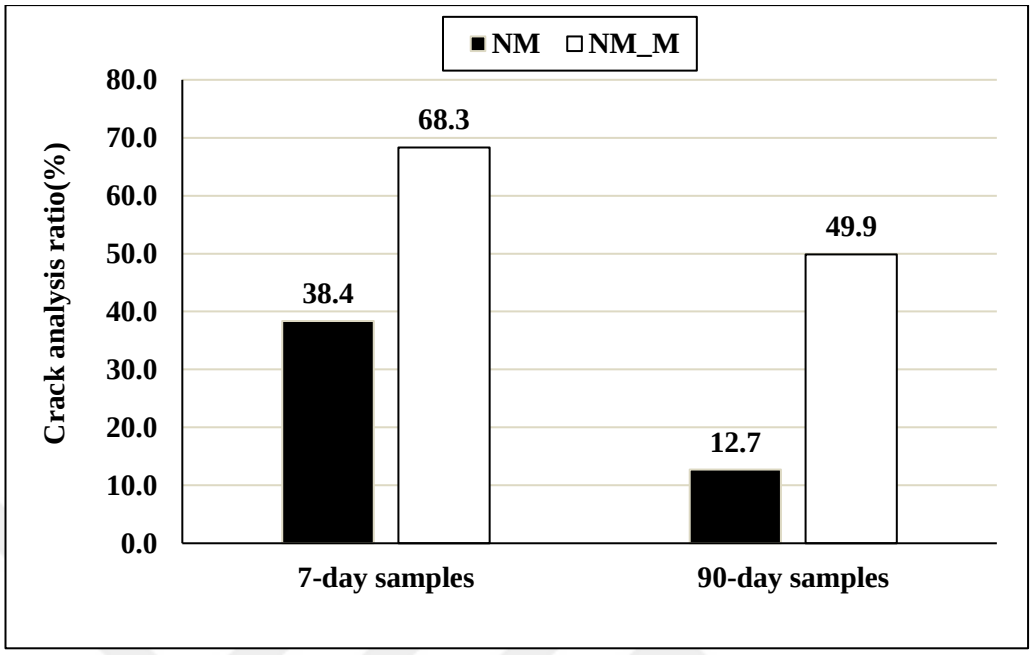

Figure 4.42 Crack closure percentages as a result of crack analysis (self-healing ratio)

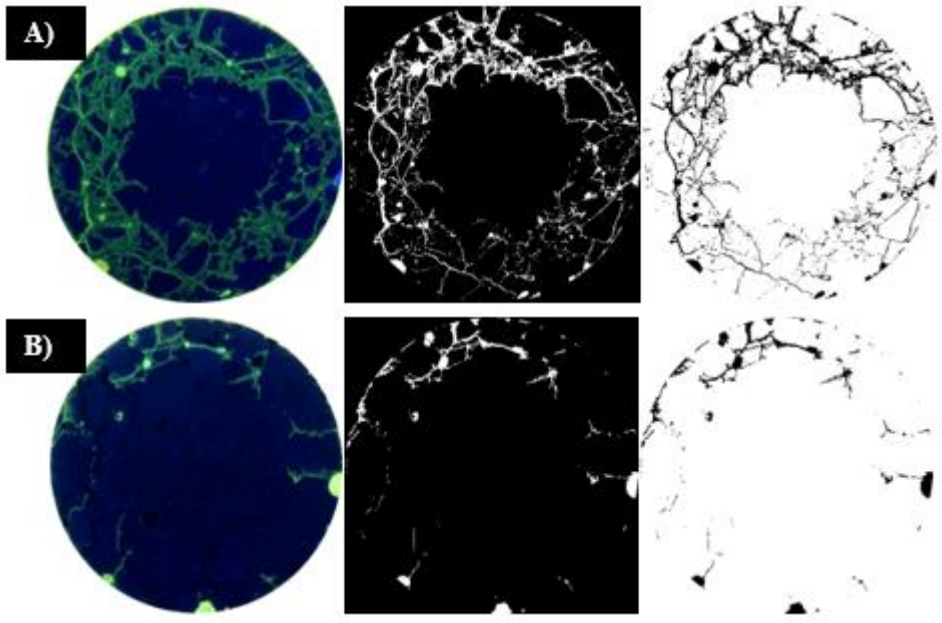

Figure 4.43 a) NM mixture after 7 days preloading, b) 7 days preloaded sample under UV light and analysis after 30 days self-healing period (Personal archive, 2019)

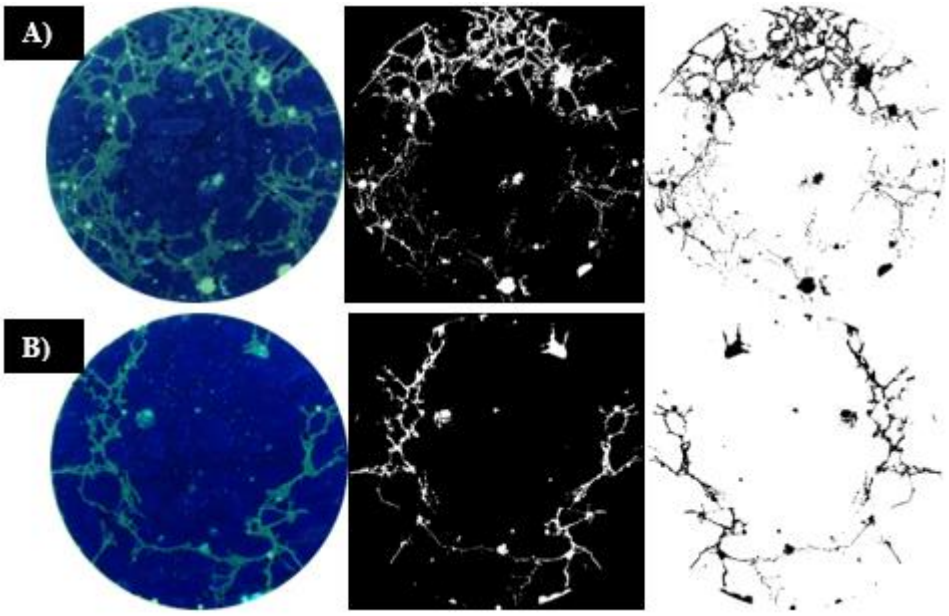

Figure 4.44 a) NM_M mixture after 7 days preloading, b) 7 days preloaded sample under UV light and analysis after 30 days self-healing period (Personal archive, 2019)

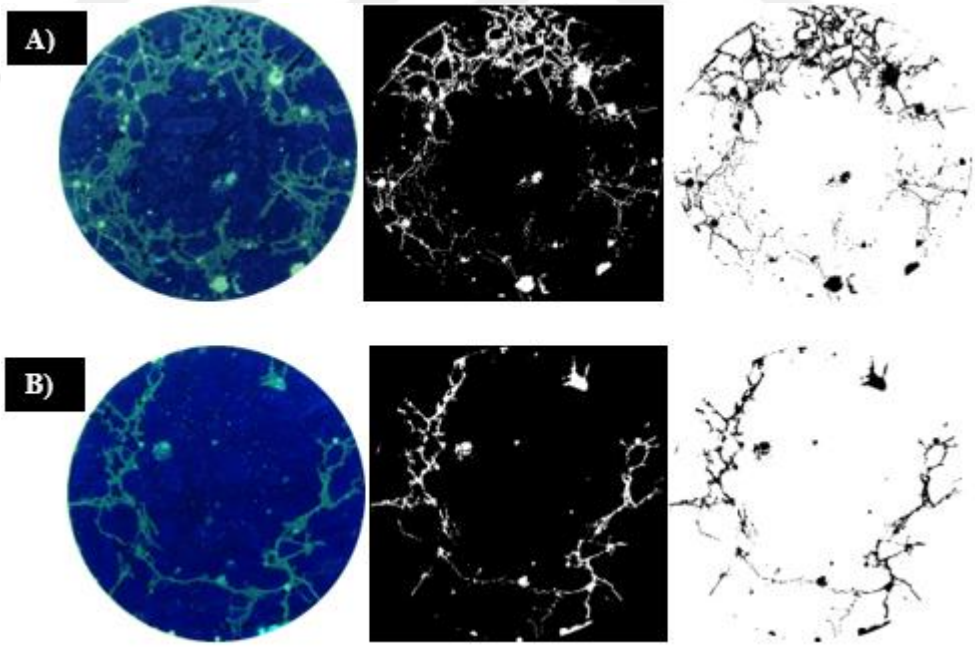

Figure 4.45 a) NM mixture after 90 days preloading, b) 90 days preloaded sample under UV light and analysis after 30 days self-healing period (Personal archive, 2019)

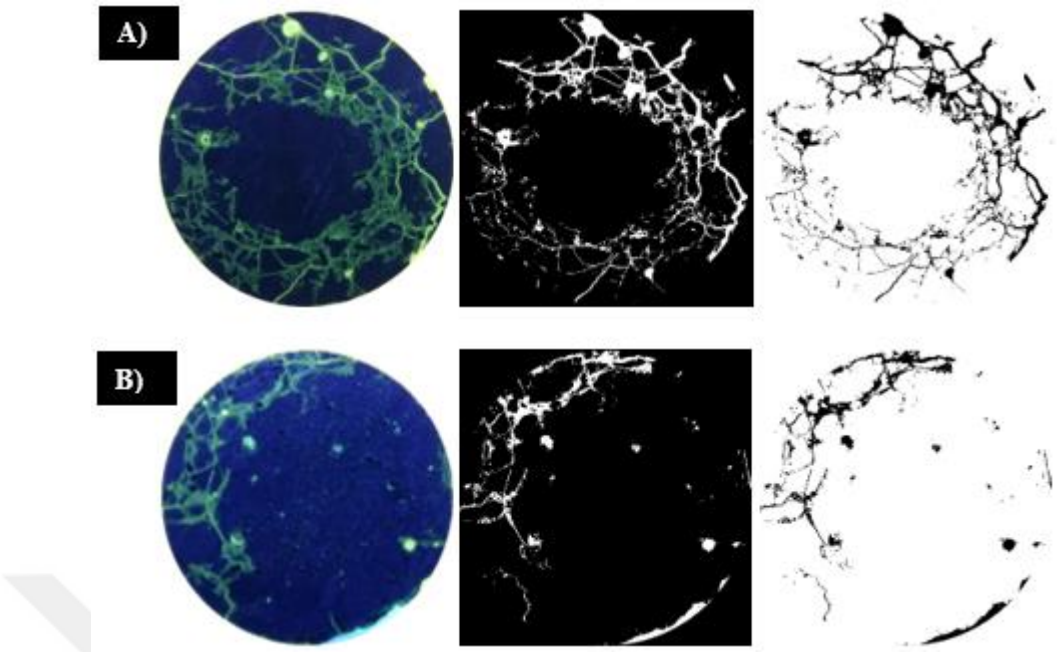

Figure 4.46 a) NM_M mixture after 90 days preloading, b) 90 days preloaded sample under UV light and analysis after 30 days self-healing period (Personal archive, 2019)

4.2.7 General Evaluation of the Effectiveness of Sodium Silicate / Polyurethane Microcapsules in Normal Mortar Mixtures

Significant amounts of self-healing activity of microcapsules in normal mortar mixtures were determined by all test methods. It has been demonstrated that the capacity of self-healing has been improved by using microcapsules in permeability with the tests of TWA / CWA and crack analysis tests; in mechanical properties with compressive strength. It has been observed that the developed microcapsules are more suitable to be used in normal mortar mixtures.

CHAPTER 5

CONCLUSIONS AND RECOMMENDATIONS

This study was carried out within the scope of the project (Project No: 215M783) financed by TUBITAK. Within the scope of the study, self-healing behaviour of ultra-high strength concretes and normal mortar mixtures was investigated by encapsulation of self-healing agents with microencapsulation technology. The self-healing mechanisms of microcracks formed under tensile and compressive loads were investigated by various mechanical tests, permeability and microstructure analysis. In addition, the microencapsulation of sodium silicate as a self-healing agent with polymeric wall materials and its healing ability in cement-based materials were carried out within the scope of this study. The conclusions obtained are as follows:

- The self-healing capacity of the ultra-high performance concrete and normal mortar mixtures was determined using various methods. From the experimental results, it was concluded that the determination of the self-healing rate is possible with a correct perspective. Especially in the compressive strength test, overly optimistic self-healing rates can be obtained, if the ongoing hydration reactions during the recovery period and especially the pozzolanic reactions are not taken into account. In addition, the effectiveness of the applied experiments can be analysed in terms of self-healing assessment. Compressive strength test, crack closure, total water absorption and capillary water absorption, crack analysis tests have been successfully used to evaluate the self-healing behaviour of preloaded and/or pre-damaged samples.

- Sodium silicate healing agent is microencapsulated with polyurethane wall. The microencapsulation process was optimized within the scope of the TUBITAK 215M783 project. Sodium silicate/polyurethane microcapsules with an average size of 60 micrometres were produced with the most efficient microencapsulation process by optimizing parameters such as the amount of

MDI, which is a wall construction material, the amount of sodium silicate, the healing agent, and the mixing procedure.

- Sodium silicate / polyurethane microcapsules were added at 5% by weight of cement to the GGBF-containing UHPC mixture (YM). It has been observed that it is more convenient to disperse the microcapsules in the mixing water before adding them to the dry components of the mixture. The results of the experiment showed that the effectiveness of these microcapsules in UHPC mixtures was less than expected. Although significant self-healing ratios were obtained in total and capillary water absorption tests, a significant self-healing ratio could not be determined in UHPC with microcapsule additive in other test methods. The large void size (60 micrometres) of the microcapsules led to decreases in strength. It has been evaluated that the long mixing time of UHPC can damage the microcapsules and reduce the effectiveness of the self-healing. Normal mortar mixtures (NM) were prepared in order to better investigate the self-healing effectiveness of microcapsules. It was found that the use of microcapsules significantly improved the self-healing ability in the mechanical properties with the compressive strength test, and the decrease in permeability with the TWA/CWA and crack analysis tests.

- In this process, the reaction between sodium silicate in the healing agent and Ca(OH)2, a product of cement hydration, is as follows (Alghamri et al., 2016; Giannaros et al., 2016; Pelletier et al., 2011):

$$Na_2SiO_3 + Ca(OH)_2 + H_2O \rightarrow {}_X(CaO \cdot SiO_2)H_2O + Na_2O$$

As can be seen, as a result of the reaction of calcium hydroxide and sodium silicate, which is a product of cement hydration, a secondary calcium-silica-hydrate (C-S-H) gel is formed and provides healing in cracks.

- Compared to UHPC, it has been determined that the developed microcapsules are more suitable to be used in normal mortar mixtures. Self-healing with

microcapsule effect was observed with compressive strength up to 23% in 7-day samples and 14% self-healing ratio in 90-days, 38.4% and 39.9% in total and capillary water absorption tests applied in 90-day samples, respectively, and 37.2% in crack analysis.

- When it is examined total improvements in which both autogenous healing and microcapsule-based healing are effective beyond the microcapsule-based healing, higher values were encountered in the normal mortars. For 7-day samples, 80%, 79%, 97%, 51% and 68% recovery rates were obtained in compressive strength, TWA, CWA crack closure tests and crack analysis, respectively. In 90-day samples, the recovery rates are 22%, 63%, 46%, 40% and 50%, respectively. A summary of self-healing results is shown in Table 5.1.

Table 5.1 Summary of Self-healing ratios

	UHPC				**Normal Mortar**			
	Microcapsule Based Healing		**Total Healing**		**Microcapsule Based Healing**		**Total Healing**	
	7-day	**90-day**	**7-day**	**90-day**	**7-day**	**90-day**	**7-day**	**90-day**
Compressive Test	-4%	8%	72%	34%	23%	14%	80%	22%
Direct Tensile Test	7%	45%	58%	64%	-	-	-	-
TWA	6%	30%	59%	57%	13%	38%	79%	63%
CWA	4%	12%	67%	54%	13%	39%	97%	46%
Crack-closing	0%	3%	100%	59%	3%	7%	51%	40%
Crack Analysis	-13%	-6%	60%	41%	30%	37%	68%	50%

The recommendations that can be made at the end of the study are as follows:

- Since the microcapsules act as voids in the matrix, optimization studies can be carried out to produce microcapsules in smaller sizes.

- Studies can be made on the microencapsulation of different healing agents by investigating the effectiveness of these agents.

- The effects on long-term durability can be examined by performing the self-healing properties with longer-term tests.

- Self-healing ability can be realized by cooperating industrial projects with private companies.

REFERENCES

Ahn, T. H., & Kishi, T. (2010). Crack self-healing behavior of cementitious composites incorporating various mineral admixtures. *Journal of Advanced Concrete Technology, 8*(2), 171-186.

Beglarigale, A. (2018). A*n investigation on self-healing ability of cement based composites.* Phd. Thesis, Dokuz Eylül University, İzmir.

Beglarigale, A., Eyice, D., Tutkun, B., Yazıcı, H., (2021). Evaluation of enhanced autogenous self-healingability of UHPC mixtures. *Construction and Building Materials, 280, 1-16.*

Bhaskar, S., Hossain, K. M. A., Lachemi, M., Wolfaardt, G., & Kroukamp, M. O. (2017). Effect of self-healing on strength and durability of zeolite-immobilized bacterial cementitious mortar composites. *Cement & Concrete Composites, 82*, 23-33.

Brown, E. N., Kessler, M. R., Sottos, N. R., & White, S. R. (2003). In situ poly(urea-formaldehyde) microencapsulation of dicyclopentadiene. *Journal of Microencapsulation, 20*(6), 719-730.

Cailleux, E., & Pollet, V. (2009). *Investigations on the development of self-healing properties in protective coatings for concrete and repair mortars.* Paper presented at the Proceedings of the 2nd International Conference on Self-Healing Materials, Chicago, IL, USA, 1-4.

Calvo, J. L. G., Perez, G., Carballosa, P., Erkizia, E., Gaitero, J. J., & Guerrero, A. (2017). Development of ultra-high performance concretes with self-healing micro/nano-additions. *Construction and Building Materials, 138,* 306-315.

de Rooij, M., Van Tittelboom, K., De Belie, N., & Schlangen, E. (2013). *Self-healing phenomena in cement-Based materials: state-of-the-art report of RILEM technical committee 221-SHC: self-Healing phenomena in cement-Based materials* (RILEM State-of-the-Art Reports; Vol. 11). Dordrecht: Springer.

Freyermuth, C. L. (2001). Life-cycle cost analysis for large bridges. *Concrete International, 23*(02), 89-95.

Giannaros, P., Kanellopoulos, A., & Al-Tabbaa, A. (2016). Sealing of cracks in cement using microencapsulated sodium silicate. *Smart Materials and Structures, 25(8),* 1-12.

Gilford, J., Hassan, M. M., Rupnow, T., Barbato, M., Okeil, A., & Asadi, S. (2014). Dicyclopentadiene and sodium silicate microencapsulation for self-healing of concrete. *Journal of Materials in Civil Engineering, 26*(5), 886-896.

Homma, D., Mihashi, H., & Nishiwaki, T. (2009). Self-healing capability of fibre reinforced cementitious composites. *Journal of Advanced Concrete Technology, 7*(2), 217-228.

Hung, C. C., Su, Y. F., & Hung, H. H. (2017). Impact of natural weathering on medium-term self-healing performance of fiber reinforced cementitious composites with intrinsic crack-width control capability. *Cement & Concrete Composites, 80,* 200-209.

Jia, Y., Wang, H. Y., Tian, K. S., Li, R. F., Zhaopeng, X., Jiao, J.,Cao, L., & Wu, Y. (2016). A combined interfacial and in-situ polymerization strategy to construct well-defined core-shell epoxy-containing SiO2-based microcapsules with high encapsulation loading, super thermal stability and nonpolar solvent tolerance. *International Journal of Smart and Nano Materials, 7*(4), 221-235.

Joseph, C., Jefferson, A. D., Isaacs, B., Lark, R., & Gardner, D. (2010). Experimental investigation of adhesive-based self-healing of cementitious materials. *Magazine of Concrete Research, 62*(11), 831-843.

Kanellopoulos, A., Giannaros, P., & Al-Tabbaa, A. (2016). The effect of varying volume fraction of microcapsules on fresh, mechanical and self-healing properties of mortars. *Construction and Building Materials, 122,* 577-593.

Kanellopoulos, A., Giannaros, P., Palmer, D., Kerr, A., & Al-Tabbaa, A. (2017). Polymeric microcapsules with switchable mechanical properties for self-healing concrete: synthesis, characterisation and proof of concept. *Smart Materials and Structures, 26* (045025), 1-15.

Kim, D. J., Kang, S. H., & Ahn, T. H. (2014). Mechanical characterization of high-performance steel-fiber reinforced cement composites with self-healing effect. *Materials, 7*(1), 508-526.

Kishi, T., Ahn, T., Hosoda, A., Suzuki, S., & Takaoka, H. (2007). *Self-healing behaviour by cementitious recrystallization of cracked concrete incorporating expansive agent.* Paper presented at the Proceedings of the First International Conference on Self-healing Materials, 18-20 April, The Netherlands, 1-10.

Kuang, Y. C., & Ou, J. P. (2008b). Self-repairing performance of concrete beams strengthened using superelastic SMA wires in combination with adhesives released from hollow fibers. *Smart Materials and Structures, 17*(025020), 1-7.

Kunieda, M., Choonghyun, K., Ueda, N., & Nakamura, H. (2012). Recovery of protective performance of cracked ultra high performance-strain hardening cementitious composites (uhp-shcc) due to autogenous healing. *Journal of Advanced Concrete Technology, 10*(9), 313-322.

Li, M., & Li, V. C. (2011). Cracking and healing of engineered cementitious composites under chloride environment. *ACI Materials Journal, 108*(3), 333-340.

Li, V. C., & Herbert, E. (2012). Robust self-healing concrete for sustainable infrastructure. *Journal of Advanced Concrete Technology, 10*(6), 207-218.

Li, V. C., Lim, Y. M., & Chan, Y. W. (1998). Feasibility study of a passive smart self-healing cementitious composite. *Composites Part B-Engineering, 29*(6), 819-827.

Liu, X., Yao, W., Zheng, X., & Wu, J. (2005). Experimental study on self-healing performance of concrete. *Journal of Building Materials, 2*, 184-188.

Lv, L., Yang, Z., Chen, G., Zhu, G., Han, N., Schlangen, E., & Xing, F. (2016). Synthesis and characterization of a new polymeric microcapsule and feasibility investigation in self-healing cementitious materials. *Construction and Building Materials, 105*, 487-495.

Mihashi, H., & Nishiwaki, T. (2012). Development of engineered self-healing and self-repairing concrete-state-of-the-art report. *Journal of Advanced Concrete Technology, 10*(5), 170-184.

Neville, A. (2002). Autogenous healing—a concrete miracle?, *Concrete International, 24*(11), 76-82.

Nishiwaki, T., Koda, M., Yamada, M., Mihashi, H., & Kikuta, T. (2012). Experimental study on self-healing capability of frcc using different types of synthetic fibers. *Journal of Advanced Concrete Technology, 10*(6), 195-206.

Nishiwaki, T., Kwon, S., Homma, D., Yamada, M., & Mihashi, H. (2014). Self-healing capability of fiber-reinforced cementitious composites for recovery of watertightness and mechanical properties. *Materials, 7*(3), 2141-2154.

Palin, D., Wiktor, V., & Jonkers, H. M. (2015). Autogenous healing of marine exposed concrete: Characterization and quantification through visual crack closure. *Cement and Concrete Research, 73*, 17-24.

Pelletier, M., Brown, R., Shukla, A., & Bose, A. (2011). *Self-Healing Concrete with a Microencapsulated Healing Agent.* Retrieved May 17, 2013 from http://energetics.chm.uri.edu/system/files/Self%20healing%20concrete%20-7-11.pdf.

Perez, G., Erkizia, E., Gaitero, J. J., Kaltzakorta, I., Jimenez, I., & Guerrero, A. (2015). Synthesis and characterization of epoxy encapsulating silica microcapsules and amine functionalized silica nanoparticles for development of an innovative self-healing concrete. *Materials Chemistry and Physics, 165*, 39-48.

Perez, G., Gaitero, J. J., Erkizia, E., Jimenez, I., & Guerrero, A. (2015). Characterisation of cement pastes with innovative self-healing system based in epoxy-amine adhesive. *Cement & Concrete Composites, 60*, 55-64.

Qian, S. Z., Zhou, J., & Schlangen, E. (2010). Influence of curing condition and precracking time on the self-healing behavior of Engineered Cementitious Composites. *Cement & Concrete Composites, 32*(9), 686-693.

Ramachandran, S. K., Ramakrishnan, V., & Bang, S. S. (2001). Remediation of concrete using micro-organisms. *ACI Materials Journal-American Concrete Institute, 98*(1), 3-9.

Sahmaran, M., Keskin, S. B., Ozerkan, G., & Yaman, I. O. (2008). Self-healing of mechanically-loaded self consolidating concretes with high volumes of fly ash. *Cement & Concrete Composites, 30*(10), 872-879.

Sahmaran, M., & Li, V. C. (2009). Durability properties of micro-cracked ECC containing high volumes fly ash. *Cement and Concrete Research, 39*(11), 1033-1043.

Sahmaran, M., Yildirim, G., & Erdem, T. K. (2013). Self-healing capability of cementitious composites incorporating different supplementary cementitious materials. *Cement & Concrete Composites, 35*(1), 89-101.

Saihi, D., Vroman, I., Giraud, S., & Bourbigot, S. (2006). Microencapsulation of ammonium phosphate with a polyurethane shell. Part II. interfacial polymerization technique. *Reactive & Functional Polymers, 66*(10), 1118-1125.

Sangadji, S., & Schlangen, E. (2012). Self healing of concrete structures - novel approach using porous network concrete. *Journal of Advanced Concrete Technology*, *10*(5), 185-194.

Sangadji, S., Wiktor, V., Jonkers, H., & Schlangen, E. (2017). The use of alkaliphilic bacteria-based repair solution for porous network concrete healing mechanism. *3rd International Conference on Sustainable Civil Engineering Structures and Construction Materials - Sustainable Structures for Future Generations, 171*, 606-613

Sherir, M. A. A., Hossain, K. M. A., & Lachemi, M. (2017a). Development and recovery of mechanical properties of self-healing cementitious composites with MgO expansive agent. *Construction and Building Materials, 148*, 789-810.

Sherir, M. A. A., Hossain, K. M. A., & Lachemi, M. (2017b). The influence of MgO-type expansive agent incorporated in self-healing system of Engineered cementitious Composites. *Construction and Building Materials, 149*, 164-185.

Siad, H., Lachemi, M., Sahmaran, M., & Hossain, K. M. A. (2017). Mechanical, physical, and self-healing behaviors of engineered cementitious composites with glass powder. *Journal of Materials in Civil Engineering, 29*(6), 04017016.

Sisomphon, K., Copuroglu, O., & Koenders, E. A. B. (2012). Self-healing of surface cracks in mortars with expansive additive and crystalline additive. *Cement & Concrete Composites, 34*(4), 566-574.

Sisomphon, K., Copuroglu, O., & Koenders, E. A. B. (2013). Effect of exposure conditions on self healing behavior of strain hardening cementitious composites incorporating various cementitious materials. *Construction and Building Materials, 42*, 217-224.

Tan, N. P. B., Keung, L. H., Choi, W. H., Lam, W. C., & Leung, H. N. (2016). Silica-based self-healing microcapsules for self-repair in concrete. *Journal of Applied Polymer Science, 133*(12), 43090.

Ter Heide, N. (2005). *Crack healing in hydrating concrete.* MSc thesis, Delft University, Delft.

Termkhajornkit, P., Nawa, T., Yamashiro, Y., & Saito, T. (2009). Self-healing ability of fly ash-cement systems. *Cement & Concrete Composites, 31*(3), 195-203.

Van Breugel, K. (2007). *Is there a market for self-healing cement-based materials.* Paper presented at the Proceedings of the First International Conference on Self-Healing Materials, Noordwijk, (1-9).

Van Tittelboom, K., & De Belie, N. (2013). Self-Healing in Cementitious Materials-A Review. *Materials, 6*(6), 2182-2217.

Wang, J., Jonkers, H. M., Boon, N., & De Belie, N. (2017). Bacillus sphaericus LMG 22257 is physiologically suitable for self-healing concrete. *Applied Microbiology and Biotechnology, 101*(12), 5101-5114.

Wang, J. Y., Snoeck, D., Van Vlierberghe, S., Verstraete, W., & De Belie, N. (2014). Application of hydrogel encapsulated carbonate precipitating bacteria for approaching a realistic self-healing in concrete. *Construction and Building Materials, 68*, 110-119.

Wang, J. Y., Soens, H., Verstraete, W., & De Belie, N. (2014). Self-healing concrete by use of microencapsulated bacterial spores. *Cement and Concrete Research, 56*, 139-152.

White, S. R., Sottos, N. R., Geubelle, P. H., Moore, J. S., Kessler, M. R., Sriram, S. R., Brown, E., N., & Viswanathan, S. (2001). Autonomic healing of polymer composites. *Nature, 409*(6822), 794-797.

Wiktor, V., & Jonkers, H. M. (2011). Quantification of crack-healing in novel bacteria-based self-healing concrete. *Cement & Concrete Composites, 33*(7), 763-770.

Wu, M., Johannesson, B., & Geiker, M. (2012). A review: Self-healing in cementitious materials and engineered cementitious composite as a self-healing material. *Construction and Building Materials, 28*(1), 571-583.

Xing, F., Ni, Z., Han, N., Dong, B., Du, X., Huang, Z., & Zhang, M. (2008). *Self-healing mechanism of a novel cementitious composite using microcapsules.* Paper presented at the Proceedings of the International Conference on Durability of Concrete Structures, Hangzhou.

Xu, J., & Yao, W. (2014). Multiscale mechanical quantification of self-healing concrete incorporating non-ureolytic bacteria-based healing agent. *Cement and Concrete Research, 64*, 1-10.

Yang, Y. Z., Lepech, M. D., Yang, E. H., & Li, V. C. (2009). Autogenous healing of engineered cementitious composites under wet-dry cycles. *Cement and Concrete Research, 39*(5), 382-390.

Yang, Z. X., Holler, J., He, X. D., & Shi, X. M. (2010). Laboratory assessment of a self-healing cementitious composite. *Transportation Research Record*(2142), 9-17.

Yazıcı, H., Beglarigale, H., Seki, Y., Eyice, D., Vahedi, H., Tutkun, B.(2019). Çimento esaslı kompozitlerin kendi kendine iyileşme kabiliyetinin araştırılması (Project no:215M783). *Tubitak Projecy report.*

Zhou, S., Zhu, H., & Yan, Z. (2014). Materials, theories and experiments of microcapsule self-healing method—A review. In *Tunneling and Underground Construction* (195-204).

Zhou, Z. H., Li, Z. Q., Xu, D. Y., & Yu, J. H. (2011). Influence of slag and fly ash on the self-healing ability of concrete. *Emerging Focus on Advanced Materials, Pts 1 and 2, 306-307*, 1020.